

Newfoundland and Labrador Hydro Hydro Place. 500 Columbus Drive P.O. Box 12400. St. John's. NL Canada A1B 4K7 t. 709.737.1400 I f. 709.737.1800 nlhydro.com

October 31, 2025

Board of Commissioners of Public Utilities Prince Charles Building 120 Torbay Road, P.O. Box 21040 St. John's, NL A1A 5B2

Attention: Jo-Anne Galarneau

Executive Director and Board Secretary

Re: Quarterly Report on Asset Performance in Support of Resource Adequacy for the Twelve Months Ended September 30, 2025

Please find enclosed Newfoundland and Labrador Hydro's ("Hydro") Quarterly Report on Asset Performance in Support of Resource Adequacy for the Twelve Months Ended September 30, 2025.¹

As included in the previous quarterly report, Hydro has included an update on the Muskrat Falls Assets to provide the Board of Commissioners of Public Utilities with additional information. This is provided as Appendix B to this report.

Should you have any questions, please contact the undersigned.

Yours truly,

NEWFOUNDLAND AND LABRADOR HYDRO

Shirley A. Walsh

Senior Legal Counsel, Regulatory

SAW/rr

Encl.

ecc:

Board of Commissioners of Public Utilities

Jacqui H. Glynn Ryan Oake Board General

Island Industrial Customer Group

Paul L. Coxworthy, Stewart McKelvey Denis J. Fleming, Cox & Palmer Glen G. Seaborn, Poole Althouse **Labrador Interconnected Group**

Senwung F. Luk, Olthuis Kleer Townshend LLP Nicholas E. Kennedy, Olthuis Kleer Townshend LLP

Consumer Advocate

Dennis M. Browne, KC, Browne Fitzgerald Morgan & Avis Stephen F. Fitzgerald, KC, Browne Fitzgerald Morgan & Avis Sarah G. Fitzgerald, Browne Fitzgerald Morgan & Avis Bernice Bailey, Browne Fitzgerald Morgan & Avis **Newfoundland Power Inc.**Dominic J. Foley
Douglas W. Wright

Regulatory Email

¹ Formerly titled "Quarterly Report of Generating Units for the Twelve Months Ended []."

Quarterly Report on Asset Performance in Support of Resource Adequacy

For the Twelve Months Ended September 30, 2025

October 31, 2025

A report to the Board of Commissioners of Public Utilities



Contents

1.0	Introduction	1
2.0	Assumptions Used in Hydro's Assessment of System Reliability and Resource Adequacy	2
3.0	Current Period Overview	5
4.0	Hydraulic Unit DAFOR Performance – Regulated Hydro	6
4.1	Granite Canal Facility	8
4.2	Paradise River Facility	<u>9</u>
5.0	Hydraulic Unit DAFOR Performance – Muskrat Falls	<u>c</u>
5.1	Muskrat Falls Unit 1	10
5.2	Muskrat Falls Unit 2	10
5.3	Muskrat Falls Unit 3	11
6.0	Thermal Unit DAFOR Performance	11
6.1	Holyrood TGS Unit 1	12
7.0	Combustion Turbine DAUFOP Performance	13
7.1	Happy Valley Gas Turbine	16
7.2	Holyrood Combustion Turbine	17
8.0	Labrador-Island Link EgFOR Performance	17

List of Appendices

Appendix A: Soldiers Pond Synchronous Condensers

Appendix B: Muskrat Falls Asset Update – Reporting period up to September 30, 2025



1.0 Introduction

- 2 In this report, Newfoundland and Labrador Hydro ("Hydro") provides data on forced outage rates of its
- 3 generating facilities and the Labrador-Island Link ("LIL"). The data provided pertains to historical forced
- 4 outage rates and assumptions Hydro uses in its assessments of resource adequacy. This report covers
- 5 the performance for the current 12-month reporting period of October 1, 2024 to September 30, 2025
- 6 ("current period").

1

- 7 This report contains forced outage rates for the current period for individual generating units at
- 8 regulated hydraulic facilities, ¹ the Holyrood Thermal Generating Station ("Holyrood TGS"), Hydro's
- 9 combustion turbines, and the non-regulated Muskrat Falls Hydroelectric Generating Facility ("Muskrat
- 10 Falls Facility"). In addition, equivalent forced outage rates are provided for the 900 MW LIL.² This report
- also provides, for comparison purposes, the individual asset forced outage rates for the 12-month
- reporting period of October 1, 2023 to September 30, 2024 ("previous period"). Further, total asset class
- data is presented based on the calendar year for the remainder of the ten most recent years—2015 to
- 14 2024—with the exception of the Muskrat Falls Facility³ and the LIL.⁴
- 15 The forced outage rates of Hydro's generating units are calculated using two measures:
- 1) Derated adjusted forced outage rate ("DAFOR") for the continuous (base-loaded) units; and
- 2) Derated adjusted utilization forced outage probability ("DAUFOP") for the standby units.
- 18 DAFOR is a metric that measures the percentage of time that a unit or group of units is unable to
- 19 generate at its maximum continuous rating due to forced outages or unit deratings. The DAFOR for each
- 20 unit is weighted to reflect differences in generating unit sizes to provide a combined total and reflect the
- 21 relative impact a unit's performance has on overall generating performance. This measure is applied to
- 22 hydraulic units and, historically, was used for the thermal units; however, it does not apply to

⁴ The LIL was officially commissioned on April 13, 2023. Annual equivalent forced outage rate ("EqFOR") data is only available for 2024 year end.



Page 1

¹ Regulated hydraulic facilities include the Bay d'Espoir Hydroelectric Generating Facility ("Bay d'Espoir Facility" or "BDE"), the Cat Arm Hydroelectric Generating Station ("Cat Arm Station" or "CAT"), the Hinds Lake Hydroelectric Generating Station ("Hinds Lake Station" or "HLK"), the Upper Salmon Hydroelectric Generating Station ("Upper Salmon Station" or "USL"), the Granite Canal Hydroelectric Generating Station ("Granite Canal Station" or "GCL"), and the Paradise River Hydroelectric Generating Station ("Paradise River Station" or "PRV").

² The LIL has been commissioned and is currently rated at 700 MW.

³ The final generating unit at the Muskrat Falls Facility was released for commercial operation on November 25, 2021. Annual DAFOR performance data is available beginning in 2022.

- 1 combustion turbines because of their operation as standby units and their relatively low operating
- 2 hours.
- 3 DAUFOP is a metric that measures the percentage of time that a unit or group of units will encounter a
- 4 forced outage and not be available when required. DAUFOP is a measure primarily used for combustion
- 5 turbines; however, this measure may be applicable to thermal units, should their operation move
- 6 towards standby operation in the future. This metric includes the impact of unit deratings.
- 7 The forced outage rates include outages that remove a unit from service completely as well as instances
- 8 when units are derated. If a unit's output is reduced by more than 2%, the unit is considered derated
- 9 under Electricity Canada guidelines. These guidelines require that the derated levels of a generating unit
- 10 be calculated by converting the operating time at the derated level into an equivalent outage time.
- 11 As the LIL is not a generating unit, the above noted forced outage rate measures do not apply to this
- 12 asset. Instead, Hydro has determined an appropriate metric to be an EqFOR to measure the
- performance of this asset as it relates to the supply of electricity to the Island. This EqFOR measures the
- 14 percentage of time that the LIL bipole is unable to deliver its maximum continuous rating⁵ to the Island
- due to forced outages, derates, or unplanned monopole outages. The effect of deratings and unplanned
- 16 monopole outages is converted to equivalent bipole outage time using the same methodology as
- 17 outlined above for generating units.
- 18 In addition to forced outage rates, this report provides details for those outages which occurred in the
- 19 current period that contributed materially to forced outage rates exceeding those used in Hydro's
- 20 resource adequacy planning analysis for both the near and long-term.

2.0 Assumptions Used in Hydro's Assessment of System Reliability and Resource Adequacy

- 23 Hydro continually assesses the reliability of its system and its ability to meet customer requirements,
- 24 filing both near- and long-term assessments with the Board of Commissioners of Public Utilities.⁶

⁶ Hydro currently files an assessment of near-term system reliability and resource adequacy annually in November, the Near-Term Reliability Report. Hydro also files an assessment of longer-term system reliability and resource adequacy. The most



21

⁵ The LIL maximum continuous rating is 700 MW at present.

- 1 As part of the ongoing Reliability and Resource Adequacy Study Review proceeding, Hydro detailed the
- 2 process undertaken for determining the forced outage rates most appropriate for use in its near-term
- 3 reliability assessments and long-term resource adequacy analysis. Table 1 and Table 2 summarize the
- 4 most recent forced outage rate assumptions, as determined using the forced outage rate methodology.⁷
- 5 Forced outage rate assumptions will be re-evaluated on an annual basis to incorporate the most recent
- 6 data available.

Table 1: Hydro's Reliability and Resource Adequacy Study Analysis Values – Generating Units (%)

Asset Type	Measure	Near-Term Analysis Value	Resource Planning Analysis Value
Hydraulic: Regulated	DAFOR	3.60	3.03
Hydraulic: Muskrat Falls	DAFOR	2.30	3.03
Thermal	DAUFOP	20.008	20.00
Combustion Turbines			
Happy Valley	DAUFOP	4.65	4.65
Hardwoods and Stephenville	DAUFOP	30.00	30.00
Holyrood	DAUFOP	4.90	4.90

- 7 A three-year, capacity-weighted average was applied to the regulated hydraulic units (Bay d'Espoir
- 8 Facility, Cat Arm Station, Hinds Lake Station, Granite Canal Station, Upper Salmon Station, and Paradise
- 9 River Station) for a near-term analysis, resulting in a DAFOR of 3.60%, while a ten-year, capacity-
- 10 weighted average was applied for use in the long-term resource planning model, resulting in a DAFOR of
- 11 3.03%. The DAFOR value was based on historical data reflective of Hydro's maintenance program over
- the long-term.
- 13 For the Muskrat Falls Facility, the near-term forced outage rate was based on the forced outage rates of
- the units to date, to reflect the possibility of outages early in the lifetime of the Muskrat Falls Facility. In
- the long-term resource planning model, the regulated hydroelectric forced outage rate was used, as it is

⁸ The Holyrood TGS base assumption is 20.00%. The sensitivity assumption is 34.00%. A sensitivity value of 34.00% was chosen to reflect actual performance at the Holyrood TGS for the 2021–2022 winter operating period.



recent filing was the "2024 Resource Adequacy Plan – An Update to the Reliability and Resource Adequacy Study," Newfoundland and Labrador Hydro, rev. August 26, 2024 (originally filed July 9, 2024), ("2024 Resource Plan").

⁷ Values indicated for Hydro's near-term analysis reflect those used in the 2024 Resource Plan and the "Reliability and Resource Adequacy Study Review – 2024 Near-Term Reliability Report – November Report," Newfoundland and Labrador Hydro, November 20, 2024 ("November 2024 Near-Term Report").

- 1 assumed that these assets will be maintained to the same standards as the remainder of the hydraulic
- 2 fleet.

- 3 Historically, forced outage rates for the three units at the Holyrood TGS have been reported using the
- 4 DAFOR metric, which is predominately used for units that operate in a continuous (base-loaded)
- 5 capacity. As presented in Hydro's RRA Study 2022 Update, 9 there are reliability concerns associated with
- 6 the operation of the units at the Holyrood TGS in an emergency standby capacity. When considering
- 7 standby or peaking operations of units at the Holyrood TGS, DAFOR is no longer the most appropriate
 - measure of forced outage rates; instead, UFOP¹⁰ and DAUFOP should be considered. Given the
- 9 frequency of deratings historically experienced by these units, DAUFOP is a more appropriate measure.
- 10 Analyses performed for a range of Holyrood TGS DAUFOP assumptions indicate the sensitivity of supply
- adequacy to changes in the availability of the Holyrood TGS. From this analysis, a forced outage rate of
- 12 20.00% was recommended in the near-term, with a sensitivity value of 34.00%. Hydro will continue to
- analyze the operational data to ensure that forced outage rate assumptions for the Holyrood TGS are
- 14 appropriate.
- 15 At present time, the operation of the units at the Holyrood TGS remains base-loaded to ensure the
- 16 availability of capacity for the power system, as the LIL is recently commissioned and in the early
- operational stages. This will remain the case as Hydro continues to monitor LIL performance and
- 18 reliability. If the LIL is found to perform well for an extended period, and system conditions permit,
- 19 Hydro will have the opportunity to incrementally remove the Holyrood TGS units from service. To
- 20 ensure alignment with the assumptions used in the resource planning model (PLEXOS)¹¹ while
- 21 appropriately reporting on current period versus historical performance, Hydro will continue to use the
- 22 DAFOR performance measure and the 20.00% forced outage rate for the units at the Holyrood TGS.
- 23 As the combustion turbines in the existing fleet vary in age and condition, each was considered on an
- 24 individual basis. For the Happy Valley Gas Turbine, a three-year, capacity-weighted average was applied
- to the unit for the near-term analysis while a ten-year capacity-weighted average was applied for use in

¹¹ The resource planning model does not differentiate between DAFOR and DAUFOP metrics; rather, it applies a forced outage rate only.



⁹ "Reliability and Resource Adequacy Study – 2022 Update," Newfoundland and Labrador Hydro, October 3, 2022 ("RRA Study 2022 Update").

¹⁰ Utilization forced outage probability ("UFOP").

- 1 the resource planning model. The DAUFOP values were based on historical data to reflect the unit's past
- 2 performance. For the Holyrood Combustion Turbine ("Holyrood CT") the DAUFOP was calculated based
- 3 on a scenario-based approach rather than historical data, due to the unit's minimal operating time and
- 4 resultant small data set. For the Hardwoods and Stephenville Gas Turbines, a fixed DAUFOP consistent
- 5 with values considered in Hydro's previous near-term reliability reports was used for the near-term and
- 6 long-term analyses. 12 As presented in Hydro's 2024 Resource Plan, the Hardwoods and Stephenville Gas
- 7 Turbines are proposed for retirement in 2030.
- 8 Now that the LIL is commissioned, multiple years of operational experience are required to better
- 9 inform the long-term selection of a bipole forced outage rate. In the interim, the bipole forced outage
- 10 rate will be addressed with a range of upper and lower limits as additional scenarios in the analysis -
- 11 currently 10% and 1%, respectively. As LIL performance statistics become available in the coming years,
- 12 the forced outage rate range may be narrowed. However, the current base-case assumption is a 5% LIL
- 13 forced outage rate.

14

Table 2: Hydro's Reliability and Resource Adequacy Study Analysis Values – LIL (%)

Asset Type	Measure	Base Planning Analysis Value	Range of Planning Analysis Values
LIL	EqFOR	5	1–10

3.0 Current Period Overview

- 15 Table 3 presents an overview of the current period performance, compared to previous period
- 16 performance and most recent Planning Analysis values.

Table 3: DAFOR and DAUFOP Overview (%)

Asset Type	Measure	1-Oct-2023 to 30-Sep-2024	1-Oct-2024 to 30-Sep-2025	Near-Term Planning Analysis Value	Resource Planning Analysis Value
Hydraulic: Regulated	DAFOR	2.17	0.49	3.60	3.03
Hydraulic: Muskrat Falls Facility	DAFOR	0.48	2.92	2.30	3.03

¹² "Reliability and Resource Adequacy Study Review – 2024 Near-Term Reliability Report – November Report," Newfoundland and Labrador Hydro, November 20, 2024.



Thermal	DAFOR/DAUFOP ¹³	47.78	28.86	20.00	20.00	
Combustion Turbines						
Happy Valley	DAUFOP	7.07	8.38	4.65	4.65	
Hardwoods/Stephenville	DAUFOP	51.19	2.25	30.00	30.00	
Holyrood	DAUFOP	0.00	15.88	4.90	4.90	

- 1 As shown in Table 3, regulated hydraulic DAFOR and thermal DAFOR performance improved for the
- 2 current period, while the Muskrat Falls Facility DAFOR performance declined for the current period,
- 3 when compared to the previous period.
- 4 The DAUFOP performance for the Hardwoods and Stephenville Gas Turbines have improved for the
- 5 current period, while the Happy Valley Gas Turbine and Holyrood CT have declined in the current period,
- 6 compared to the previous period.
- 7 Table 4 presents LIL data for the current and the previous period. Since the previous filing, the
- 8 performance of the LIL has improved, with no significant impacts to the EqFOR because of any
- 9 operational events that have occurred.

Table 4: EqFOR Overview (%)

		1-Oct-2023 to	1-Oct-2024 to	Base Planning Analysis	Range of Planning Analysis
Asset Type	Measure	30-Sep-2024	30-Sep-2025	Value	Values
LIL	EgFOR	3.28	0.7614	5	1-10

4.0 Hydraulic Unit DAFOR Performance – Regulated Hydro

- Detailed results for the current period and the previous period are presented in Table 5 and Chart 1.
- 12 These results are compared to Hydro's near-term and resource planning analysis values for forced
- 13 outage rates, as used in the 2024 Resource Plan and the November 2024 Near-Term Report. Any
- 14 individual unit with forced outage rates which exceed the established near-term and/or resource
- planning analysis values is discussed herein.

¹⁴ This EqFOR is calculated on a base LIL capacity of 700 MW. On a base capacity of 900 MW, the EqFOR is calculated to be approximately 1.06%. Following the completion of the 900 MW test, all calculations will be adjusted to reflect the change in assumptions.



¹³ The resource planning model does not differentiate between DAFOR and DAUFOP; rather, it requires the selection of a forced outage rate percentage.

Table 5: Hydraulic Weighted DAFOR – Regulated Hydro

Generating Unit	Maximum Continuous Unit Rating (MW)	12 Months Ended Sep 2024 (%)	12 Months Ended Sep 2025 (%)	Near-Term Analysis Value (%)	Resource Planning Analysis Value (%)
All Hydraulic Units – Weighted	954.4	2.17	0.49	3.60	3.03
Hydraulic Units					
BDE Unit 1	76.5	0.00	0.00	3.60	3.03
BDE Unit 2	76.5	0.00	0.00	3.60	3.03
BDE Unit 3	76.5	2.64	0.00	3.60	3.03
BDE Unit 4	76.5	0.13	0.48	3.60	3.03
BDE Unit 5	76.5	3.83	0.00	3.60	3.03
BDE Unit 6	76.5	9.55	0.00	3.60	3.03
BDE Unit 7	154.4	3.87	0.00	3.60	3.03
CAT Unit 1	67	1.06	0.02	3.60	3.03
CAT Unit 2	67	0.07	0.00	3.60	3.03
HLK Unit	75	0.94	1.42	3.60	3.03
USL Unit	84	1.37	0.84	3.60	3.03
GCL Unit	40	1.88	5.60	3.60	3.03
PRV Unit	8	7.73	3.38	3.60	3.03



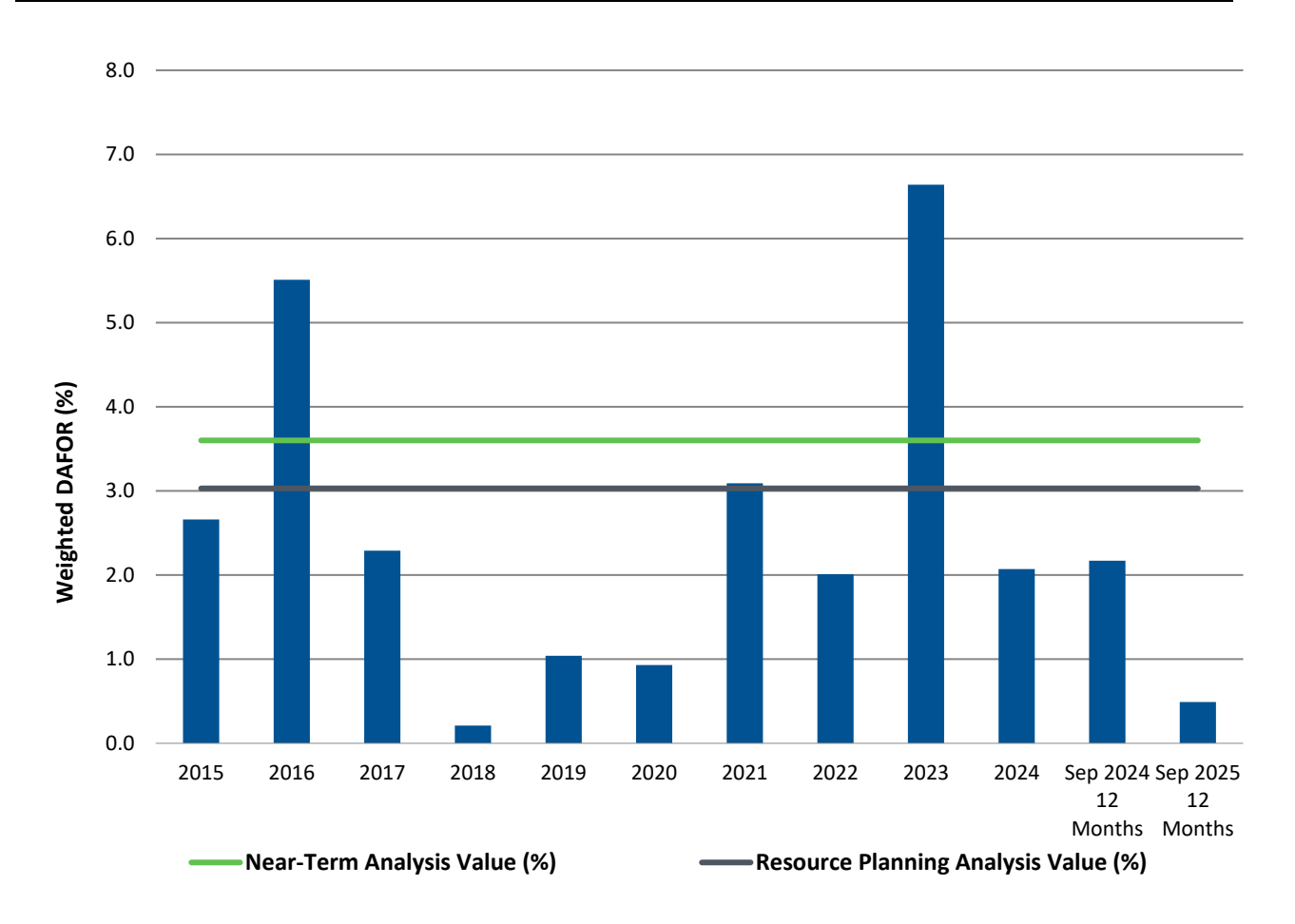


Chart 1: Hydraulic Weighted DAFOR - Regulated Hydro

4.1 Granite Canal Facility

- 2 The Granite Canal unit DAFOR of 5.60% for the current period is above the resource planning analysis
- 3 value of 3.03% and the near-term planning analysis value of 3.60% for an individual hydraulic unit. This
- 4 increase in DAFOR is the result of eleven forced outages in the current period, including four that
- 5 occurred since the previous filing.
- 6 Since the previous filing, an outage was required on August 11, 2025 to address communications issues
- 7 at the Granite Canal Facility. This outage lasted less than two hours. On September 11, 2025 the unit
- 8 tripped due to vibration while operating in the hydraulic rough zone. On September 17, 2025 the unit
- 9 experienced issues during start-up associated with a cooling water valve resulting in a forced outage. On
- 10 September 19, 2025 the unit tripped while shutting down, and subsequent investigation revealed a
- 11 loose wire on the shear pin circuit.



4.2 Paradise River Facility

- 2 The Paradise River unit DAFOR of 3.38% is above the resource planning analysis value of 3.03% but is
- 3 below the near-term planning analysis value of 3.60% for an individual hydraulic unit. Although above
- 4 the resource planning analysis value, this is an improvement in performance over the previous period.
- 5 The elevated DAFOR was the result of four forced outages in the current period, including one that
- 6 occurred since the previous filing.
- 7 Since the previous filing, an outage was required from September 9 to 11, 2025 after inadvertent
- 8 operation of the generator deluge system. The generator was thoroughly dried and returned to service
- 9 without issue.

1

10

5.0 Hydraulic Unit DAFOR Performance – Muskrat Falls

- Detailed results for the current period and the previous period are presented in Table 6 and Chart 2.
- 12 These results are compared to Hydro's near-term and resource planning analysis values for forced
- outage rates, as used in the 2024 Resource Plan and the November 2024 Near-Term Report. Overall, the
- 14 plant performance for the Muskrat Falls Facility shows a decline over the previous period. Any individual
- unit with performance not meeting the established near-term and resource planning analysis values are
- 16 discussed below.

Table 6: Hydraulic Weighted DAFOR – Muskrat Falls

	Maximum Continuous	12 Months Ended	12 Months Ended	Near-Term Analysis	Resource Planning
	Unit Rating	Sep 2024	Sep 2025	Value	Analysis Value
Generating Unit	(MW)	(%)	(%)	(%)	(%)
Muskrat Falls Units - weighted	824	0.48	2.92	2.30	3.03
Muskrat Falls Units					
Muskrat Falls 1	206	1.29	6.24	2.30	3.03
Muskrat Falls 2	206	0.52	4.11	2.30	3.03
Muskrat Falls 3	206	0.10	2.52	2.30	3.03
Muskrat Falls 4	206	0.03	0.00	2.30	3.03



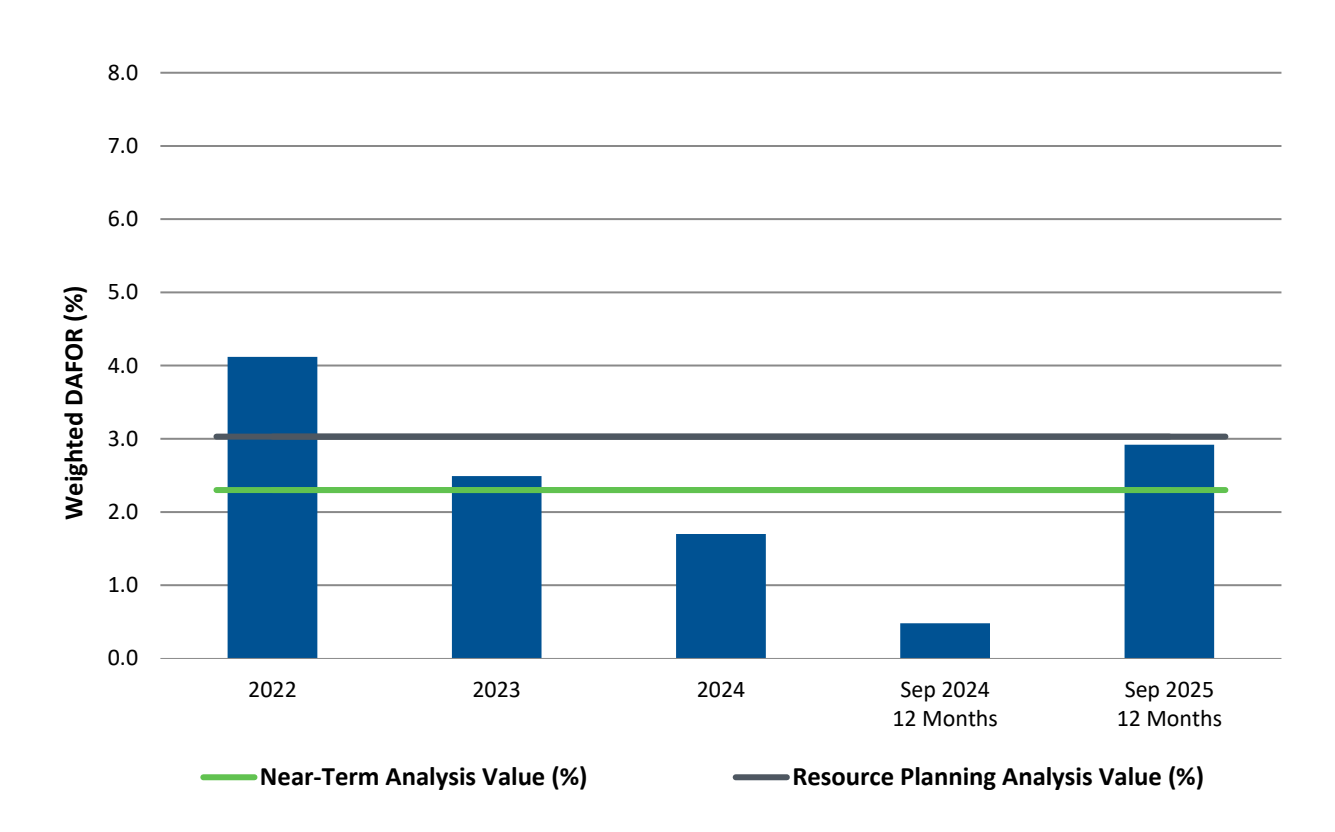


Chart 2: Hydraulic Weighted DAFOR – Muskrat Falls

1 5.1 Muskrat Falls Unit 1

- 2 The Muskrat Falls Unit 1 DAFOR of 6.24% is above the resource planning analysis value of 3.03% and the
- 3 near-term planning analysis value of 2.30% for an individual Muskrat Falls unit. As previously reported,
- 4 the elevated DAFOR was the result of two forced outages in the current period, which have been
- 5 resolved with the exception of final repair outstanding. ¹⁵ No new outages have occurred since the
- 6 previous filing.

7

5.2 Muskrat Falls Unit 2

- 8 The Muskrat Falls Unit 2 DAFOR of 4.11% is above the resource planning analysis value of 3.03% and the
- 9 near-term planning analysis value of 2.30% for an individual Muskrat Falls unit. Muskrat Falls Unit 2 was
- taken offline on a planned outage for major turbine repairs on October 16, 2024, and was unavailable
- for most of 2025 due to this work. The unit returned to service in August of 2025 and experienced a
- 12 brief forced outage on September 7, 2025. Due to the minimal operating time of the unit in the current

¹⁵ Final repairs to the intake civil works as a result of concrete which had dislodged from the intake and travelled through the unit are planned during the Unit 1 annual outage in 2026.



- 1 period, this one outage elevated the DAFOR mathematically. As the unit continues to accumulate
- 2 operating hours in the coming months, the DAFOR is anticipated to normalize.

3 5.3 Muskrat Falls Unit 3

- 4 The Muskrat Falls Unit 3 DAFOR of 2.52% is below the resource planning analysis value of 3.03% but is
- 5 above the near-term planning analysis value of 2.30% for an individual Muskrat Falls unit. This elevated
- 6 DAFOR is the result of three forced outages in the current period, two of which were less than 24 hours
- 7 in duration. The first, a unit trip on February 21, 2025 caused by an unseated PLC card in the Governor
- 8 Cabinet lasted approximately 12 hours. The second outage, caused by a water passage low pressure trip
- 9 on June 30, 2025, occurred as the Operator was draining the piezometer panel and lasted approximately
- 10 1.5 hours. The third outage, which was the largest impact to current period performance, occurred on
- August 26, 2025 as a result of suspected excessive shaft seal leakage, and continued until the start of the
- 12 annual outage on September 3, 2025. The annual outage was completed on September 30, 2025, with
- 13 no abnormal findings on the shaft seal, and the unit returned to normal operation. Investigation is
- ongoing as to the cause of the shaft seal low pressure anomaly that initiated the forced outage.

6.0 Thermal Unit DAFOR Performance

Detailed results for the current and previous periods are presented in Table 7 and Chart 3. These results are compared to Hydro's near-term and resource planning analysis values for forced outage rates, as used in the 2024 Resource Plan and the November 2024 Near-Term Report. Any individual unit with forced outage rates which exceed the established near-term and/or resource planning analysis values is discussed herein.

Table 7: Thermal Weighted DAFOR

Generating Unit	Maximum Continuous Unit Rating (MW)	12 months Ended Sep 2024 (%)	12 months Ended Sep 2025 (%)	Near-Term Planning and Resource Planning Analysis Value (%)
All Thermal Units – Weighted	490	47.78	28.86	20.00
Thermal Units				
Holyrood TGS Unit 1	170	11.13	68.32	20.00
Holyrood TGS Unit 2	170	95.54	9.84	20.00
Holyrood TGS Unit 3	150	19.24	3.67	20.00



15

16

17

18

19

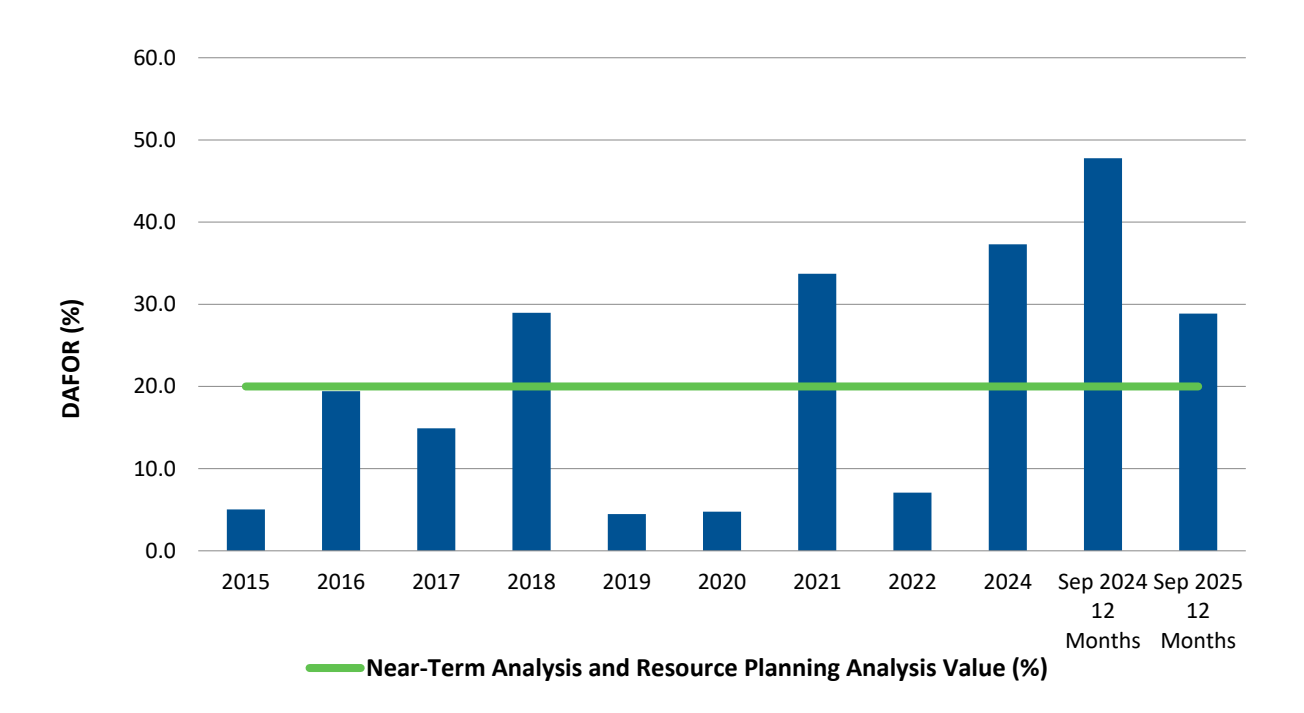


Chart 3: Thermal DAFOR

- 1 For the current period, the weighted DAFOR for all thermal units of 28.86% is above the 20.00% near-
- 2 term and resource planning analysis values. The individual unit DAFOR outcome for the current period
- 3 of 9.84% for Unit 2 and 3.67% for Unit 3 at the Holyrood TGS are below the 20.00% analysis value. The
- 4 performance of Unit 1 at the Holyrood TGS is discussed in Section 6.1.

6.1 Holyrood TGS Unit 1

5

6

7

8

9

10

11

12

13

14

Considering individual thermal unit performance, the DAFOR of 68.32% for Unit 1 at the Holyrood TGS is above the near-term and resource planning analysis value of 20.00% for a unit at the Holyrood TGS, and shows a decline in performance over the previous period. This elevated DAFOR is the result of a forced extension to the planned unit outage to overhaul the Unit 1 turbine and replace the L-0 and L-1 blades at the General Electric ("GE") shop in the United States. ¹⁶ The blades were replaced; however, it was found that additional work was required to restore the bearing journals, which resulted in extension to the outage. All work was completed and the rotor was shipped back to Holyrood site in late 2024. Startup activities in January 2025 were delayed due to issues found with the turbine stop valve, which were resolved and the unit brought online on February 12, 2025. Following return to service, an issue with the

¹⁶ "2024 Capital Budget Application," Newfoundland and Labrador Hydro, rev. September 21, 2023 (originally filed July 12, 2023), sch. 6, prog. 2.



- 1 main steam controls valves prevented movement beyond 56% opening, which resulted in a forced
- derating to 105 MW. This derating remained until March 10, 2025, when a planned outage was taken to
- 3 investigate and correct the issue with the control valves. The unit returned to operation on
- 4 March 17, 2025 at full capacity.
- 5 Holyrood Unit 1 entered the annual planned outage on May 4, 2025 and returned to operation on
- 6 September 18, 2025. Since returning to service the unit has experienced issues with the main steam
- 7 control valves, similar to the issues earlier in 2025, restricting the unit to 100 MW. Hydro is currently
- 8 working with the turbine contractor to develop a plan to remedy the control valve issues. Unit 1 will
- 9 remain online, derated to 100 MW, until that time.

7.0 Combustion Turbine DAUFOP Performance

- 11 DAUFOP Performance for the Hardwoods, Stephenville and Happy Valley Gas Turbines as well as the
- 12 Holyrood Combustion Turbine for the period are presented in the charts and tables below.
- 13 The combined DAUFOP for the Hardwoods and Stephenville Gas Turbines was 2.25% for the current
- period, as shown in Table 8 and Chart 4. This is below the near-term and resource planning analysis
- 15 value of 30.00%.

- 16 The Stephenville Gas Turbine DAUFOP for the current period is 4.39%, which is below the near-term and
- 17 resourcing planning assumption of 30.00%. The Hardwoods Gas Turbine DAUFOP for the current period
- is 0.41%, which is below the near-term and resource planning assumption of 30.00%.



Table 8: Hardwoods/Stephenville Gas Turbine DAUFOP

	Maximum	12 months	12 months	Near-Term Planning and Resource
	Continuous	Ended	Ended	Planning
	Unit Rating	Sep 2024	Sep 2025	Analysis Value
Gas Turbine Units	(MW)	(%)	(%)	(%)
Gas Turbines	100	51.19	2.25	30.00
Ctanhanvilla	F0	00.53	4.20	20.00
Stephenville	50	98.52	4.39	30.00
Hardwoods	50	0.00	0.41	30.00

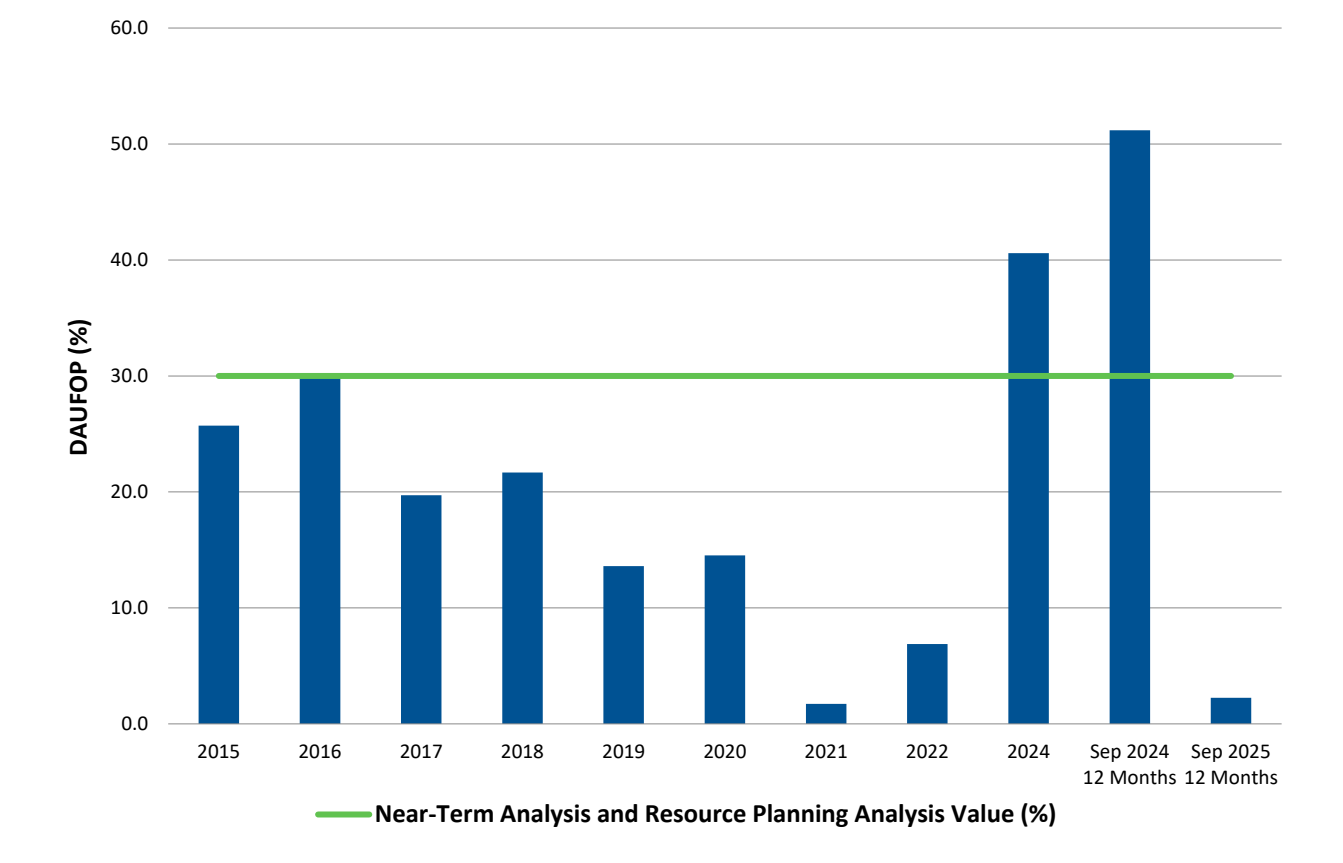


Chart 4: Gas Turbine DAUFOP: Hardwoods/Stephenville Units

- 1 The DAUFOP for the Happy Valley Gas Turbine was 8.38% for the current period, as shown in Table 9
- 2 and Chart 5. This is above the near-term and resource planning analysis value of 4.65% and indicates a
- 3 decline in performance over the previous period. As the forced outage rate for the Happy Valley Gas



- 1 Turbine exceeds the established near-term and resource planning analysis values, a discussion on same
- 2 is included in Section 7.1.

Table 9: Happy Valley Gas Turbine DAUFOP

Gas Turbine Unit	Maximum Continuous Unit Rating (MW)	12 months Ended Sep 2024 (%)	12 months Ended Sep 2025 (%)	Near-Term Planning and Resource Planning Analysis Value (%)
Happy Valley	25	7.07	8.38	4.65

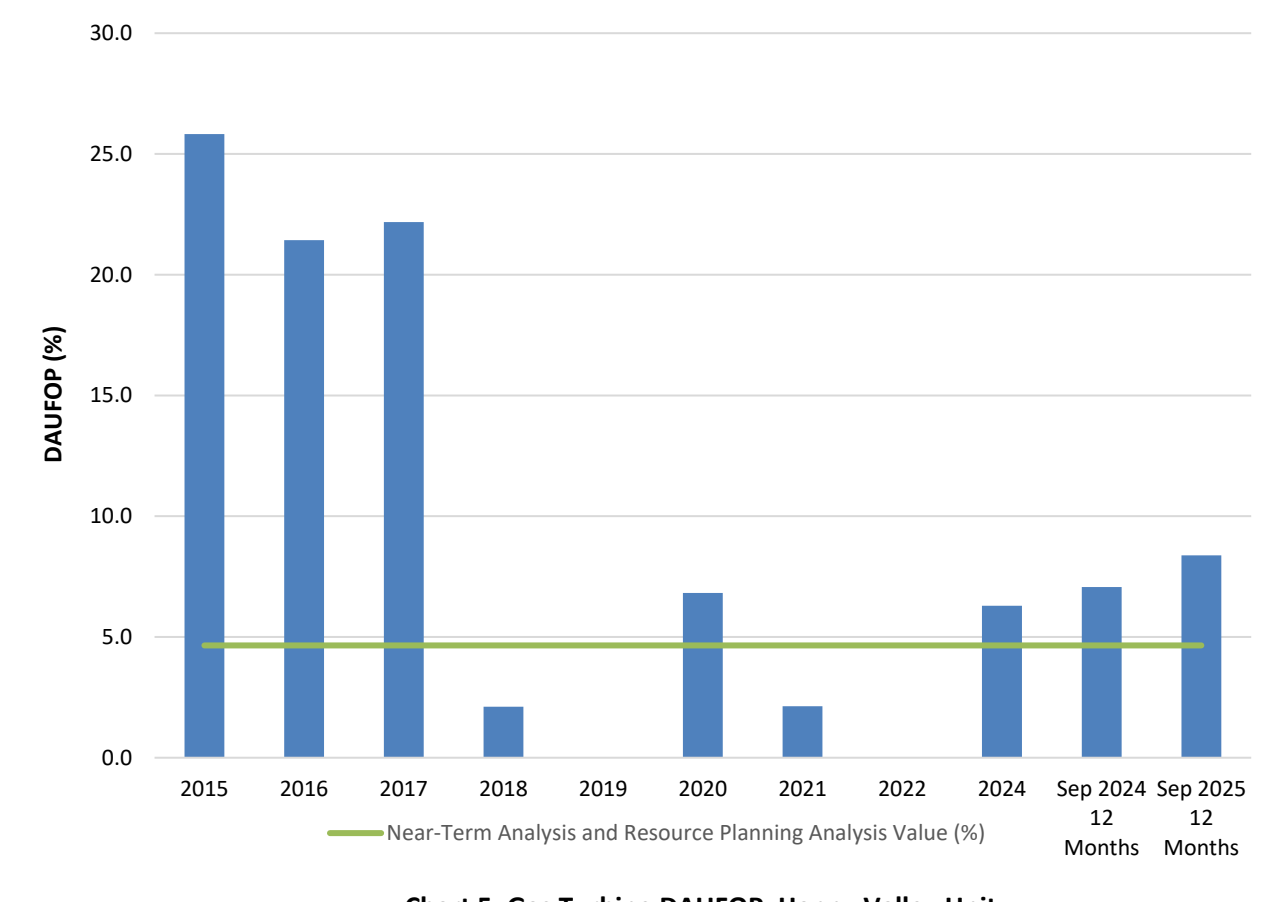


Chart 5: Gas Turbine DAUFOP: Happy Valley Unit

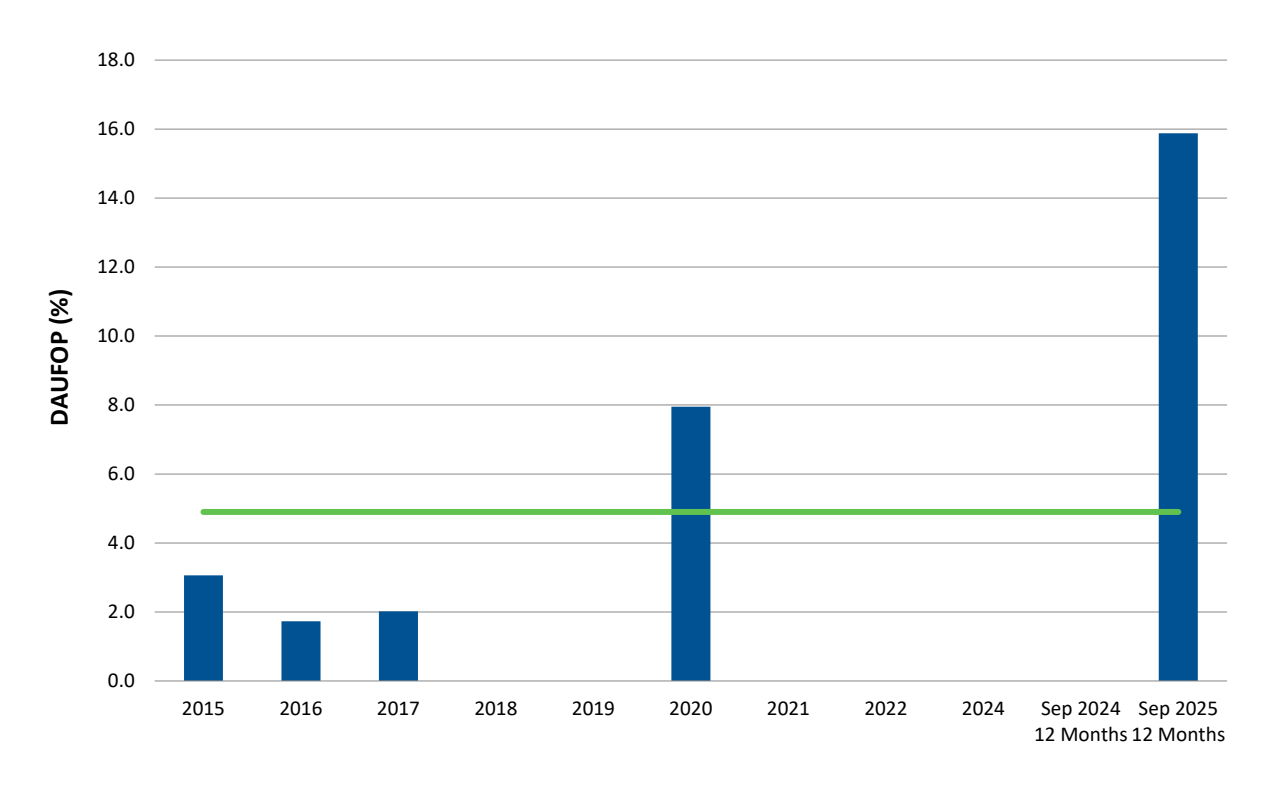
- 3 The Holyrood Combustion Turbine DAUFOP of 15.88% for the current period is above the near-term and
- 4 resource planning analysis value of 4.90%, and indicates a decline in performance when compared to
- 5 the previous period, as show in Table 10 and Chart 6. As the forced outage rate for the Holyrood CT



- 1 exceeds the established near-term and resource planning analysis values, a discussion on same is
- 2 included in Section 7.2.

Table 10: Holyrood Combustion Turbine DAUFOP

Combustion Turbine Unit	Maximum Continuous Unit Rating (MW)	12 Months Ended Sep 2024 (%)	12 Months Ended Sep 2025 (%)	Near-Term Planning and Resource Planning Analysis Value (%)
Holyrood	123.5	0.00	15.88	4.90



——Near-Term Analysis and Resource Planning Analysis Value (%)

Chart 6: Combustion Turbine DAUFOP- Holyrood Unit

7.1 Happy Valley Gas Turbine

- 4 The Happy Valley Gas Turbine DAUFOP was 8.38% for the current period, which is above the near-term
- 5 and resource planning analysis value of 4.65%. This decline in performance is a result of outages
- 6 experienced on July 12, 2025. During start-up, the unit experienced two starting failures which resulted



- 1 in approximately four hours of outage time. Due to the low percentage of operating time experienced
- 2 by the Happy Valley unit, forced outages have significant impact on the DAUFOP performance.

7.2 Holyrood Combustion Turbine

- 4 The Holyrood CT DAUFOP was 15.88% for the current period, which is above the near-term and resource
- 5 planning analysis value of 4.90%. This decline in performance is the result of two forced outages as
- 6 previously reported, and one outage which occurred since the previous filing. As previously reported,
- 7 the unit was unavailable from February 12–14, 2025 and February 25–26, 2025. Since the previous filing,
- 8 the unit experienced a brief outage following a starting failure on August 12, 2025 which lasted less than
- 9 one hour.

10

8.0 Labrador-Island Link EqFOR Performance

- 11 The EqFOR for the LIL was 0.76%¹⁷ for the current period, as shown in Table 11. This is below the range
- of values used by Hydro in the resource planning analysis scenarios.

Table 11: LIL EqFOR (%)

		12 Months Ended Sep 2024	12 Months Ended Sep 2025	Base Planning Analysis	Range of Planning Analysis
Asset Type	Measure	(%)	· (%)	Value	Values
LIL	EaFOR	3.28	0.76	5	1-10

- 13 The availability of the three Soldiers Pond synchronous condensers ("SC") is critical to the reliable
- delivery of electricity to the Island Interconnected System via the LIL. No operational issues concerning
- 15 the Soldiers Pond SCs resulted in outages or derating to the LIL in the current period.
- A fulsome update on the total number of hours of operation for the Soldiers Pond SCs for the rolling 12-
- month period is provided in in Appendix A of this report.

¹⁷ This EqFOR is calculated on a base LIL capacity of 700 MW. On a base capacity of 900 MW, the EqFOR is calculated to be approximately 1.06%. Following the completion of the 900 MW test, all calculations will be adjusted to reflect the change in assumptions.



_

Appendix A

Soldiers Pond Synchronous Condensers



Table A-1: Quarterly Rolling 12-Month Operating Hours for Soldiers Pond Synchronous Condensers ("SC")

Unit	Operating Hours ¹	% Availability ²		
SC1	8708.57	99.41		
SC2	8302.68	94.78		
SC3	7553.72	86.23		

Further information on the operation of the Soldiers Pond SC is provided in Appendix B.

¹ Hydro has provided its best estimate of operating hours for each unit for the 12 months ended September 30, 2025 based on an assumption of 24/7 operation of all three SCs, and known outages (both planned and unplanned) recorded in its database. ⁵ SC availability is calculated on the basis of the unit's operating hours, and therefore assumes that the unit is operating when available.



Appendix B

Muskrat Falls Assets Update

Reporting period up to September 30, 2025



Contents

1.0	Introduction				
2.0	Muskrat Falls Hydroelectric Generating Facility				
2.1	Capital Projects				
3.0	Soldiers Pond Synchronous Condensers	2			
3.1	Operations Items	2			
4.0	Labrador-Island Link	3			
4.1	Operations Items	3			
4.2	Capital Projects	5			
4.3	High-Power Testing	(
4.4	Software	7			
4.5	Engineering Studies and Reports	7			
4.6	Ongoing Investigations	8			
4.7	Restoration Plans and Operational Strategy	8			
5.0	Conclusion	c			

List of Attachments

Attachment 1: L3501 Failure Investigation – Ice Storm Central Labrador – January 2025



1.0 Introduction

1

- 2 The Muskrat Falls Assets, made up of the LIL, the Labrador Transmission Assets including the Soldiers
- 3 Pond Synchronous Condensers ("SC"), and Muskrat Falls have all been commissioned in recent years and
- 4 are in the early years of their asset lifespan.
- 5 As is normal for the early operation of assets, Newfoundland Labrador Hydro ("Hydro") has encountered
- 6 some challenges with equipment due to manufacturing issues or defective components. Such issues are
- 7 expected early in the equipment's life. Equipment failure rates plotted over time generally exhibit a
- 8 'bathtub-shaped curve.' Incidents of failure tend to be high when equipment is new and again near the
- 9 end of the equipment's useful life, depending on equipment type. In addition to routine ongoing
- 10 preventative maintenance activities and sustaining capital programs for each of these assets, there are a
- 11 number of one-off capital projects, corrective maintenance activities and engineering studies ongoing
- 12 with the purpose of addressing and repairing these early life issues, with the ultimate goal of improving
- asset reliability over time to expected levels.
- 14 Hydro provides the following update to the Board of Commissioners of Public Utilities ("Board") on the
- status of these activities and other information as requested by the Board.

16 2.0 Muskrat Falls Hydroelectric Generating Facility

- 17 Muskrat Falls was commissioned in November 2021. The Muskrat Falls plant continues to outperform
- similar units across Canada with a total plant derated adjusted forced outage rate performance through
- 19 the end of the second quarter of 2025 was significantly better than the Electricity Canada average of
- 20 5.27%.

21

2.1 Capital Projects

- 22 Muskrat Falls Repair Unit 2 Turbine
- 23 As recommended by the original equipment manufacturer ("OEM") and reported by The Liberty
- 24 Consulting Group in its June 2023 monitoring report, vibration issues observed on Unit 2 required
- 25 permanent corrective action, including full unit dismantling, to be completed under warranty by the
- turbine OEM. There have been no issues with vibration, or the identification of other characteristics
- 27 through internal inspections, which would indicate a problem similar to that of Unit 2 on Units 1, 3, or 4.



- 1 As a result, Unit 2 was offline through the 2024–2025 winter season and was placed back online on
- 2 September 3, 2025. The issue is resolved and the unit is operating normally.

3.0 Soldiers Pond Synchronous Condensers

- 4 Hydro continues to address the remaining items that were noted in punch list reports submitted with
- 5 the commissioning certificate and outstanding warranty claims.

6 **3.1 Operations Items**

- 7 Brush Gear
- 8 Brush equipment performance on the Soldiers Pond SCs decreased in December 2023, resulting in
- 9 several scheduled outages to replace damaged brushes, springs and brush holders.
- 10 Hydro, in consultation with the OEMs for the brush equipment and the synchronous condensers, has
- 11 been working to identify the root cause of the brush performance issues. Hydro has continued with the
- 12 modified brush configurations and operational controls to ensure optimal operating conditions for
- 13 patina development. These changes have had positive results with regards to brush performance in
- 14 2025.
- 15 In spring 2024, the existing slip ring was removed from synchronous condenser 1 and sent for machining
- to correct a runout causing excessive brush vibration. At this time, a modified brush with the ability to
- 17 operate in a higher vibration environment was also provided by the OEM and installed. These
- 18 modifications have resulted in improved performance to date. Hydro will continue to monitor the
- 19 overall impact of these changes.
- 20 General Electric ("GE") has been working with a different brushgear manufacturer; however, given the
- 21 positive brush gear performance in 2025, both GE and Hydro recommended not changing the design at
- 22 this time. As performance of a new brush and holder is unknown until they are installed and tested, the
- 23 recommendation is to continue to operate under the existing design. GE has provided Hydro with
- 24 operational limits based on the number of brushes installed per ring to help maintain patina film.
- 25 Corrective actions on all three units have yielded positive results, and changes performed in 2024 have
- aided in achieving acceptable brush performance across all three synchronous condensers.



1 Forced Outages

- 2 Outside of planned outages, the Soldiers Pond SCs have been in operation at all times during the
- 3 quarter.

4 4.0 Labrador-Island Link

- 5 Since commissioning in April 2023, the Labrador Island Link ("LIL") has been in service and successfully
- 6 providing power to the provincial grid. During the quarter, the LIL has been operating at various power
- 7 transfer levels, as required by the system. In total, approximately 699 GWh were delivered over the LIL
- 8 from July 1, 2025 to September 30, 2025. Hydro continues to ensure the availability of generation at the
- 9 Holyrood Thermal Generating Station ("Holyrood TGS"); however, energy and capacity delivered over
- the LIL are used to minimize thermal generation whenever possible.
- 11 In the early stages of its operation, as is normal for the operation of assets early in life, the current
- reliability of the LIL is anticipated to be lower than in the long-term, due to failures associated with new
- assets (e.g., due to manufacturing issues or defective components). In addition to routine ongoing
- 14 corrective and preventative maintenance activities and sustaining capital programs, there are a number
- of capital projects identified to repair these issues.

16 **4.1 Operations Items**

17 Forced Outages

- 18 During the third quarter of 2025, there was one trip event on the LIL which occurred on
- 19 September 20, 2025. Pole 2 tripped while in monopole mode as a result of an electrode imbalance
- 20 protection following a temporary fault. Pole 1 was on a planned maintenance outage at this time.
- 21 Impacted customers were returned to service within an hour. The faulted pole was returned to service
- 22 on September 21, 2025 following an inspection that confirmed no issues. Outage follow-up actions
- 23 include review of protection settings improvements, which is ongoing.



1 Cable Switching

- 2 As reported in Hydro's final 2024–2025 Winter Readiness Report, 1 new equipment was successfully
- 3 installed to mitigate cable switching transients at the LIL Transition Compounds in mid-October 2024.
- 4 Since the Winter Readiness Report, Hydro has identified an icing issue with transition compound
- 5 disconnects that can impact cable switching in winter conditions. Hydro continues to work with GE to
- 6 engineer a solution to resolve this issue. In the interim, Hydro is developing operating procedures to
- 7 ensure reliable operation in winter conditions.

8 Replacement of Direct Current Current Transformers ("DCCT")

- 9 In 2023, the OEM and Hydro determined that very low air temperatures at Muskrat Falls Converter
- 10 Station were influencing the measurement accuracy of DCCTs, resulting in false protection trips and
- power control issues on the LIL. The OEM identified the root cause of the issue to be a manufacturing
- defect with the Delay Coil Fiber Optical Cable located within the DCCTs; this issue occurred with a select
- 13 batch of fiber optic cables, affecting six DCCTs at the Muskrat Falls HVdc Converter Station, which have
- 14 since been replaced.²
- 15 Hydro will continue to work with GE, the OEM, to ensure proper mitigation of the issue. GE has
- 16 identified a manufacturing facility to replenish spare DCCTs, and Hydro will be actively involved in the
- 17 design and testing process to ensure that the new units meet operational requirements.
- 18 In addition, GE is preparing a revised plan to address DCCTs which have low risk indicators of the issues
- 19 related to cold weather operation. GE has indicated that the plan will be provided in the fourth quarter
- 20 of 2025. Hydro will continue to work with the OEM to ensure proper mitigation of the issue.

21 Conductor Testing

- 22 Following a bipole trip on March 30, 2024, line patrol determined that the electrode conductor was
- 23 broken and damaged during an ice storm at several locations in Southern Labrador. As a result,
- 24 conductor testing was completed and determined no material issues with the conductor, and found that
- 25 the failure was due to overload, which is consistent with past findings. There is evidence that cyclic

² One of these DCCTs has an operation rating to -40°C and will be replaced with a DCCT rated to -50°C in 2025.



¹ Reliability and Resource Adequacy Study Review – 2024–2025 Winter Readiness Planning Report – Final Report," Newfoundland and Labrador Hydro, December 10, 2024.

- 1 loading due to ice and wind on the conductor may be causing fatigue and could contribute to the failure.
- 2 This was consistent with previous testing results. Additional conductor testing has been completed,
- 3 which has been provided in Attachment 1 to this report and determined that there were no significant
- 4 new findings.

5

4.2 Capital Projects

- 6 Replace Turnbuckles and Install Airflow Spoilers Program
- 7 With regard to the Turnbuckles Replacement and Airflow Spoiler Installation Program, Hydro continues
- 8 to actively address the recommendations resulting from the localized failures experienced on the LIL
- 9 over the past three winters. Hydro's capital programs to replace turnbuckles and install airflow spoilers
- 10 intended to reduce galloping are ongoing, prioritizing the high-priority areas of the LIL first.
- 11 At the end of 2024, Hydro had completed 100% of the planned replacements of turnbuckles for that
- 12 year, and as of the end of September 2025, 100% of air spoilers have now been installed.³
- 13 **Optimizing Clamp Designs**
- 14 Hydro has identified, through its preventative maintenance program and component failure
- 15 investigations, multiple opportunities for clamp and conductor inspection, with refurbishment or
- 16 replacement of parts made according to findings. As a result, Hydro has optimized clamp designs for the
- 17 electrode conductor and optical ground wires ("OPGW").
- 18 Three alternative suspension clamp designs have been installed on the electrode conductor at ten
- 19 structures in critical sections of the line and will be inspected for performance on an annual basis.
- 20 New electrode line suspension assemblies have been designed that will reduce the forces on the tower
- and conductor. These assemblies will be purchased and installed as required.

³ Based on the outcome of its galloping study, Hydro installed airflow spoilers on priority areas of the LIL to control galloping and mitigate further damage to the line. Hydro has mitigated the risk of prolonged customer outage as a result of fatigue failures due to galloping by prioritizing the most remote locations where galloping has been observed.



- 1 An alternate OPGW clamp assembly with improved slip strength was selected, ordered and received in
- 2 January 2025. The clamp will be installed in additional locations along the line as required. As the OPGW
- 3 relates to communications functionality, Hydro does not anticipate that further occurrences of similar
- 4 damage would result in a prolonged power interruption or customer outage.

5 Top Plate Design

- 6 In December 2022 there were two incidents impacting two adjacent structures of the LIL where the
- 7 connection of the top plate of the OPGW suspension detached from the tower, falling onto the cross
- 8 arm. As a result, Hydro has completed the reinforcement of the top plate on all 61 A3 type towers.
- 9 The design of the top plate reinforcement is complete for all required tower types, and alternate designs
- 10 have been received from the consultant. There are two A4 towers that require top plate reinforcement;
- tower reinforcement will be purchased and installed as required. Installation work to replace the two
- 12 remaining top plates is expected to begin in 2026 with expected completion in 2028. ⁴ To date, there
- have been minimal issues with other tower types. Hydro will keep the alternate design in stock as a
- 14 precaution and will schedule installation on other tower types as required if deformation of the top
- 15 plate occurs.

16 *Ice Monitoring*

- 17 In response to icing experienced on the LIL, Hydro has undertaken capital projects in 2025 for the
- installation of a real-time weather station, as well as the installation of on-line ice and galloping
- 19 monitoring equipment. In-line monitoring equipment has been installed in all three locations.

20 4.3 High-Power Testing

- 21 As previously reported, Hydro is planning to conduct the 900 MW test in late 2025. While Hydro
- 22 continues to plan for execution of the high-power test in the fourth quarter of 2025, this
- 23 timing is subject to system conditions. The high-power test may be deferred as a result of Hydro's

⁵ "Reliability and Resource Adequacy Study Review – Labrador-Island Link Update for the Quarter Ended September 30, 2025, Newfoundland and Labrador Hydro, October 3, 2025.



⁴ Analysis confirmed that 63 towers across two tower types (A3 and A4) were identified to have top plates replaced; the two remaining top plates are on A4 tower types.

- 1 prioritization of reliable service to customers during the winter period, including supporting reservoir
- 2 levels to meet peak load requirements.
- 3 Subject to the completion of high-power testing, the LIL will be able to be operated up to 900 MW as
- 4 system conditions permit. As previously reported, the following are prerequisite conditions for the test
- 5 to occur:

8

9

21

- Satisfactory system conditions are present, including both those in Newfoundland and Labrador,
 where a high system load can be reasonably expected to occur, and neighbouring jurisdictions;
 - Successful coordination with all relevant neighbouring system operators is attained; and
 - Identification of risks and implementation of all necessary risk mitigation actions are in place.

10 **4.4 Software**

- 11 New LIL software was commissioned in October 2024. This software, as with the previous version,
- 12 allows for full operation of the LIL up to 900 MW. Through dynamic commissioning, non-critical
- 13 software-related issues were identified. Hydro continues to work with GE on the development of a
- 14 version of software to resolve these issues, and installation is anticipated once Factory Acceptance
- 15 Testing is completed and system conditions allow. A version of software was already delivered by GE,
- and an attempt was made to install it in April of 2025; however, a version control error prevented full
- installation, and the software had to be removed. The new version of the software is expected to be
- delivered in the fourth quarter of this year; however, due to system constraints within the
- 19 Newfoundland and Labrador Interconnected System as well as neighbouring provinces, software
- 20 installation is planned for spring 2026.

4.5 Engineering Studies and Reports

- 22 Since its commissioning in April 2023, Hydro has gained valuable insight into LIL operations. Using
- 23 Hydro's operating experience and recommendations from its investigations, supplemented by the
- 24 recommendations made by Haldar and Associates Inc., Hydro has identified three potential
- 25 reinforcements to LIL assets to sustain reliability, address common failure modes, and mitigate risks to
- the Island Interconnected System. While these potential reinforcements have been identified, further
- engineering assessment is required to determine the benefits, costs, schedule, and feasibility of these
- 28 modifications. These include:



- Review of unbalanced ice loads for the entire line length to determine appropriate design unbalanced ice loading, followed by design and cost estimates for tower design modifications to meet unbalanced design loads;
 - Feasibility assessment and cost estimates for installation of mid-span structures to reduce tower loading in critical areas; and
 - Engineering design and cost estimates to relocate electrode conductors from towers to wood
 poles in some sections, to reduce tower loading, improve access and logistics, and minimize
 outages to address electrode line issues in critical areas.
- These assessments, designs and cost estimates have now been completed, and Hydro will evaluate
 these projects based on their anticipated reliability benefits and their estimated cost through the fourth
 quarter of 2025 to determine next steps. Hydro will provide a report to the Board once complete.

4.6 Ongoing Investigations

1

2

3

4

5

6

7

8

12

16

17

18 19

20

21

22

23

24

25

26

Investigations are completed for incidents related to the Muskrat Falls Assets as required, and the results are reviewed and finalized by Hydro. Hydro has provided the investigation report and material testing outcome for the January 2025 electrode conductor investigation as Attachment 1 to this report.

4.7 Restoration Plans and Operational Strategy

In addition to engineering studies to inform potential reinforcements to mitigate the risk of component failures and outages, Hydro is currently in the process of contracting a consultant to review Hydro's restoration plans, including review and development of specific restoration plans for a variety of potential and previously experienced scenarios. It is expected that this review will include the identification of alternative restoration approaches that can be selected based on the situation for the most efficient and effective execution of the work. Restoration plans will consider geographic and weather challenges. Restoration plan reviews will include estimates of the time to effect the repairs, as well as time challenges and opportunities for restoration duration and provide cost and benefit information to identify incremental investment in restoration time improvement and quantify the associated benefits.



₁ 5.0 Conclusion

- 2 Hydro recognizes the criticality of the Muskrat Falls Assets to the supply of the Island Interconnected
- 3 System, which helps to limit the thermal generation required from the Holyrood TGS and impacts the
- 4 overall reliability of the grid will continue to monitor the performance of these assets address early life
- 5 incidents such as those due to manufacturing issues or defective components.



Attachment 1

L3501 Failure Investigation

Ice Storm Central Labrador – January 2025



L3501 Failure Investigation

Ice Storm Central Labrador

January 2025

ILK-EG-ED-6200-TL-H15-0010-01



L3501 Failure Investigation – Ice Storm Central Labrador – January 2025

Revision				Remarks		
No	Ву	Rev.	Chk.	Appr.	Date	
1	RM	00	MV	KR	Oct 30, 2025	Issued for Review
2						
3						

Prepared By: Rebecca Manuel

Rebecca Manuel

Checked By: _____ Waria Veitch

Maria Vetich

Digitally signed by **krirogps**Date: 2025.10.31
10:27:24 -02'30'

Kris Rogers



Contents

1.0	Abbreviations and Acronyms	1			
2.0	Introduction				
3.0	Background	1			
4.0	Purpose	3			
5.0	Failure Description	4			
5.1	Location	7			
5.2	Engineering Recommendations for Repairs	9			
5.3	Restoration Summary	. 10			
6.0	Weather Information	. 10			
7.0	Construction Quality and Maintenance Review	. 18			
8.0	Material Testing	. 19			
9.0	Analysis of Loads Causing Failures	. 19			
9.1	Ice Loading	. 20			
9.	1.1 Balanced Ice Loading	. 20			
9.	1.2 Unbalanced Ice Loading	. 22			
10.0	Summary and Conclusions	. 24			
11.0	Recommendations	. 24			

List of Appendices

Appendix A: Maps of Loading Zones (from Overhead Transmission - Meteorological Loading for the Labrador- Island Transmission Link Attachment B.1.

Appendix B: NL Hydro Transmission Line Failure (Conductor EL-1 at Suspension Tower 127) report by Wayland Engineering Ltd.



1.0 Abbreviations and Acronyms

2 DE - Dead end

1

- 3 EL1 Electrode Line 1
- 4 EL2 Electrode Line 2
- 5 HVdc High Voltage direct current
- 6 L3501/2 Line number of the 350 kV HVdc transmission line
- 7 L3501 Pole 1 of the line
- 8 L3502 Pole 2 of the line
- 9 LIL Labrador Island Transmission Link
- 10 OPGW Optical Ground Wire
- 11 P1 Pole 1
- 12 P2 Pole 2
- 13 ROW Right of way

14 2.0 Introduction

- 15 On Monday, January 13, 2025, during a helicopter patrol of the electrode line 1 (EL1), broken conductor
- was identified at Structure 127 (S127). Review of the electrode currents indicate that EL1 open circuited
- 17 at approximately 23:50 on January 11, 2025. The protection activated approximately 55 minutes later at
- 18 00:46 on January 12, when the next scheduled unbalancing occurred. After closer inspection, it was
- identified that the main failure occurred at S127 with cross arm damage between S127 and S130.

20 3.0 Background

- 21 The Labrador-Island Link (LIL) is an important transmission line for the provincial energy grid due to its
- 22 power carrying capacity that is used to deliver a large portion of the winter peak energy and demand to
- the Island Interconnected System. Line L3501/2 is the 350 kV HVdc overland transmission line portion of



- the LIL, traversing a distance of approximately 1,100 km through three major meteorological loading
- 2 zones: average, alpine, and eastern. As shown in Figure 1, the HVdc line has two poles; one OPGW, and
- 3 two electrode conductors. The electrode conductor is attached to the lattice towers for a part of the line
- 4 from Muskrat Falls to approximately 384 km southeast of Muskrat Falls, where it diverts to a separate
- 5 right of way (ROW) on wood pole structures. From there, the electrode line travels to an electrode site
- 6 approximately 16 km away, located in the L'Anse-au-Diable area. There are sections of L3501/2 without
- 7 the electrode on the towers, these structures do not have electrode cross arms.

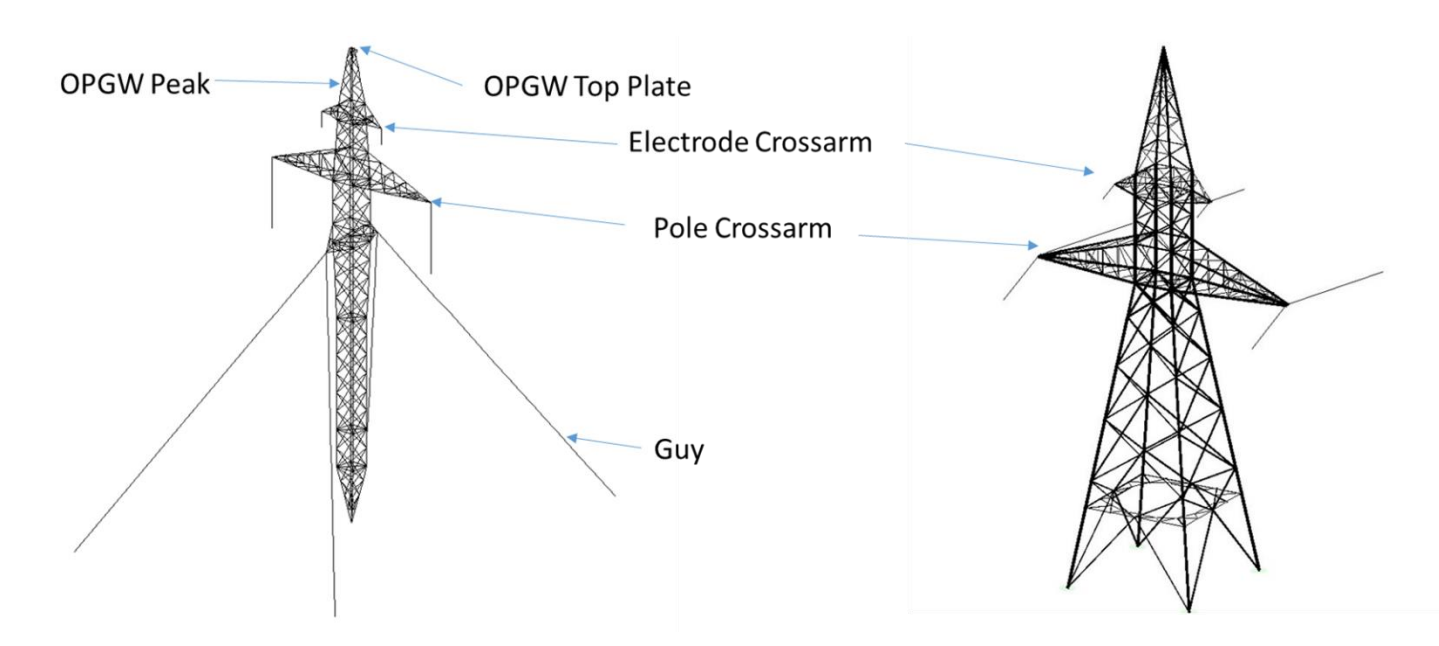


Figure 1: Suspension and Deadend Tower Diagram

- 8 The HVdc transmission line corridor has been divided into three major meteorological loading zones
- 9 referenced above in combination with eight further subcategories related to loads, pollution levels
- 10 (inland and costal), and geographic location. This combination results in 19 separate loading zones.
- 11 Eleven tower types (A1, A2, A3, A4, B1, B2, C1, C2, D1, D2, and E1) were designed to meet the loading
- requirements, which consist of a specified wind load, ice load, and combination of both applied to the
- 13 line. The tower types consist of both guyed towers and self-support towers. The tower types are
- summarized in Table 1 and a depiction of the structure types is shown in Table 1.



Tower Type	Structure Type	Insulator Assembly Type	Deflection Angle Limit (degree)
A1, A2, A3, A4	Guyed	Suspension	0-1
B1	Guyed	Suspension	0-3
B2	Self-Support	Suspension	0-3
C1, C2	Self-Support	Dead End	0-30
D1, D2	Self-Support	Dead End	0-45
E1	Self-Support	Dead End	45-90

Table 1: Tower Types

- 1 Of the total number of towers on L3501/2, ninety percent are suspension towers, types A1, A2, A3, A4,
- 2 B1, and B2. Chart 1 provides a break down of the tower distribution on L3501/2, with suspension
- 3 towers shown in red and dead end towers shown in blue.

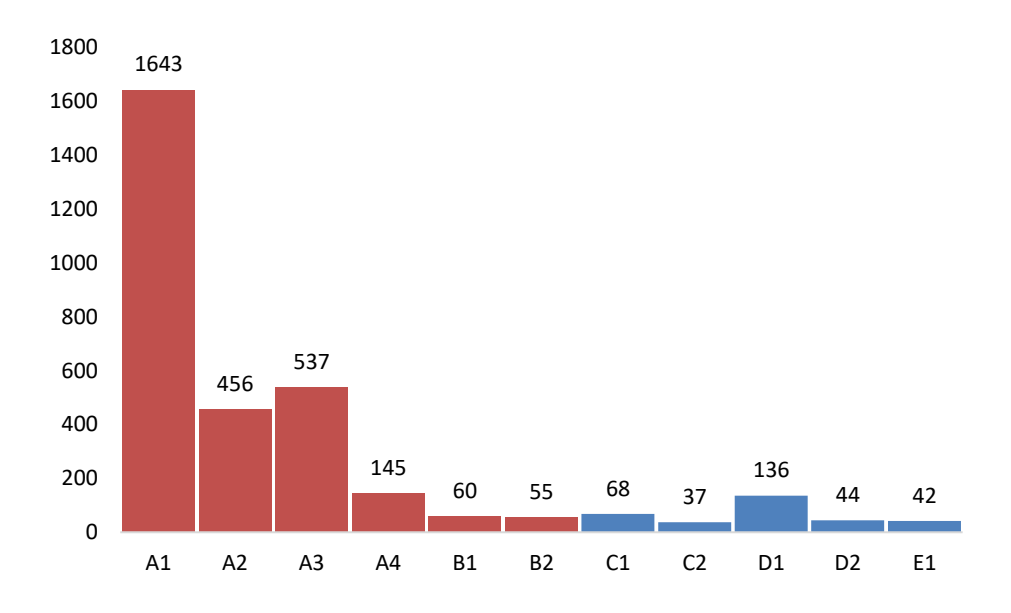


Chart 1: Distribution of Tower Type on L3501/2

4 4.0 Purpose

- 5 Due to the importance of L3501/2 to the provincial energy grid and the need to understand the line's
- 6 performance, a detailed investigation was completed to determine the root cause of the failures, and to
- 7 recommend actions to mitigate further damage to the line.
- 8 The investigation will be described in detail within this report and includes the following components:



- 1 **1)** Failure Description;
- 2 **2)** Weather;
- 3 3) Construction Quality and Maintenance Review;
- 4 4) Material Testing;
- 5 Analysis of Loads Causing Failures.

5.0 Failure Description

- 7 Broken conductor was identified on EL1 during a helicopter patrol on January 13, 2025. The conductor
- 8 was found to have fully broken at the S127 clamp. After closer inspection, cross arm damage was
- 9 identified between S127 and S130. During ice clearing, the peaks of S120 and S121 were damaged, and
- 10 OPGW clamps were pulled between S114 and S131. As a result, an aerial ice removal procedure has
- been developed to provide guidance and mitigate damage caused by ice removal activities. Damage due
- to the weather event is summarized in Table 2 and shown in Figure 3 through Figure 7 below.

Table 2: Summary of Structure and Conductor Damage

Tower	Crossarm I	Damage	Conductor Dama	r Damage
Tower	EL1	EL2	EL1	El2
114	No	No	No	No
115	No	No	No	No
116	No	No	No	No
117	No	No	No	No
118	No	No	No	No
119	No	No	No	No
120	No	No	No	No
121	No	No	No	No
122	No	No	No	No
123	No	No	No	No
124	No	No	No	No
125	No	No	No	No
126	No	No	No	No
127	Yes	No	Yes	No
128	Yes	No	No	No
129	Yes	No	No	No
130	Yes	No	Yes	No
131	No	No	No	No



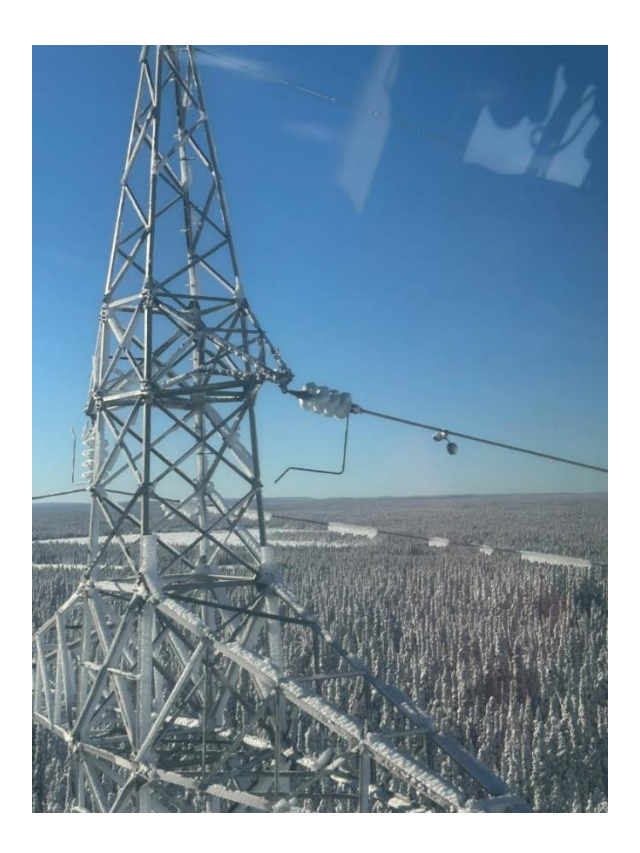


Figure 3: S127 EL1 Cross Arm and Conductor Failure



Figure 4: S128 EL1 Cross Arm Failure





Figure 5: S130 EL1 Cross Arm Failure



Figure 6: S120/121 OPGW Peak Failure due to Ice Removal





Figure 7: Pulled OPGW due to Ice Removal

1 5.1 Location

- 2 Structures are numbered sequentially along the transmission line, starting at Muskrat Falls. Structure
- 3 numbers that sustained damage related to the initial weather event are S127 to S130. Additional
- 4 structure damage from ice removal activities impacted S114 to S131. Damage sustained due to ice
- 5 removal activities were omitted from this investigation report, as the cause of that damage is known.
- 6 The damaged structures are located approximately 46 km south of Happy Valley Goose Bay as shown
- 7 in Figure 8. The structures are located 0.1 to 0.4 km from Highway 510.





Figure 8: Map of Portion of Newfoundland and Labrador Showing Location of Damaged Structures

- 1 The structures that sustained damage are located in Loading Zone 1. Zone 1 is classified as an average
- 2 loading zone in terms of ice, wind and a combination of the two. Figure 9 summarizes the wind and ice
- 3 conditions for which this zone is designed. Attachment B.1. from "Overhead Transmission -
- 4 Meteorological Loading for the Labrador- Island Transmission Link Attachment" can be found in
- 5 Appendix A.



Zone 1, 8b and 10 (see Attachment B.1)

The following load case is to be applied in the location shown in attachment B.1. Please note that this loading is valid for the northern corridor alternative only.

Maximum Ice 50 mm radial glaze, 0.9 g/cm³ density

Maximum Wind 105 km/h (10 minute average wind speed at 10 m height

above ground)

Combined Ice and Wind 25 mm radial glaze, 0.9 g/cm³ density

60 km/h (10 minute average wind speed at 10 m height

above ground)

Maximum wind and combined wind values assume Terrain Type C as per CSA C22.3 NO 60826-10. Any deviation for this terrain type for select locations along the corridor must be included in the HVdc tower design criteria.

Figure 9: Zone 1 Wind and Ice Design Loading¹

- 1 The four structures that sustained steel or conductor damage are all Type A1 tangent towers. The tower
- 2 body extension, and electrode and OPGW attachment heights are summarized in Table 3. All towers had
- 3 a suspension attachment. All structures are within the same dead-end to dead-end section.

Table 3: Damaged Structure Information Summary

	Str.	Str.	Height to Electrode	Height to OPGW
Str. #	Type	Height	Attachment (m)	Attachment (m)
127	A1	A1+12.0	39.97	46.81
128	A1	A1+1.5	29.47	36.31
129	A1	A1+13.5	41.47	48.31
130	A1	A1+6.0	33.97	40.81

4 5.2 Engineering Recommendations for Repairs

5 It was recommended by Hydro Engineering to restore the line to its as-built condition.

CSA 22.3 No. 60826 - Overhead transmission lines - Design criteria



¹ Terrain Type C as defined by CSA 22.3 No. 60826: Terrain with numerous small obstacles of low height (hedges, trees and buildings)

5.3 Restoration Summary

1

18

- 2 Hydro transmission crews were mobilized to site to begin restoration work on January 16, 2025. Snow
- 3 clearing operations were required in order to access the site. Prior to the start of work, construction of
- 4 the bearing pads was required, and backer anchors were installed to secure them. Two wheeled 50 ton
- 5 cranes with fixed baskets were brought to site. A helicopter from Churchill Falls was engaged and
- 6 arrived to site on January 14, 2025 to facilitate patrols and ice removal.
- 7 To restore the transmission line to its original condition, external contractors were engaged to replace
- 8 the OPGW peaks and dampers, assist in the use of implosion sleeves for splicing conductor, and replace
- 9 tower peaks that were damaged during ice removal. Due to a forecasted snow event on
- 10 January 20, 2025 and the projected demand for additional power, external resources were also engaged
- 11 to support the restoration of failed electrode conductor, and the repair and replacement of damaged
- 12 structure components, in order to facilitate the completion of repairs ahead of the storm.
- 13 Repair work began on January 16, 2025, following snow clearing efforts and bearing pad construction.
- 14 The damaged conductor was removed and the connection of new conductor using implosion sleeves
- was completed. Damaged cross arms were replaced on S128 and S130, and repaired on S127 and S129.
- 16 Transmission crews determined that the S125 and S126 crossarms did not require repair or
- 17 replacement. All repair work was completed by January 20, 2025.

6.0 Weather Information

- 19 There were observations of significant icing on the lines on January 13, 2025, as seen in Figure 10. An ice
- 20 sample that fell from EL1 was collected, measured, and weighed. The sample measured approximately
- 21 6"×5"×4.5" and weighed 4 lbs. From this sample, the equivalent radial thickness was estimated to be 50
- 22 75 mm at a density of 0.7 g/cm³. Figure 11 through Figure 14 contain photos of various ice samples
- 23 collected from the event.



Paae 10



Figure 10: Ice conditions at Time of Helicopter Patrol Discovering Damage



Figure 11: Ice Sample from EL1





Figure 12: Ice Sample from EL1



Figure 13: Ice Sample from EL1





Figure 14: Ice Sample from EL1

- 1 Weather data was gathered from the "Goose Bay A" weather station, located as shown in Figure 15.
- 2 Temperature, precipitation, and wind data from the weather station is shown in Figure 16 and Figure 17.
- 3 This station is located approximately 32 km north of the damaged structures. The elevation of the
- 4 weather station is approximately 49 m, and the elevation at the damaged structures ranges from 385.8
- 5 to 406.2 m. The higher elevation of the damaged structures may have exposed them to stronger winds
- 6 and colder temperatures than those recorded at the weather station. Based on the weather data
- 7 available for the Goose Bay A Station, there were no particularly unusual wind or temperature
- 8 conditions experienced immediately before the damage event. However, in the days leading up to the
- 9 event, the temperatures had increased to 3°C, with freezing rain, fog, rain, snow and snow showers. The
- wind during this time ranged from approximately 15 km/h to 52 km/h, with gusts as high as 70 km/h.



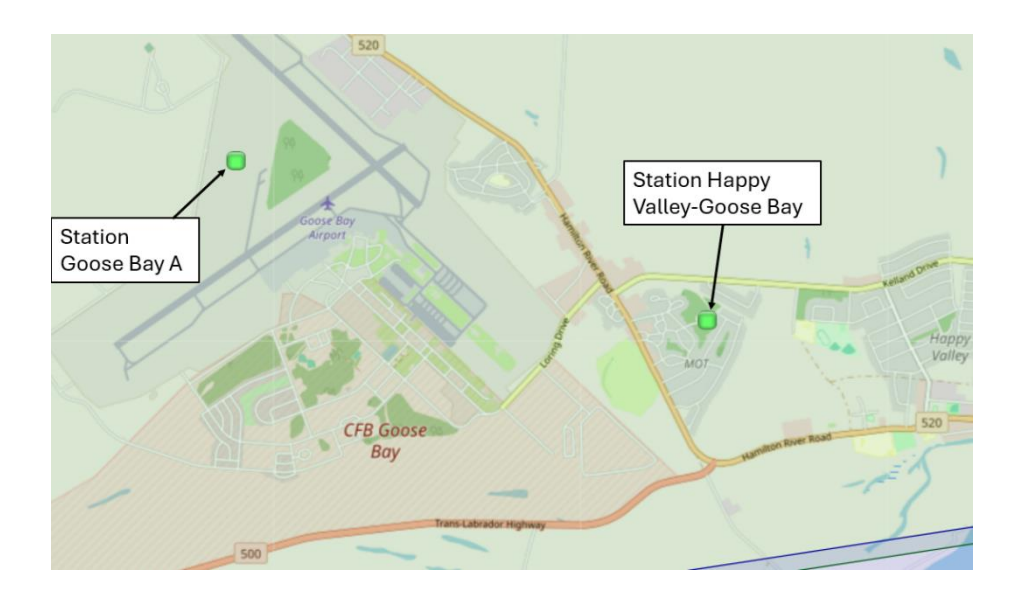


Figure 15: Weather Station Location

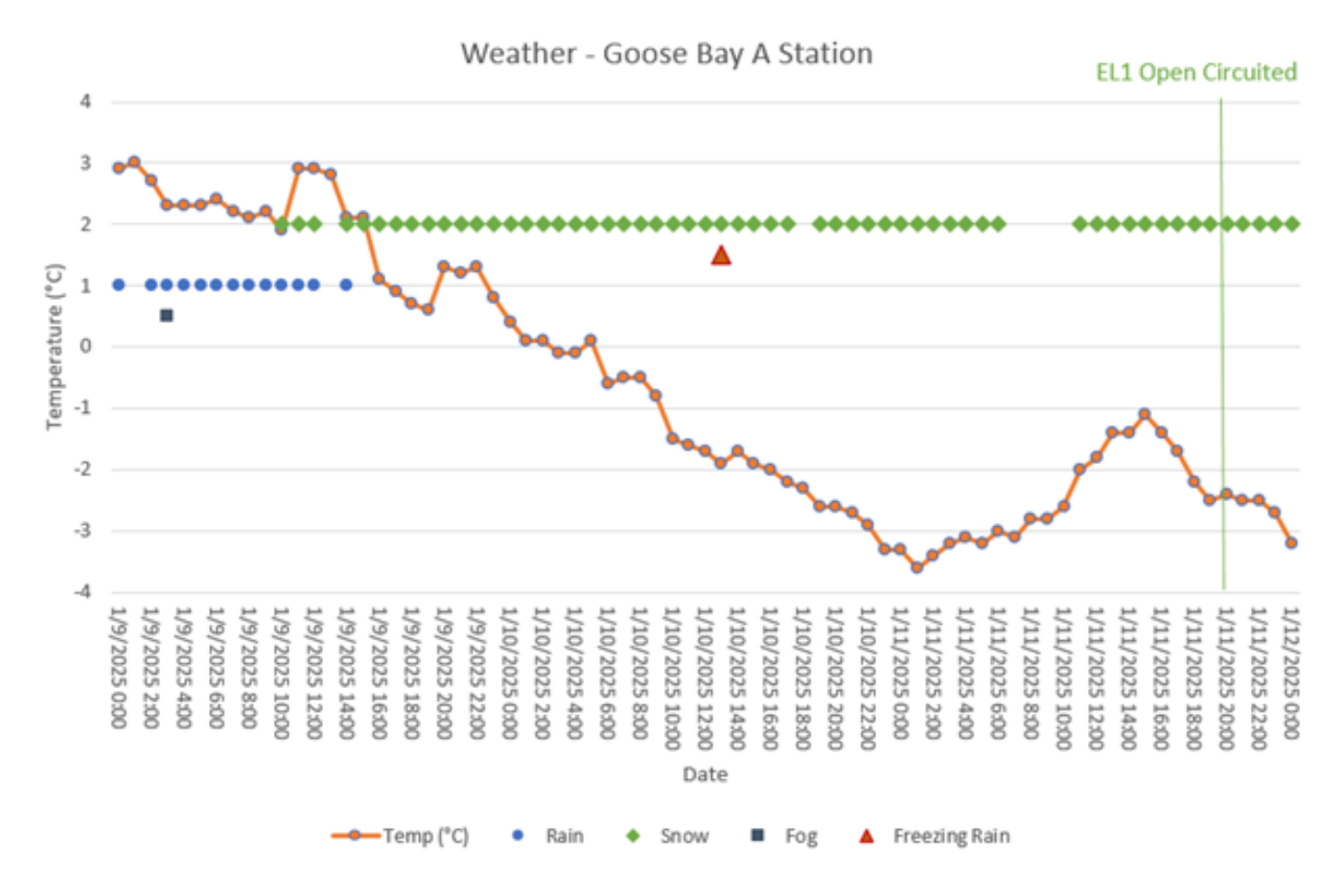


Figure 16: Temperatures and Precipitation Type at Goose Bay A Weather Station



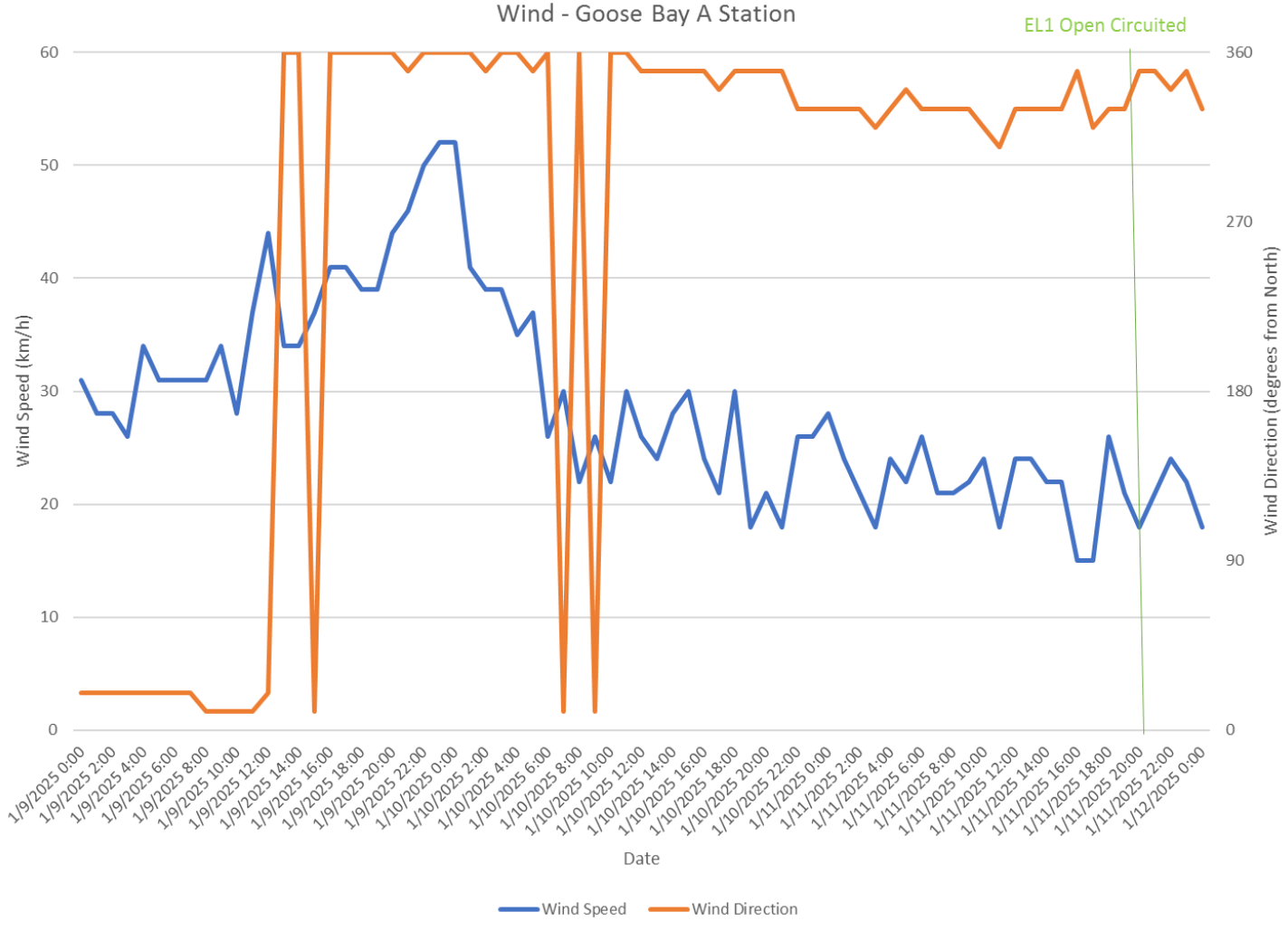


Figure 17: Wind Speed and Direction at Goose Bay A Weather Station

- 1 Following the event, a significant increase in snow and ice accumulation was observed near the location
- 2 of the damaged structures. Refer to Figure 18 and Figure 19 for comparison of the minimal snow and ice
- 3 on the trees near Goose Bay, as compared to the significant snow and ice accumulation near the
- 4 damaged structures.





Figure 18: Accumulation of Ice and Snow on Trees Near Goose Bay

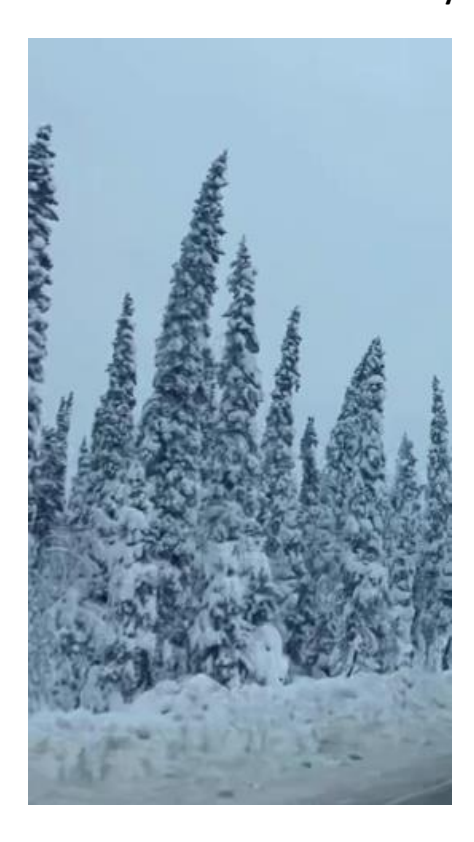


Figure 19: Accumulation of Ice and Snow on Trees Near Damage Site



- 1 Due to this significant change in meteorological conditions, another weather station located in Kenamu
- 2 River was utilized to more accurately determine the conditions at the location of the damaged
- 3 structures leading up to the failure. The location of the Kenamu River station, shown in Figure 20, is
- 4 closer to the site of the damage event and situated at an elevation of 224m.

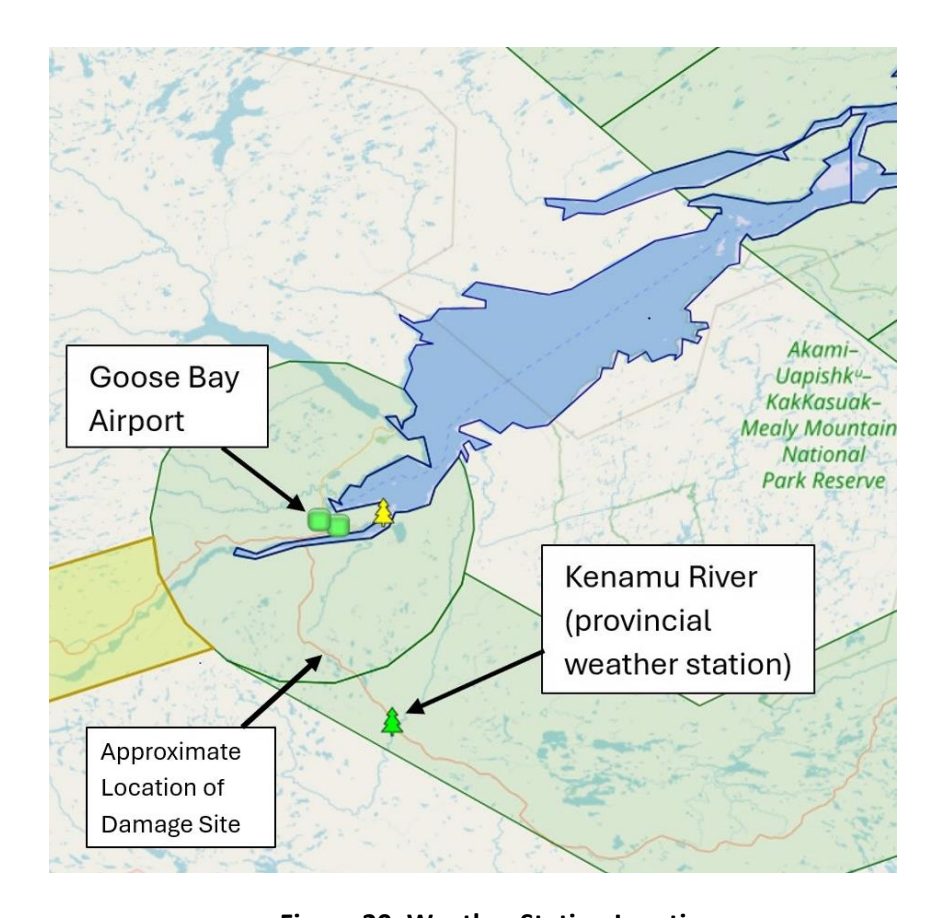


Figure 20: Weather Station Locations

- 5 Weather data was gathered from the Kenamu River provincial weather station for the timeframe of
- 6 January 8 to January 12, 2025. A total of 1.8 mm of precipitation was recorded at the station over
- 7 January 8 and January 9. As a result of the temperature, precipitation likely fell mostly as rain, mixed
- 8 with some snow. No precipitation was recorded between January 9 and January 12. At this point,
- 9 precipitation had likely changed from rain to light snow as a result of temperature, and may not have
- 10 been picked up by the station sensor. The maximum wind gust reported for the event was 73.6 km/h,
- occurring on January 9. Temperatures over the five day period are shown in Table 4. Comparative data
- 12 from Goose Bay A Station and Kenamu River Station show that the Kenamu River site experienced
- 13 temperatures approximately 1–2 °C lower with marginally higher wind gusts, than those observed at
- 14 Goose Bay A.



Table 4: Kenamu River Weather Station Temperatures

Date	Maximum Temperature (Degrees Celsius)	Minimum Temperature (Degrees Celsius)
January 8, 2025	0.8	0.0
January 9, 2025	1.3	-1.2
January 10, 2025	-1.2	-4.9
January 11, 2025	-1.7	-5.2
January 12, 2025	-4.6	-6.2

1 7.0 Construction Quality and Maintenance Review

- 2 The final construction quality control inspection of S127 to S130 was completed in August and
- 3 September 2017. There were six non-conformances noted for the tower steel. These non-conformances
- 4 were for steel deficiencies on the guy cross arms, conductor cross arms, and the mast members, with
- 5 none related to the electrode cross arms. All deficiencies were remediated. The electrode conductor for
- 6 this section of line was strung on January 12, 2016, with no quality control issues noted at that time.
- 7 On the four structures that experienced conductor or tower damage, there were eight previous
- 8 corrective work orders. These work orders included a loose splice plate, damaged dampers (OPGW and
- 9 electrode), and the OPGW pulled through the suspension assembly. The root cause of these issues
- 10 remains unidentified considering further investigation was not warranted as they were isolated
- incidents. Hydro believes that the OPGW pull through is likely caused by unbalanced ice load from ice
- shedding, and that galloping² or Aeolian vibration³ may have been the cause of damper damage.
- 13 Further, it is possible the loose splice plate was a result of an isolated construction error. All work orders
- 14 were remediated, and there is no evidence to suggest these deficiencies contributed to the January
- 15 2025 electrode failure.

³ Aeolian vibration is a high-frequency, low-amplitude oscillation of the overhead power lines that is caused by low-velocity, steady wind.



² Galloping is a high-amplitude, low-frequency oscillation of overhead power lines due to wind; it can be caused by specific wind conditions and is sometimes observed on lines with small amounts of icing.

8.0 Material Testing

1

- 2 Material testing of the electrode conductor was completed by Wayland Engineering Ltd. ("Wayland") to
- 3 determine the cause of failure and any potential issues with the conductor. The summary of conclusions
- 4 and recommendations is included in this section and the complete report can be found in Appendix B.
- 5 Wayland concluded that the physical, chemical and metallurgical evidence indicates that the conductor
- 6 failure is consistent with ductile limit load fracture (i.e. overload) of the aluminum and steel reinforcing
- 7 core wire strands. Tension testing of intact sections of service wire indicated that the ultimate strength
- 8 of the wire was approximately 6% below the specified minimum rated tensile strength for the conductor
- 9 (tested strength was 175 kN, and the minimum rate tension strength is 187 kN); however, diameter
- 10 measurements and tensile testing of individual strands met or exceeded the material strength
- 11 requirements. The 6% is not considered material, as the conductor would have likely failed even if the
- rated tensile strength had met the specification. Wayland concludes that while the decrease in breaking
- 13 strength of the conductor may have contributed to the failure, the primary cause of the failure is likely
- 14 the combination of accumulated ice and wind conditions exceeding the conductors design criteria. It
- was also noted that while galloping has not been historically observed in this area, forces from galloping
- 16 cannot be excluded as a potential additional source of loading on the conductor.
- 17 Wayland recommended that Hydro investigate mechanical and/or thermal means to reduce ice
- 18 accumulation on the transmission lines. Investigation may also be completed to determine why the
- 19 conductor assembly rated strength is reduced while the individual strands meet or exceed
- 20 requirements. Hydro has begun preliminary work to complete the recommended investigations, which
- 21 are complex in nature.

9.0 Analysis of Loads Causing Failures

- 23 Hydro completed analysis of the possible failure loads utilizing an existing PLS-CADD as-built model of
- 24 L3501/2. The model includes the existing terrain and as-built tower locations and heights, with complete
- 25 finite element tower models. PLS-CADD is a transmission line design program that allows the user to
- 26 enter a variety of loading conditions to analyze how they will affect the line and structures under the as-
- 27 built conditions. The program enables users to perform in-depth analysis of how increased loading will
- 28 affect tower performance, ultimately predicting how the towers will fail under extreme loading
- 29 conditions.

22



- 1 Tower failure is defined in the analysis as any component of the tower exceeding its maximum damage
- 2 limit. The reaction of the tower to the load cases can be quantified by the maximum utilization, which is
- 3 the ratio of the force applied to any member from the specified loads divided by the damage limit
- 4 capacity, expressed as a percentage. Any value greater than 100% is considered a tower failure.

$$Maximum\ Utilization = \frac{Force}{Damage\ Limit\ Capacity} \times 100\%$$

6 9.1 Ice Loading

- 7 As discussed in Section 6, there were observations of significant icing on the lines on January 13, 2025.
- 8 An ice sample that fell from EL1 was collected, measured, and weighed. The sample measured
- 9 approximately 6"×5"×4.5" and weighed 4 lbs. From this sample, the equivalent radial thickness was
- estimated to be approximately 58 mm at a density of 0.7 g/cm³. This estimate slightly exceeds the
- design ice load of 50 mm of radial glaze ice with a density of 0.9 g/cm³.
- 12 Modeling of the section of line was completed with both (i) balanced observed ice conditions and with
- 13 (ii) unbalanced observed ice loads. Refer to Section 9.1.1 for discussion of the balanced ice loading
- analysis and section 9.1.2 for results of the unbalanced ice loading analysis.
- 15 Additionally, modelling of the electrode conductor shows that the rated strength of the cable was not
- 16 exceeded during this event. However, the cable tension limits previously selected as per the design
- 17 criteria and CSA-22.3 No 1-10 were exceeded. Those limits were selected to prevent conductor failure
- 18 under extreme weather conditions, as well as the occurrence of excessive plastic stretch when stresses
- are applied to conductors in the range of 80 to 95% of their ultimate tensile strength (UTS). The cable
- 20 limit selected for this particular cable was 60% UTS as per the project design basis. Additionally, CSA-
- 21 22.3 No 1-10 suggests a cable tension limit of around 75% UTS⁴. Modelling of the applied loads from this
- weather event show a 77% UTS utilization of the cables, roughly 2% above the suggested CSA cable
- 23 tension limit.

24 9.1.1 Balanced Ice Loading

- 25 The balanced load cases place 40 to 140 mm of radial ice with a density of 0.7 g/cm³ on the conductors.
- lce modeling was completed with the thickness of the pole conductor ice reduced by 70%, due to ice

⁴ The cable tension limit is a value selected for how close the conductor can approach its UTS under the expected loading conditions. The Hydro design basis adopts a more conservative approach than what is suggested in CSA-22.3 No. 1-10.



Page 20

- 1 accretion modeling and in-field experience that have proven there is less ice accretion on the larger
- 2 diameter conductor(s).
- 3 Balanced modelling showed failures on S127 at the electrode cross arms starting at 80 mm of radial ice.
- 4 This result is above the in-field observations for this particular icing event. Table 5 shows the comparison
- of the structure damaged in the field to the structures above 100% utilization in the model based on
- 6 balanced loading conditions.
- 7 Figure 21 and Figure 22 show the model results under various radial ice thicknesses for balanced loading
- 8 conditions for S127. The results indicate that the balanced ice loads would have to be higher than what
- 9 was observed in order to induce failure at S127.

Table 5: Comparison of Field Damage and Modeling Results for Balanced Ice Loading

	Field Damage		Modelling 70mm	Modeling 80 mm	Modeling 90 mm	
	Crossarm	n Damage	EL Crossarm Damage	EL Crossarm Damage	EL Crossarm Damage	
Tower	EL1	EL2	(% Utilization)	(% Utilization)	(% Utilization)	
127	Yes	No	97	117	140	
128	Yes	No	91	110	132	
129	Yes	No	79	97	116	
130	Yes	No	79	97	117	

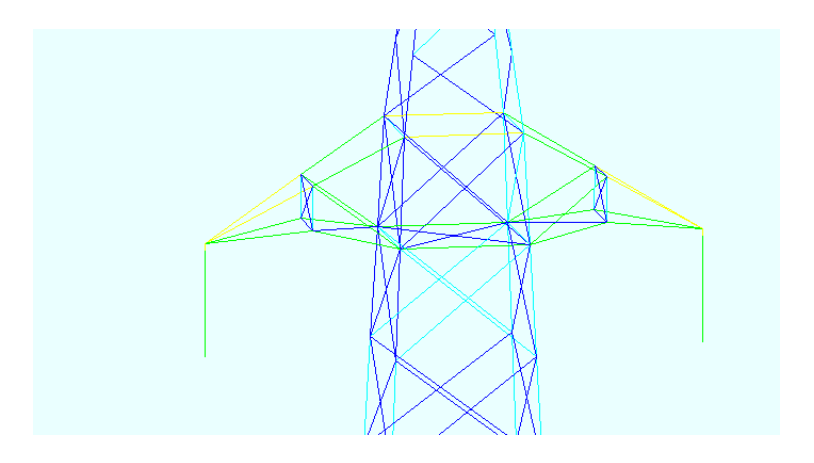


Figure 21: Model of S127 with 70mm of Balanced Radial Ice - No Failures



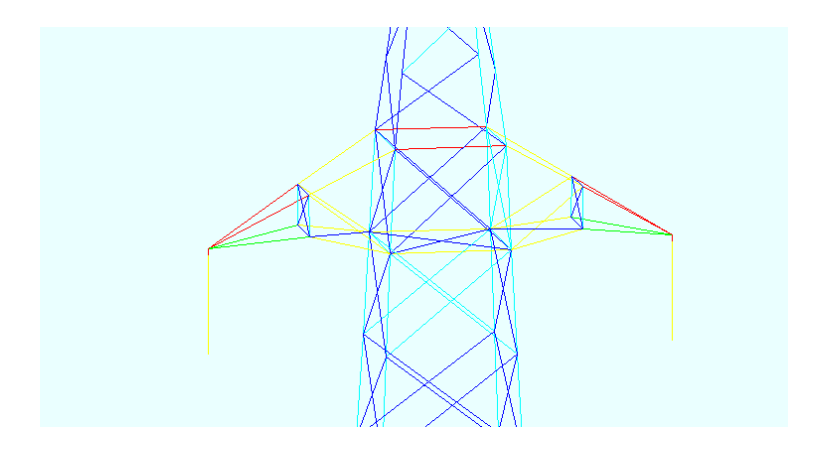


Figure 22: Model of S127 with 80mm of Balanced Radial Ice – Electrode Cross Arm Failures

1 9.1.2 Unbalanced Ice Loading

- 2 Modelling of the line was completed with 100% of the ice on the back span and values between 30-
- 3 100% ice on the front span (or vice versa). This was completed utilizing maximum ice thicknesses of 58
- 4 mm at a density of 0.7 g/cm³, and resulted in failure of the OPGW wire at 60% and below, and failure of
- 5 all cables at 40% and below. As the percentage of ice on the adjacent span decreases, the loading
- 6 becomes more unbalanced, resulting in failures. Table 6 shows the comparison of the structure
- 7 damaged in the field to the structures above 100% utilization in the model based on unbalanced loading
- 8 conditions. From this exercise it was determined that ice of 58 mm radial thickness with an unbalanced
- 9 load of 100/40% could produce the cross arm damage observed, as shown in Figure 23 and Figure 24.

Table 6: Comparison of Field Damage and Modeling Results for Unbalanced Ice Loading

	Field Damage		Field Damage Modelling 100/50%		Modeling 100/30%	
Tower	Crossar EL1	rm Damage EL2	EL Crossarm Damage (% Utilization)	EL Crossarm Damage (% Utilization)	EL Crossarm Damage (% Utilization)	
127	Yes	No	95	114	131	
128	Yes	No	95	113	130	
129	Yes	No	94	112	129	
130	Yes	No	94	112	129	



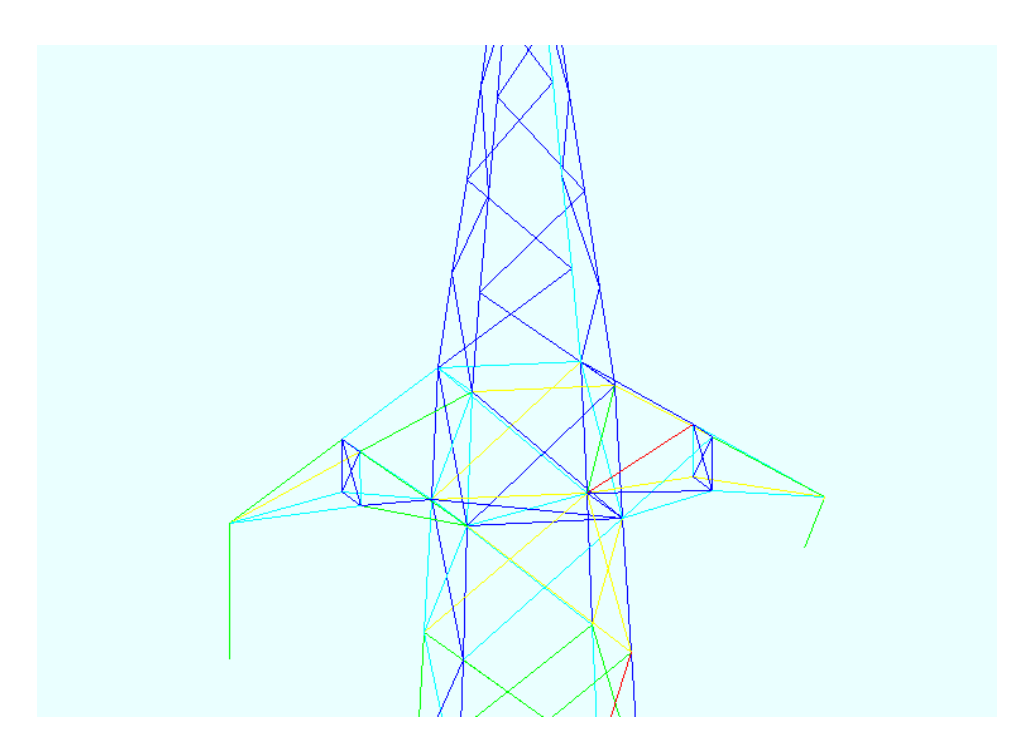


Figure 23: Model of S127 Unbalanced Ice Load Case Showing Failed Members in the Electrode Crossarm Exceeding Capacity at 100/40% Unbalanced Loading

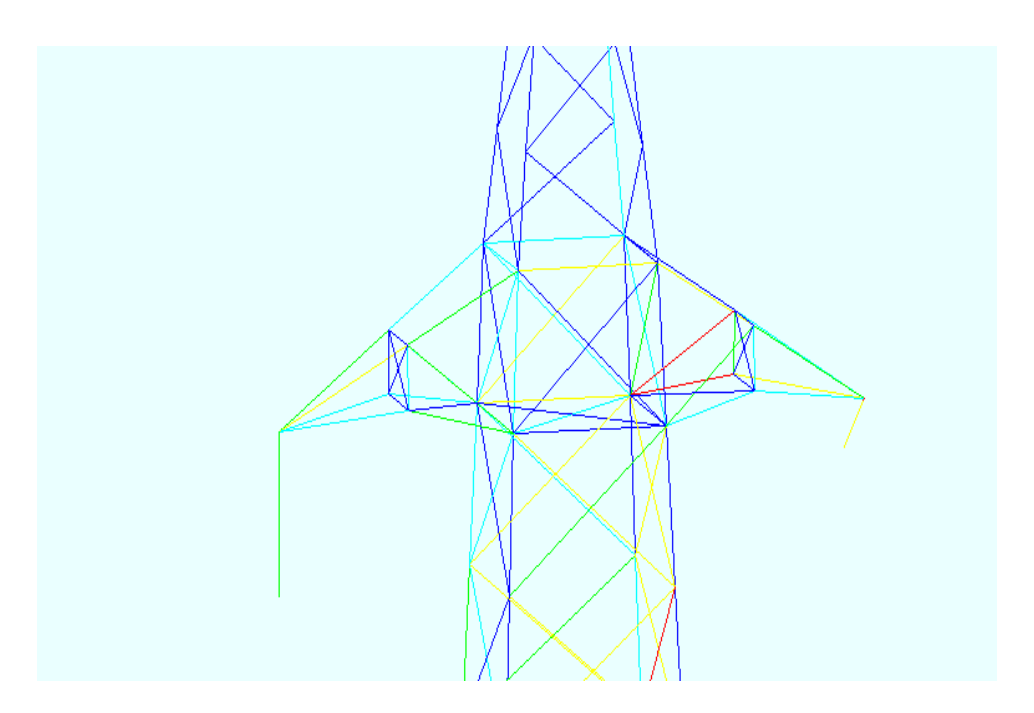


Figure 24: Model of S127 Unbalanced Ice Load Case Showing Failed Members in the Electrode Crossarm Exceeding Capacity at 100/30% Unbalanced Loading



10.0 Summary and Conclusions

1

- 2 The primary cause of the damage to the electrode crossarms and the electrode conductor was overload
- 3 failure due to ice loads exceeding the design for this section of the line.
- 4 Ice loads in the area at the time of the failure were estimated to be approximately 58 mm of radial glaze
- 5 ice with a density of 0.7 g/cm³. This estimate slightly exceeds the design loads of this section of the line,
- 6 which is 50 mm of radial glaze ice with a density of 0.9 g/cm³.
- 7 Modelling of the electrode conductor shows that the rated strength of the cable was not exceeded
- 8 during this event. While the cable limits were exceeded, tension was estimated to be approximately
- 9 77%, which is less than the 80-95% which can result in potential excessive plastic stretch.
- 10 Modeling shows the damage to the electrode crossarms could be caused by ice loading greater than 80
- mm to 90 mm of balanced radial ice with a density of 0.7 g/cm³. This is higher than the observed ice field
- conditions, and therefore unlikely to be the cause of the failure in this instance.
- 13 Modelling was also completed for unbalanced loading and showed that 58 mm of radial ice thickness
- 14 with an unbalanced load of 100/40% could produce the Electrode Line damage observed. Therefore, ice
- 15 shedding resulting in unbalanced loading could result in the crossarm damage observed.
- 16 Material testing found that the physical, chemical and metallurgical evidence indicates the conductor
- 17 failures were consistent with ductile limit load fracture. The testing also concluded that the ultimate
- 18 strength of the wire was 6% below the specified minimum rated tensile strength. Though the capacity of
- 19 the wire was reduced, the ductile failure was likely caused by overloading due to ice accumulation and
- 20 wind loads at the time of the failure. It is also noted that galloping due to wind could have contributed
- 21 to the failure by causing cyclic loading on the conductor.

11.0 Recommendations

- 23 Recommendations for consideration to mitigate future failures includes the following:
- Monitoring of ice conditions along the line;
- Investigate thermal and mechanical methods to reduce ice accumulation;
- Strengthening of the tower to withstand higher ice loads;



22

- Modifying the line to reduce the loads on towers;
 - Relocating the electrode line to adjacent wood pole structures;
- Look at alternative suspension assemblies and clamp designs; and
- Investigate using radiography to evaluate conductor issues.
- 5 These recommendations stem from previous failures. Investigation or implementation of many of these
- 6 recommendations is already underway. Refer to Table 7 for a list of Failure Investigation Reports
- 7 completed to date.

2

Table 7: Failure Investigation Reports

Document Title	Document Number
Failure Investigation Report - TL3501/2 Tower and Conductor	ILK-EG-ED-6200-TL-H15-0001-
Damage - Icing Event January 2021 in Labrador ⁵	01
Failure Investigation Report - L3501/2 Pole Assembly Turnbuckle	ILK-EG-ED-6200-TL-H15-0002-
Failure - Failure Event February 2021 in Labrador ⁶	01
L3501/2 Failure Investigation - Turnbuckle Failures Structure	ILK-EG-ED-6200-TL-H15-0003-
1872, 1806 and 1014 ⁷	01
L3501/2 Failure Investigation - OPGW Tower Peaks - Structure	ILK-EG-ED-6200-TL-H15-0004-
1230 and 1231 ⁸	01
L3501/2 Failure Investigation - OPGW Top Plates - Structure 2135	ILK-EG-ED-6200-TL-H15-0005-
and 2136 ⁹	01
L3501/2 Failure Investigation - OPGW Tower Peaks - Central	ILK-EG-ED-6200-TL-H15-0006-
Newfoundland ¹⁰	01
L3501/2 Failure Investigation – Ice Storm Southern Labrador	ILK-EG-ED-6200-TL-H15-0007-
Structures 514 to 517 ¹¹	01
Failure Investigation Report - Icing Event December 2022 in	ILK-EG-ED-6200-TL-H15-0008-
Labrador ¹²	01

¹² Supra footnote 5



⁵ Filed within "Reliability and Resource Adequacy Study Review – Labrador-Island Link Failure Investigation Reports", Newfoundland and Labrador Hydro, May 31, 2021.

⁶ Supra, footnote 3

⁷ Filed within "Reliability and Resource Adequacy Study Review - Summary of Findings from L3501/2 Failure Investigations," Newfoundland and Labrador Hydro, October 23, 2024.

⁸ Supra footnote 5

⁹ Supra footnote 5

¹⁰ Filed as Attachment 1 to Appendix B within "Quarterly Report on Asset Performance in Support of Resource Adequacy for the Twelve Months Ended March 31, 2025" Newfoundland and Labrador Hydro, April 30, 2025.

¹¹ Filed as Attachment 2 to Appendix B within "Quarterly Report on Asset Performance in Support of Resource Adequacy for the Twelve Months Ended March 31, 2025" Newfoundland and Labrador Hydro, April 30, 2025.

1 Monitoring can include line patrol, in-line ice load monitoring equipment, and test spans with ice load 2 and weather monitoring equipment near the line route. While monitoring itself will not prevent failures, 3 it is possible on occasion to remove ice from the lines or prevent it from originally accruing. Monitoring 4 can also help find and prepare for failures, and it can be used to better understand the amount of ice on 5 the lines for future work. Investigation is ongoing to determine potential mechanical and thermal 6 methods to prevent ice accretion and to remove ice that has accumulated. 7 Monitoring of ice conditions is currently accomplished by line patrol. Based on past recommendations, 8 line crews have increased helicopter patrols to four times a winter, with additional patrols as needed. 9 The amount of ice on the lines can be estimated visually from fallen samples and from pictures. Ice that 10 has fallen from the lines can be weighed and measured. Check sheets and forms have been created and 11 shared with Engineering and Operations to ensure the necessary information is being collected when 12 possible. 13 A test span has been constructed near \$1225, with plans to install another test span in 2026. The test span consists of one span of conductor between two wood poles with a load cell to monitor ice load, 14 15 and equipment to monitor wind and temperature. Unfortunately, icing near S1225 at the time of the 16 failures also caused damage to the existing test span, with data currently unavailable from this site. 17 Repairs are scheduled for completion by the end of 2025. A second real-time monitoring station is 18 planned for installation in Central Labrador in late 2026. In addition, in-line monitors have been installed 19 on the line in 2025 to monitor ice loading at three locations. Investigation is ongoing into the use of 20 various scanning technologies that may allow the condition of the conductors to be evaluated and areas 21 of concern to be identified prior to a failure. 22 The tangent towers on the line are designed for unbalanced ice loads of 70% maximum design ice thickness on one wire on one side of the tower, and 100% on one wire on the other side of the tower. If 23 24 the differential in ice thickness is higher, there is a chance the tower will fail. In 2024, the unbalanced ice 25 loading design used for L3501/2 was evaluated and updated to account for the loads being observed in 26 the field. A consultant has since completed a scope of work to provide design and cost estimate options 27 for tower modification that are required to meet this new unbalanced ice load design. Any 28 recommended changes to the towers would have to consider the slip strength of the clamps, the 29 redistribution of loads within the towers, and the constructability of the reinforcements considering the 30 line is built and in service. The resulting options are currently under review internally, and will be



- evaluated based on feasibility and cost. These options will need to meet the new design loads by
- 2 reducing the loads on the towers or increasing the tower capacity, including installing mid span
- 3 structures between existing tangent structures, removing the electrode conductor from the towers and
- 4 installing it on wood pole structures for sections of the line as required, and reinforcing existing
- 5 structures.
- 6 The conductor failures occurred at the suspension clamp. As part of the 2024-2025 tower analysis
- 7 project, an assessment of the electrode suspension assembly and a re-design of the assembly was
- 8 completed in 2025. There is also an ongoing analysis where three different electrode suspension clamps
- 9 have been installed at 10 structures (20 clamps in total) to determine if they perform better than the
- 10 existing clamp under unbalanced ice loading conditions. The conductor at these clamp locations will be
- inspected on an annual basis to look for signs of wear or damage.
- 12 Hydro will progress investigation into the possibility of conductor damage from extreme weather events
- 13 and excessive plastic deformation resulting from exceedance of the conductor tension limits as a
- 14 potential contributing factor to failure. The installation of ice and weather monitoring equipment will
- provide information that will help inform this investigation.
- 16 Additionally, Hydro has initiated investigation of radiography and other methods of non-destructive
- 17 testing by performing a preliminary corona discharge survey of conductor and substation equipment in
- 18 Labrador. The results are currently under review, and next steps will be determined based on the
- 19 findings.



Paae 27

Appendix A

Maps of Loading Zones



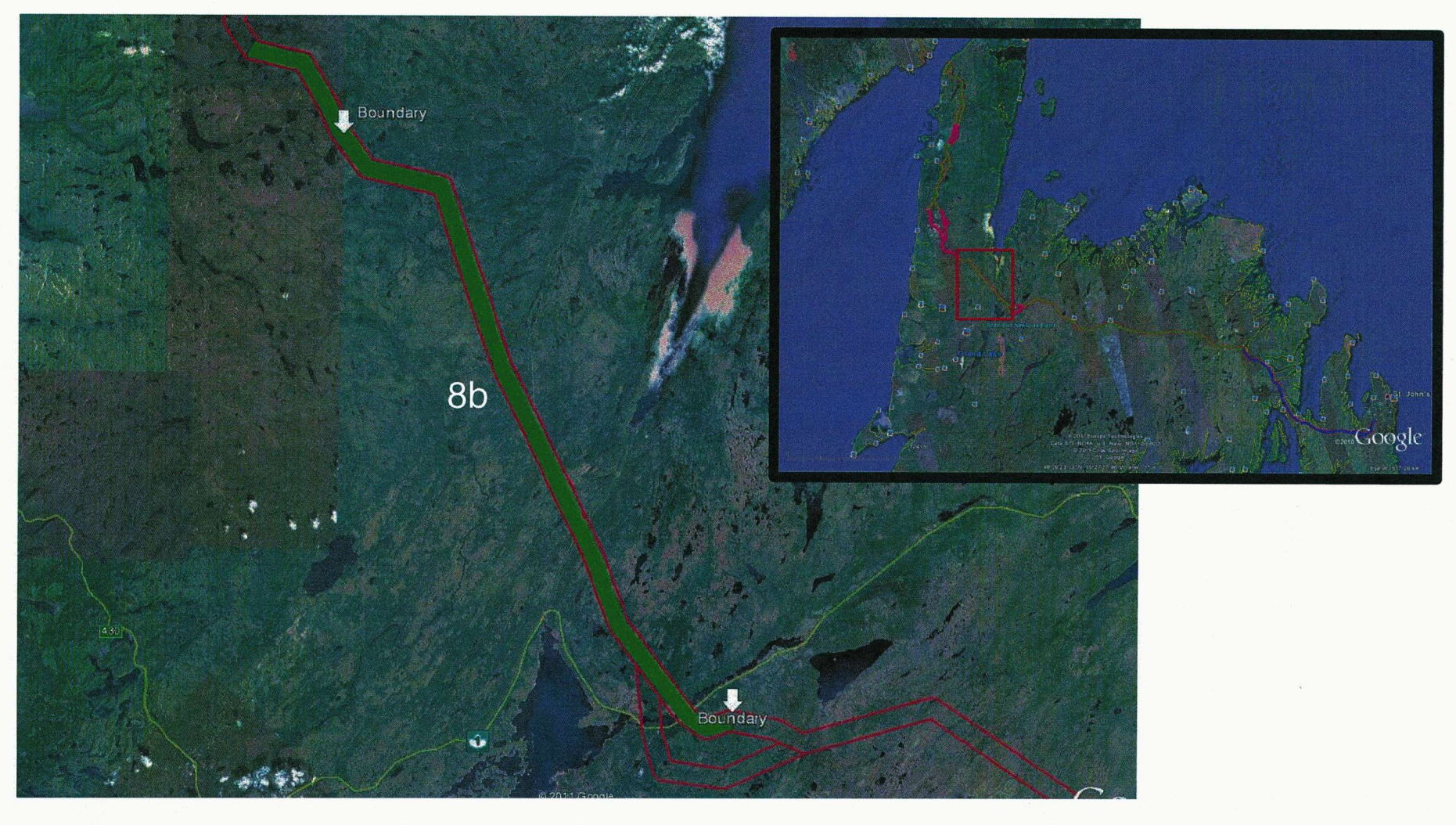


Zone 1 – Inner Labrador

Average Meteorological Loading Zone

Maximum Ice: 50 mm glaze, Maximum Wind: 105 km/h, Combined Ice and Wind: 25 mm glaze and 60 km/h



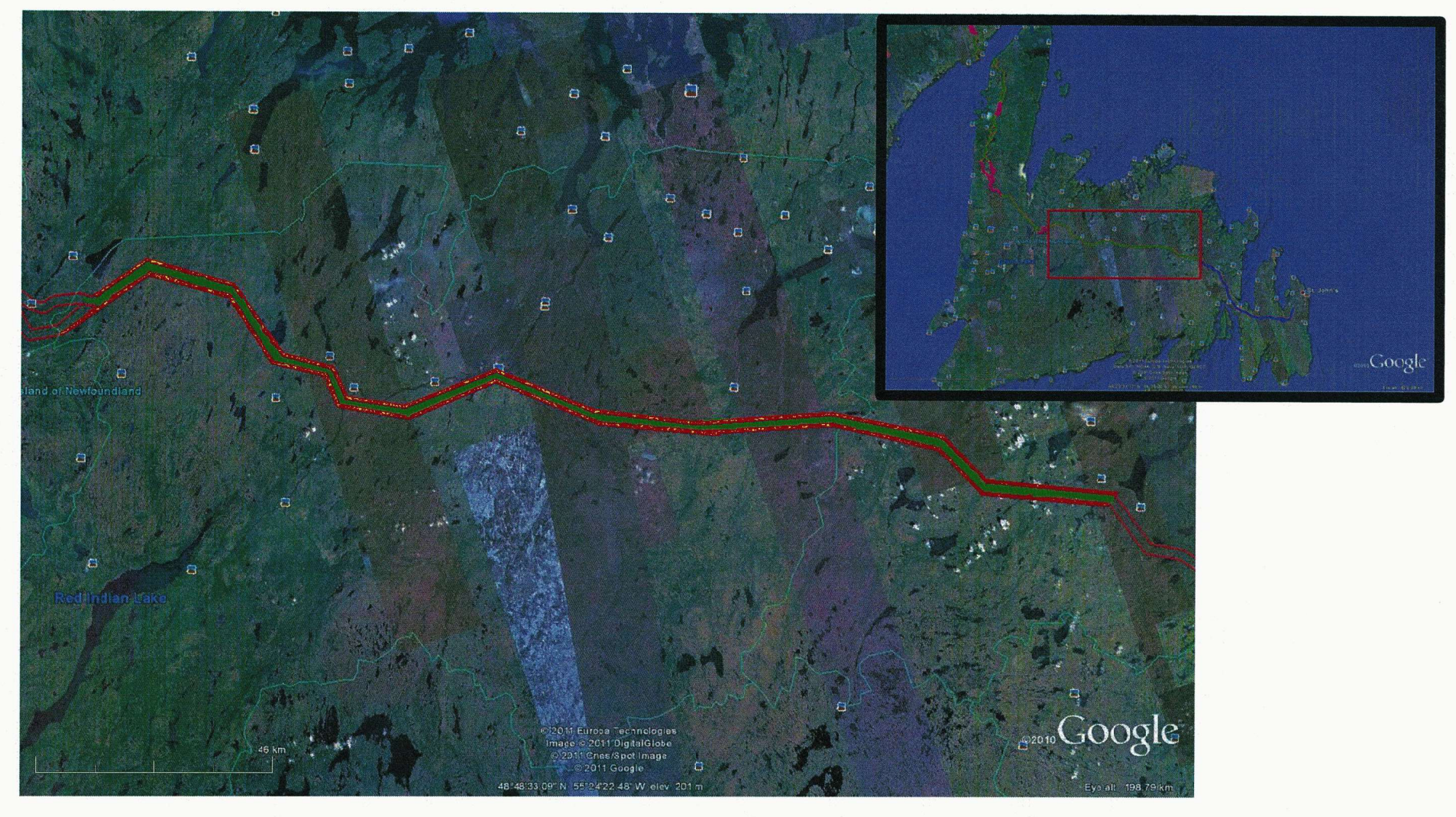


Zone 8b - Central-West Newfoundland

Average Meteorological Loading Zone

Maximum Ice: 50 mm (Glaze), Maximum Wind: 105 km/h, Combined Ice and Wind: 25 mm (Glaze) and 60 km/h





Zone 10 – Central-East Newfoundland

Average Meteorological Loading Zone

Maximum Ice: 50 mm (Glaze), Maximum Wind: 105 km/h, Combined Ice and Wind: 25 mm (Glaze) and 60 km/h



Appendix B

NL Hydro Transmission Line Failure Report

Wayland Engineering Ltd.



NL HYDRO TRANSMISSION LINE FAILURE

(Conductor EL-1 at Suspension Tower 127)

Prepared By:

K.J. KarisAllen, P.Eng. Wayland Engineering Ltd. Unit 9B, 2 Beechville Park Drive

Beechville, NS B3T 1L7

DATE 17/07/23 CE STATE OF NONE SECTION OF NONE

Prepared For: Maria Veitch, P.Eng. Newfoundland and Labrador Hydro 500 Columbus Drive St. John's, NL A1E 0A1

Wayland Engineering Ltd.

Wayland Engineering Ltd – Report No. J2512A July 2025

Executive summary

Wayland Engineering Ltd. was asked by Newfoundland and Labrador Hydro (NL Hydro) to conduct an investigation on an electrical conductor (EL-1) removed from suspension Tower #127. The conductor routed electrical power along the approximately 1090 km long transmission corridor between Muskrat Falls and Soldiers Pond. On January 11, 2025, the electrode current monitoring system indicated that EL-1 open circuited at approximately 23:50. A subsequent inspection conducted on the lines identified that the main failure of conductor EL-1 was located at suspension Tower #127. NL Hydro requested that Wayland Engineering provide an opinion on the mechanism(s) responsible for the failure sustained by conductor EL-1 from Tower #127.

A summary of the primary conclusions and recommendations generated by the investigation conducted includes:

- The physical, chemical and metallurgical evidence indicates that the mechanism responsible for the failure of conductor EL-1 at Tower #127 is consistent with ductile limit load fracture (i.e. overload) of the aluminum and steel reinforcing core wire strands.
- Uniaxial tension testing of duplicate samples from a length of intact service exposed conductor provided by NL Hydro indicated that the ultimate strength of the composite assembly was approximately 6 percent below the specified minimum rated tensile strength for a Grackle ACSR 54/19 (size 1192.5 kcmil) conductor.
- Diameter measurements and uniaxial tension testing of the individual strands from the failed EL-1 conductor and the intact service exposed conductor indicated that both the wire strand dimensional and material strength requirements either met or exceeded the requirements for a Grackle ACSR 54/19 (size 1192.5 kcmil) conductor.
- While the decrease in the ultimate breaking strength of the conductor assembly observed may have contributed to the failure of the EL-1 conductor, both the current failure on January 11, 2025 and a previous failure investigated by Wayland Engineering, which occurred on March 30, 2024, have been primarily attributed to the combination of accumulated ice and wind conditions which exceeded the design criteria for the conductor.
- It is recommended that NL Hydro consider exploring either mechanical and/or thermal methods which effectively reduce ice accumulation on the transmission lines when atmospheric conditions are conducive to ice build-up.

Table of contents

Exe	ecutive	summary	ii
Tal	ole of c	contents	iii
Lis	t of fig	gures	iv
Lis	t of tab	bles	viii
1	BAC	KGROUND	1
2	PREL	IMINARY EXAMINATION OF FAILED CONDUCTOR EL-1	4
3		LUATION OF THE CONDUCTOR MECHANICAL AND DIMENSIONAL PERTIES	. 10
	3.1	Uniaxial Tension Testing of an Intact Service Exposed (Used) Conductor	. 10
	3.2	Dimensional Characterization of Failed Conductor EL-1 Wire Strands	. 16
	3.3	Dimensional Characterization of the Tension Test Wire Strands (Subsequent to Testing)	. 17
	3.4	Uniaxial Tension Testing of Individual Wire Strands for the Failed Conductor EL-1	. 18
	3.5	Uniaxial Tension Testing of Individual Wire Strands Subsequent to the Tension Test of the Composite Conductor Assembly	. 18
4		ALLURGICAL CHARACTERIZATION OF THE FAILED CONDUCTOR [AGE (EL-1)	. 20
5	SUM	MARY AND DISCUSSION OF THE PHYSICAL EVIDENCE	. 26
	5.1	Summary of the Physical Evidence	. 26
	5.2	General Discussion	. 27
6	CON	CLUSIONS AND RECOMMENDATIONS	. 29
Re	ference	es	. 30
An	nex A	Data Sheet for the ACSR Grackle (Zinc Coated) Conductor	. 31
An		Dimensional Characterization of the Failed Section of ACSR Grackle (Zinc ed) Conductor EL-1	. 33
An		Dimensional Characterization of the Intact Service Exposed Section of ACSR kle (Zinc Coated) Conductor Provided for Uniaxial Tension Testing	. 35
An		Uniaxial Tension Test Results of Individual Wire Strands for the Failed Conductor	
An		Uniaxial Tension Testing of Individual Wire Strands Subsequent to the Tension of the Composite Conductor Assembly	. 37

List of figures

Figure 1-1:	Close-up view of suspension Tower #127 subsequent to the EL-1 conductor failure on January 11, 2025 [1]. The image shows the locations of conductors EL-1 and EL-2 (arrows), which were attached to the crossarms of the tower via suspension insulators
Figure 1-2:	Google map image provided by NL Hydro [1] showing the general compass directions of the segments of the transmission lines between Tower #125 and Tower #134. The map also shows the reported direction of the wind (northerly) during the day of the failure [1].
Figure 1-3:	Schematic showing the general configuration of an ACSR Grackle 54/19 conductor specification.
Figure 2-1:	General view of the mating sections of the failed conductor EL-1 from suspension Tower #127 as received for analysis
Figure 2-2:	Side view of the Stockbridge damper observed attached to the south side section at a distance of approximately 38 inches from the failed end of the conductor
Figure 2-3:	Image showing the evidence of moderate birdcaging of the outer layer wire strands observed on the south side section at a distance of approximately 24 inches from the failed end of the conductor.
Figure 2-4:	Image showing a side view of a typical wire clamp (from 2024 conductor failures), which was utilized for the attachment of the conductor to the crossarm suspension insulator.
Figure 2-5:	Image showing the wire strands associated with the individual layers (L1-L6) of the conductor subsequent to disassembly
Figure 2-6:	Close-up view of a representative example of the first fracture failure morphology observed for the aluminum strands associated with conductor EL-1. The first morphology was characterized by a tapered (necked) interval immediately adjacent to the strand fracture surface
Figure 2-7:	Close-up view of a representative example of the second fracture failure morphology observed for the aluminum strands associated with conductor EL-1. The second morphology was characterized by an oblique fracture plane extending across the diameter of the strand.
Figure 2-8:	Close-up view of a representative example of a partial through wire indication detected in an aluminum strand (arrows)

Figure 2-9	: Close-up view of a representative example of the strand on strand brinelling (localized deformation) observed on the individual aluminum wire strands	. 9
Figure 2-1	0: Close-up view of a representative example of the fracture failure morphology observed for the steel reinforcing core strands associated with conductor EL-1. The morphology was characterized by a tapered (necked) interval immediately adjacent to the strand fracture surface.	. 9
Figure 3-1	: Image showing the approximately 13 foot length of the service exposed (used) conductor provided by NL Hydro as received for analysis	10
Figure 3-2	: Photograph showing the epoxy filled socket fixture (ellipse) utilized to terminate the conductor at both ends	11
Figure 3-3	: Photograph showing the load train utilized to test the intact service exposed conductor in uniaxial tension (the arrow indicates the conductor)	12
Figure 3-4	: Photograph showing the two tensile test samples subsequent to failure. The axial positions of the conductor failures ranged between approximately 50 cm and 60 cm from the beginning of one of the epoxy filled terminations.	13
Figure 3-5	: Representative example showing the relative positions of the outer aluminum and the inner steel reinforcing wire strand failures subsequent to tension testing	13
Figure 3-6	: Close-up view of a representative example of the first fracture failure morphology observed for the aluminum strands subsequent to uniaxial tension testing. The first morphology was characterized by a tapered (necked) interval immediately adjacent to the strand fracture surface.	14
Figure 3-7	: Close-up view of a representative example of the second fracture failure morphology observed for the aluminum strands subsequent to uniaxial tension testing. The second morphology was characterized by an oblique fracture plane extending across the diameter of the strand.	14
Figure 3-8	: Close-up view of a representative example of the fracture failure morphology observed for the steel reinforcing core strands subsequent to uniaxial tension testing. The morphology was characterized by a tapered (necked) interval immediately adjacent to the strand fracture surface.	15
Figure 3-9	: Close-up view of a representative example of a partial through wire indication detected in an aluminum strand subsequent to uniaxial tension testing (arrows)	15
Figure 3-1	0: Close-up view of a representative example of the strand on strand brinelling (localized deformation) observed on the individual aluminum wire strands subsequent to uniaxial tension testing.	16

Figure 4-1: Low magnification SEM secondary image of a representative example of the fracture surface (ellipse) associated with the tapered-end (necked) geometry observed terminating the failed aluminum wire strands during the preliminary examination of conductor EL-1 (Figure 2-6). The image shows the general cup and cone morphology of the failed end of the wire strand	reinforcing strand for the failed conductor EL-1. The image shows the variation in the thickness of the zinc coating observed around the circumference of the steel reinforcing strand.	17
centroid shown in Figure 4-1. The image indicates that the strand fracture mechanism was dominated by void coalescence (i.e. ductile fracture) at the site 21 Figure 4-3: Low magnification SEM secondary image of a representative example of the fracture surface associated with the oblique geometry observed terminating the failed aluminum wire strands during the preliminary examination of conductor EL-1 (Figure 2-7)	fracture surface (ellipse) associated with the tapered-end (necked) geometry observed terminating the failed aluminum wire strands during the preliminary examination of conductor EL-1 (Figure 2-6). The image shows the general cup	21
fracture surface associated with the oblique geometry observed terminating the failed aluminum wire strands during the preliminary examination of conductor EL-1 (Figure 2-7)	centroid shown in Figure 4-1. The image indicates that the strand fracture	21
centroid shown in Fugure 4-3. The image shows the topological features associated with the strand fracture mechanism. Similar to Figure 4-2, the image suggests that the strand fracture mechanism was dominated by void coalescence (i.e. ductile fracture) at the site	fracture surface associated with the oblique geometry observed terminating the failed aluminum wire strands during the preliminary examination of conductor	22
partial through wire indication (rectangle). The image also shows the spacial relationship between the partial through wire indication and the fractured end of the wire strand	centroid shown in Fugure 4-3. The image shows the topological features associated with the strand fracture mechanism. Similar to Figure 4-2, the image suggests that the strand fracture mechanism was dominated by void coalescence	22
indication shown in Figure 4-5. The indication was characterized by a singular propagation morphology which was orientated at an oblique angle with respect to the longitudinal axis of the wire strand	partial through wire indication (rectangle). The image also shows the spacial relationship between the partial through wire indication and the fractured end of	23
brinelling observed in conductor EL-1. The image shows the localized severe distortion (plastic deformation) of the wire material observed at the sites where brinelling was observed on the external surface of the aluminum wire strand	indication shown in Figure 4-5. The indication was characterized by a singular propagation morphology which was orientated at an oblique angle with respect to	23
(arrows)	brinelling observed in conductor EL-1. The image shows the localized severe distortion (plastic deformation) of the wire material observed at the sites where	24

Figure 4-8: Low magnification SEM secondary image of a representative example of the
fracture surface (ellipse) associated with the tapered-end (necked) geometry
observed terminating the failed steel reinforcing wire strands during the
preliminary examination of conductor EL-1 (Figure 2-10). The image shows the
general cup and cone morphology of the failed end of the wire strand
Figure 4-9: High magnification fractographic image within the proximity of the strand centroid shown in Figure 4-8. The image indicates that the strand fracture mechanism was dominated by void coalescence (i.e. ductile fracture) at the site 25
Figure B-1: SEM backscatter image of representative examples of the zinc coated steel reinforcing strands for failed conductor EL-1. The image shows the variation in the thickness of the zinc coating observed around the circumference of the steel
reinforcing strands

List of tables

Table 1-1:	Summary of the damage detected by the field inspection conducted subsequent to the failure event on January 11, 2025 [1]	. 2
Table 3-1:	Summary of wire strand diameter results for the 6 layers associated with the failed conductor EL-1. The detailed measurement results have been provided in Annex B.	17
Table 3-2:	Summary of wire strand diameter ranges for the 6 layers associated with the conductor subjected to a uniaxial tension test. The detailed measurement results have been provided in Annex C.	18
Table 3-3:	Summary of wire strand ultimate force ranges for the 6 layers associated with the failed conductor EL-1. The detailed measurement results have been provided in Annex D.	18
Table 3-4:	Summary of wire strand ultimate force ranges for the 6 layers associated with the intact service exposed (used) conductor subsequent to the tension test of the composite wire assembly. The detailed measurement results have been provided in Annex E.	19
Table A-1:	Manufacturer's data sheet for the ACSR Grackle conductor (zinc coated steel reinforcing core)	31
Table B-1:	Summary of the outer aluminum conductor and inner steel reinforcing wire strand diameter measurements for the failed section of conductor EL-1	33
Table C-1:	Summary of the outer aluminum conductor and inner steel reinforcing wire strand diameter measurements for the used intact service exposed conductor provided for uniaxial tension testing.	35
Table D-1:	Summary of the ultimate uniaxial tension force results for select individual outer aluminum conductor and inner steel reinforcing wire strands for the failed conductor EL-1	36
Table E-1:	Summary of the ultimate uniaxial tension force results for select individual outer aluminum conductor and inner steel reinforcing wire strands for the used intact service exposed conductor provided for uniaxial tension testing	37

1 BACKGROUND

Wayland Engineering Ltd. was asked by Newfoundland and Labrador Hydro (NL Hydro) to conduct an investigation on an electrical conductor (EL-1) removed from suspension Tower #127. The conductor routed electrical power along the approximately 1090 km long transmission corridor between Muskrat Falls and Soldiers Pond [1]. On January 11, 2025, the electrode current monitoring system indicated that EL-1 open circuited at approximately 23:50 [1]. A subsequent inspection conducted on the lines identified that the main failure of conductor EL-1 was located at suspension Tower #127 (Figure 1-1) [1]. The inspection also detected various forms of additional damage at Tower #128 and Tower #130 (Table 1-1 [1]). It has been indicated that there was significant ice accumulation on the line prior to failure (estimated radial thickness of the ice glaze was in the range between 50 - 75 mm with a density of 0.7 g/cm³) [1]. It was also assumed that based on the observed icing conditions after the failure, there were unbalanced ice loads on the line due to ice shedding prior to the failure event on January 11 [1]. It was reported that during the day of the conductor failure, the wind velocity ranged between approximately 20 km/h and 35 km/h from a generally northerly direction at the closest weather station [1]. It has been indicated that the line was designed for a maximum wind velocity of 105 km/h in the absence of accumulated ice [1]. For a radial ice accumulation of approximately 25 mm (with a density of 0.9 g/cm³), the design criterion for the maximum wind velocity reduces to approximately 60 km/h [1]. The combination of the ice accumulation and wind velocities reported suggests that the line was operating in excess of the design criteria during the day of the failure sustained by conductor EL-1.

Figure 1-2 is a map showing the general compass directions of the line segments between suspension Tower #125 and Tower #134. It was reported that the distances from Tower #126 to Tower #127 and Tower #127 to Tower #128 were approximately 363.1 m and 408.3 m, respectively [1]. It has been indicated that conductor EL-1 at Tower 127 was installed in 2016 and had been subjected to approximately 9 years of service prior to the failure in 2025 [1]. Figure 1-2 also shows the direction of the northerly wind velocity reported during the day of the conductor failure event. Of relevance to the current investigation was the high attack angle of the wind direction with respect to the axis of the conductors, which may impose significant additional lateral forces on the lines (particularly for conditions of significant ice accumulation on the conductors). It was reported that galloping of the conductors has not been historically observed in the vicinity of Tower #127 since the installation of the lines in 2016 [1].

Figure 1-1 also shows the general electrode attachment arrangement. The image shows the locations of conductors EL-1 and EL-2, which were attached to the crossarms of the tower via suspension insulators. It was reported that both conductors EL-1 and EL-2 conformed to an ACSR Grackle conductor specification. The Grackle 54/19 conductor specification with a 1192.5 kcmil size is a concentric-lay-stranded configuration with 54 outer aluminum conductors and 19 inner zinc coated steel reinforcing wires (Figure 1-3). The nominal diameters of the outer aluminum and inner steel wire strands were reported as 3.77 mm and 2.26 mm, respectively [2]. Annex A contains the detailed data sheet for the ACSR Grackle conductor utilized by NL Hydro at Tower #127 [2]. NL Hydro requested that Wayland Engineering provide an opinion on the mechanism(s) responsible for the failure sustained by the section of conductor EL-1 provided for analysis.

Table 1-1: Summary of the damage detected by the field inspection conducted subsequent to the failure event on January 11, 2025 [1].

Tower No.	Description of Damage Sustained			
EL-1 conductor completely broken at insulator clamp. Electrode crossarm				
127	observed.			
128	Electrode crossarm damage observed.			
130	Electrode crossarm damage observed. Minor conductor damage (a few strands).			

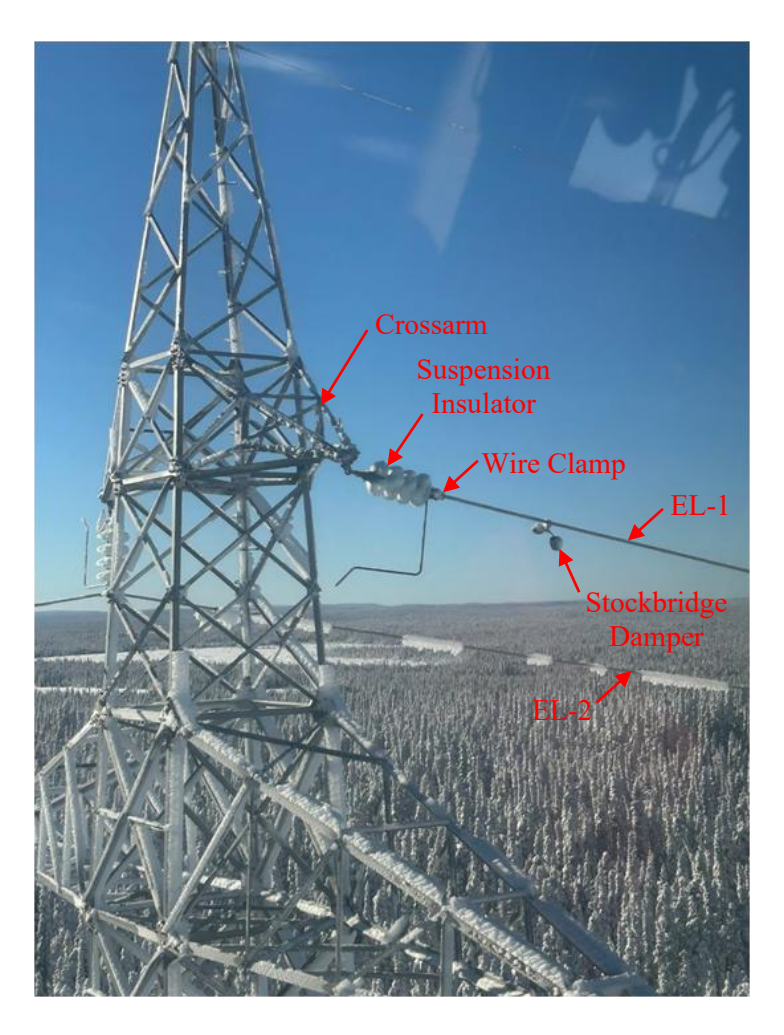


Figure 1-1: Close-up view of suspension Tower #127 subsequent to the EL-1 conductor failure on January 11, 2025 [1]. The image shows the locations of conductors EL-1 and EL-2 (arrows), which were attached to the crossarms of the tower via suspension insulators.



Figure 1-2: Google map image provided by NL Hydro [1] showing the general compass directions of the segments of the transmission lines between Tower #125 and Tower #134. The map also shows the reported direction of the wind (northerly) during the day of the failure [1].

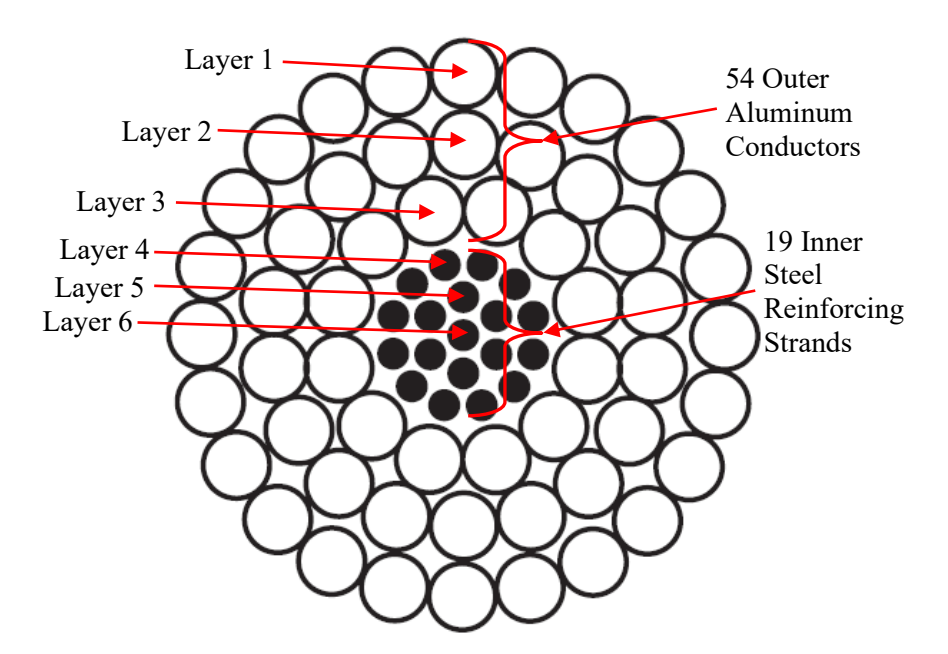


Figure 1-3: Schematic showing the general configuration of an ACSR Grackle 54/19 conductor specification.

2 PRELIMINARY EXAMINATION OF FAILED CONDUCTOR EL-1

Figure 2-1 shows the mating sections of the failed conductor EL-1 from suspension Tower #127 as received for analysis. The conductor section from the north side of the tower was approximately 48 inches in length and consisted of the fractured ends of individual wire strands at one end of the section and mechanically cut strands at the opposing end. The conductor section from the south side of the tower was approximately 74 inches in length and consisted of the fractured ends of individual wire strands at one end of the section and mechanically cut strands at the opposing end. A Stockbridge damper (Figure 2-2) was also attached to the south side section at a distance of approximately 58 inches from the failed end of the conductor. Evidence of moderate birdcaging of the outer layer wire strands was also observed on the south side section at a distance of approximately 24 inches from the failed end of the conductor (Figure 2-3). It was reported that the fracture of the line occurred at an axial position where a wire clamp (Figure 2-4) attached the conductor to the crossarm suspension insulator (Figure 1-1) [1].

Subsequently to the general external inspection, the fractured ends were removed from the failed conductor for further characterization of the damage sustained by the aluminum and steel reinforcing core wire strands during the failure event. Figure 2-5 shows the wire strands associated with the individual layers of the conductor subsequent to disassembly. Figure 2-6 and Figure 2-7 show close-up views of representative examples of the fracture failure morphologies observed for the aluminum wire strands. The first morphology was characterized by a tapered (necked) interval immediately adjacent to the strand fracture surface (Figure 2-6). The second morphology was characterized by an oblique fracture plane extending across the diameter of the strand (Figure 2-7). Evidence of partial through wire indications was also detected in a few of the aluminum strands (Figure 2-8).

Evidence of significant strand on strand brinelling (localized deformation) was also observed on the individual aluminum wire strands (Figure 2-9). The brinelling was more prevalent in adjacent strands corresponding to approximately half of the circumference of individual layers. The severity of the brinelling was also observed to increase towards the fractured ends of the aluminum strands.

Figure 2-10 shows a close-up view of a representative example of the fracture failure morphology observed for the steel reinforcing core wire strands. The morphology was characterized by a tapered (necked) interval immediately adjacent to the strand fracture surface. Section 4.1 includes the metallurgical characterization of the aluminum and steel strand fracture failures, as well as the partial through wire indications and strand to strand brinelling observed in the aluminum strands.

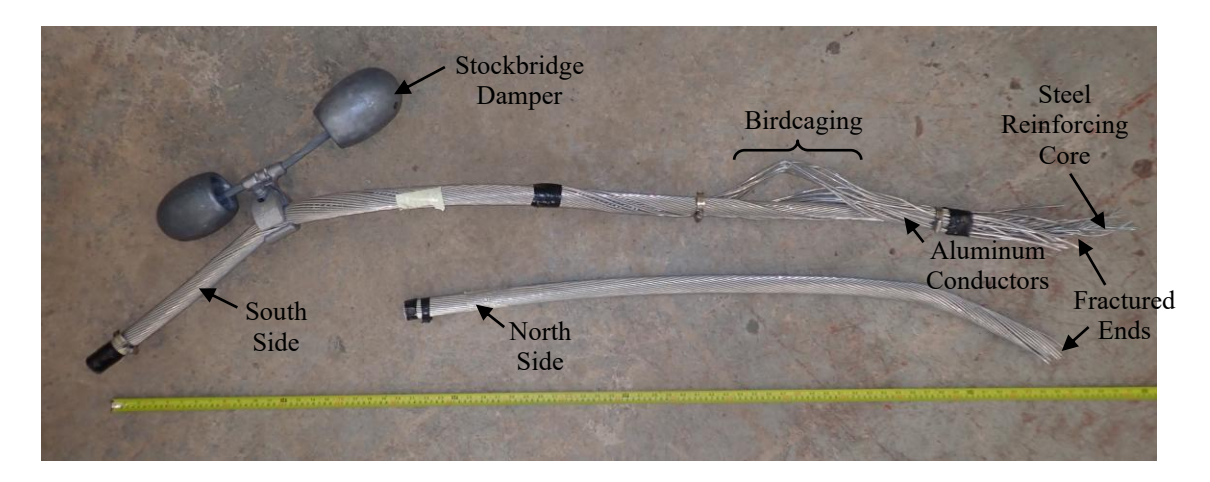


Figure 2-1: General view of the mating sections of the failed conductor EL-1 from suspension Tower #127 as received for analysis.

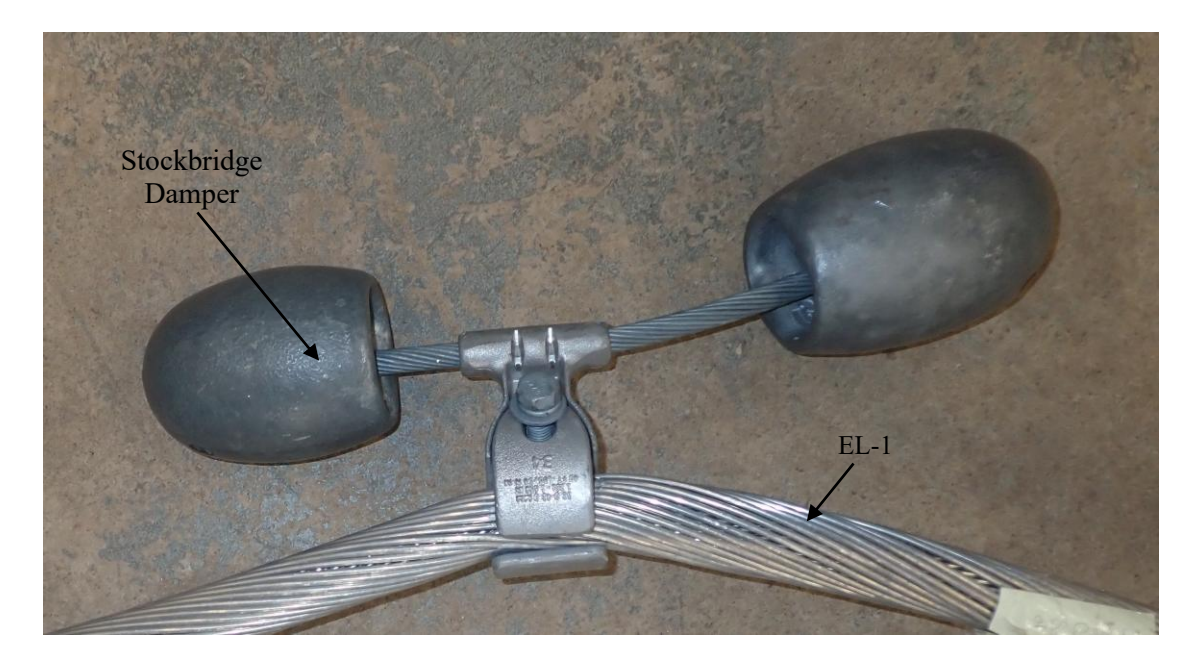


Figure 2-2: Side view of the Stockbridge damper observed attached to the south side section at a distance of approximately 38 inches from the failed end of the conductor.

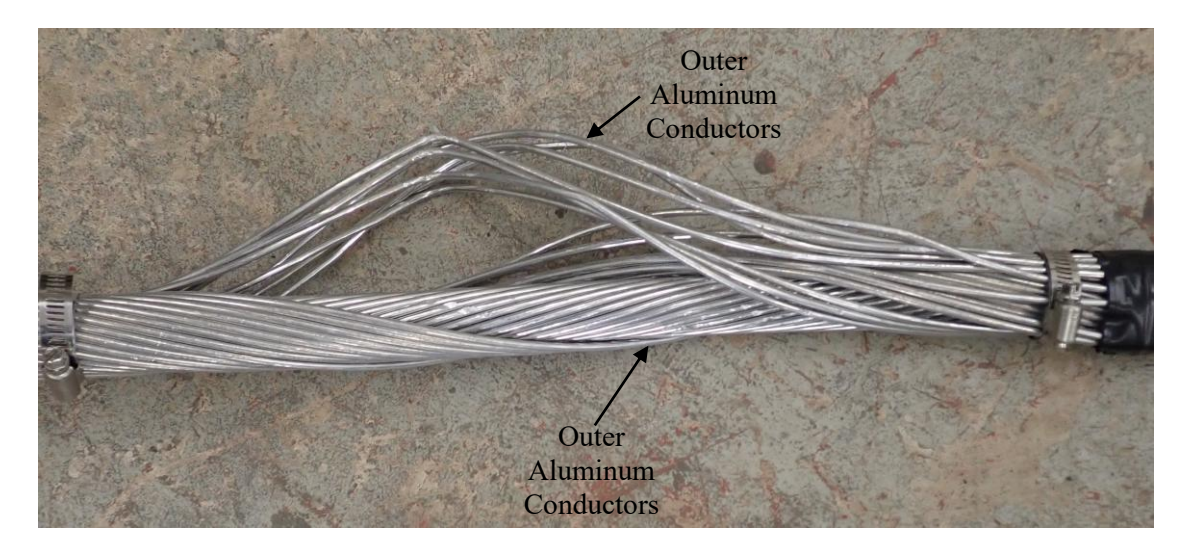


Figure 2-3: Image showing the evidence of moderate birdcaging of the outer layer wire strands observed on the south side section at a distance of approximately 24 inches from the failed end of the conductor.

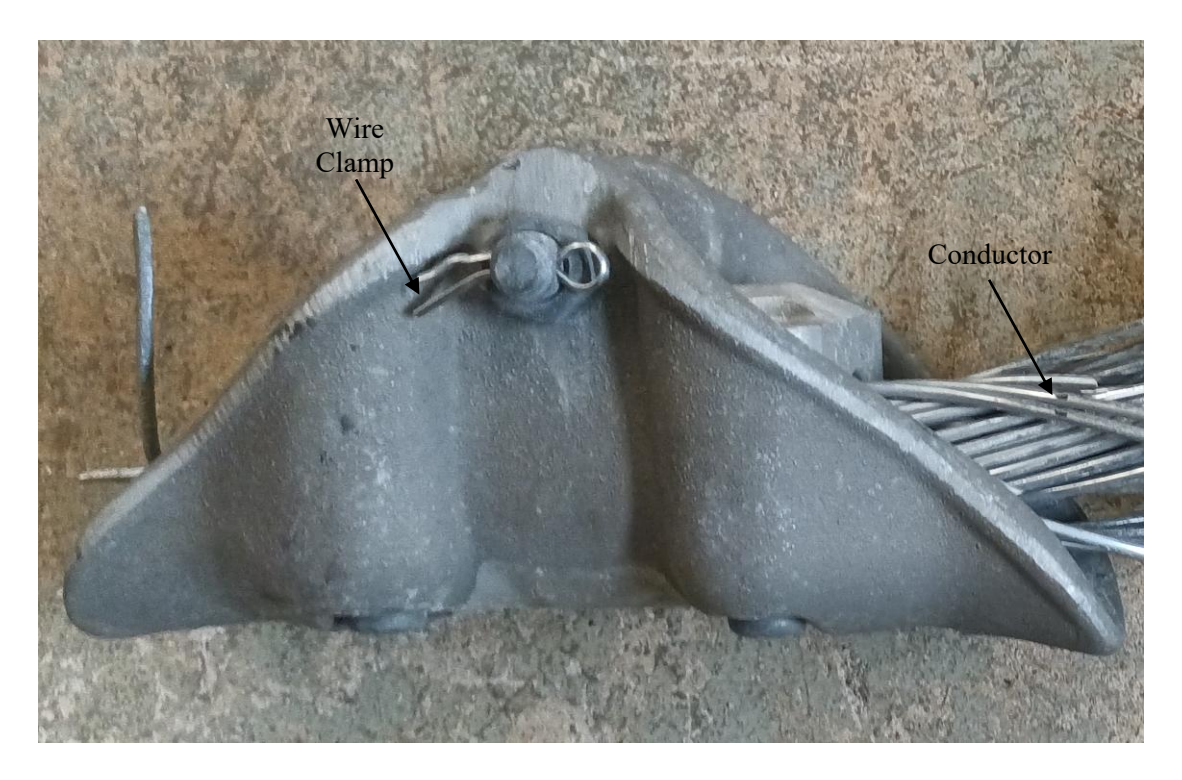


Figure 2-4: Image showing a side view of a typical wire clamp (from 2024 conductor failures), which was utilized for the attachment of the conductor to the crossarm suspension insulator.

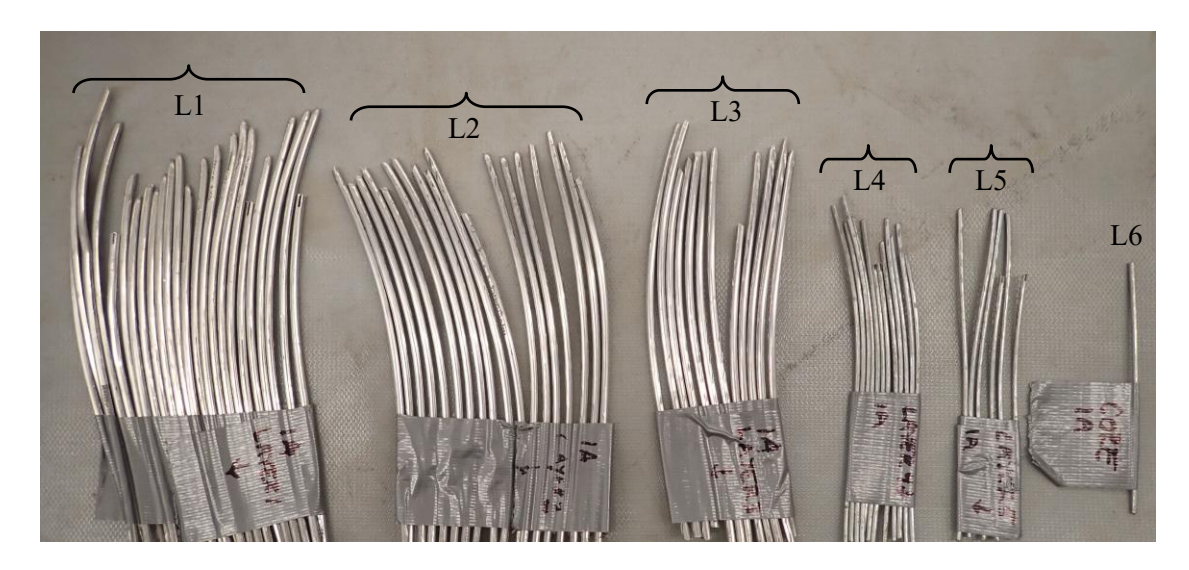


Figure 2-5: Image showing the wire strands associated with the individual layers (L1-L6) of the conductor subsequent to disassembly.



Figure 2-6: Close-up view of a representative example of the first fracture failure morphology observed for the aluminum strands associated with conductor EL-1. The first morphology was characterized by a tapered (necked) interval immediately adjacent to the strand fracture surface.

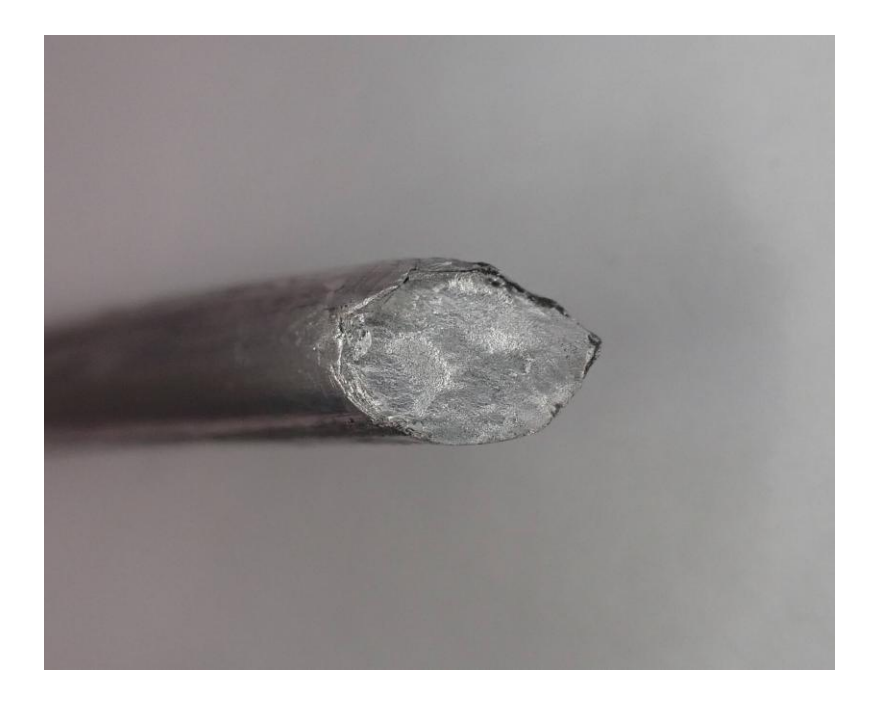


Figure 2-7: Close-up view of a representative example of the second fracture failure morphology observed for the aluminum strands associated with conductor EL-1. The second morphology was characterized by an oblique fracture plane extending across the diameter of the strand.



Figure 2-8: Close-up view of a representative example of a partial through wire indication detected in an aluminum strand (arrows).



Figure 2-9: Close-up view of a representative example of the strand on strand brinelling (localized deformation) observed on the individual aluminum wire strands.



Figure 2-10: Close-up view of a representative example of the fracture failure morphology observed for the steel reinforcing core strands associated with conductor EL-1. The morphology was characterized by a tapered (necked) interval immediately adjacent to the strand fracture surface.

3 EVALUATION OF THE CONDUCTOR MECHANICAL AND DIMENSIONAL PROPERTIES

Duplicate uniaxial tension tests were conducted on the approximately 13 foot long segment of intact, service exposed conductor provided by NL Hydro (Figure 3-1) to determine if the conductor met the original rated tensile strength requirements for a Grackle ACSR 54/19 conductor. Section 3.1 details the results of the uniaxial tension tests conducted.

Subsequent to the tension tests conducted, two intervals were removed and dissembled from the one of the conductors. The first interval (adjacent to the fractured wire strand ends) was utilized to conduct a dimensional characterization of the wire strand diameters. The second interval (approximately 16 inches away from the fractured wire strand ends) was utilized to conduct uniaxial tension tests of the individual wire strands to determine if the strands met the specified ultimate tensile strength requirements. Similar intervals were also removed and dissembled from one of the sections of the in service failed EL-1 conductor for the determination of the wire strand diameters and ultimate tensile strength for comparison purposes. For the failed EL-1 conductor internal steel reinforcing core strands, the thickness of the protective zinc coating layer was also measured on representative wire strands using scanning electron microscope (SEM) imaging. Section 3.2 and Section 3.3 detail the results of the dimensional characterization of the wire strand diameters for the failed EL-1 conductor and for the intact conductor subsequent to the tension test of the composite wire assembly, respectively. Section 3.4 and Section 3.5 detail the results of the uniaxial tension tests of the individual wire strands for the failed EL-1 conductor and for the intact conductor subsequent to the tension test of the composite wire assembly, respectively.



Figure 3-1: Image showing the approximately 13 foot length of the service exposed (used) conductor provided by NL Hydro as received for analysis.

3.1 Uniaxial Tension Testing of an Intact Service Exposed (Used) Conductor

Two lengths of the intact service exposed (used) conductor provided by NL Hydro (Figure 3-1) were tested in uniaxial tension in accordance with the procedure specified in ASTM A931 [3]. Duplicate test samples with a gauge length of approximately 1.55 m were terminated at both ends with epoxy filled socket fixtures (Figure 3-2). Figure 3-3 shows the load train utilized to test the terminated samples. The load train was used to apply a monotonic, stroke controlled, quasi-static deflection rate to the samples until the ultimate rupture of both the outer aluminum and inner steel reinforcing wire strands occurred.

The results of the testing indicated that the applied forces when the outer aluminum wire strands selectively fractured for the two tests were approximately 175.3 kN and 175.7 kN, respectively. The selective fracture of the outer aluminum wire strands resulted in a reduction of the applied forces for the two tests to approximately 83.6 kN and 82.7 kN, respectively. With continued applied deflection to the samples, the applied forces for the two tests increased to approximately 114.8 kN and 114.3 kN, respectively, which resulted in the fracture failure of the inner steel reinforcing wire strands. Measurements indicated that the overall fracture failure of the two conductors occurred between a distance of approximately 50 cm and 60 cm from the beginning of one of the epoxy filled terminations (Figure 3-4). Of relevance to the current investigation was that the maximum force generated by both of the tests conducted (175.3 kN and 175.7 kN) were approximately 6 percent below the minimum rated tensile strength requirements for a Grackle ACSR 54/19 (size 1192.5 kcmil) conductor specification (187 kN) [2].

Figure 3-5 is a close-up view of one of the conductors showing the relative positions of the outer aluminum and the inner steel reinforcing wire strand failures subsequent to testing, which is consistent with that expected for the failure of a Grackle ACSR conductor. Samples of the fractured ends of the outer aluminum wire strands were removed from the failed conductor for additional characterization. Figures 3-6 through Figure 3-8 contain side view images of representative examples of the fractured aluminum wire strands and the steel core strands. Of note was the similarity between the fracture surfaces generated by the uniaxial tension testing and the fracture surfaces associated with in service failure of conductor EL-1 (Figure 2-6, Figure 2-7 and Figure 2-10). Also similar to the in service failure of conductor EL-1 was the presence of a few partial through wire indications (Figure 3-9), as well as localized strand on strand brinelling (Figure 3-10) in the individual aluminum wire strands associated with the uniaxial tension tests.



Figure 3-2: Photograph showing the epoxy filled socket fixture (ellipse) utilized to terminate the conductor at both ends.



Figure 3-3: Photograph showing the load train utilized to test the intact service exposed conductor in uniaxial tension (the arrow indicates the conductor).

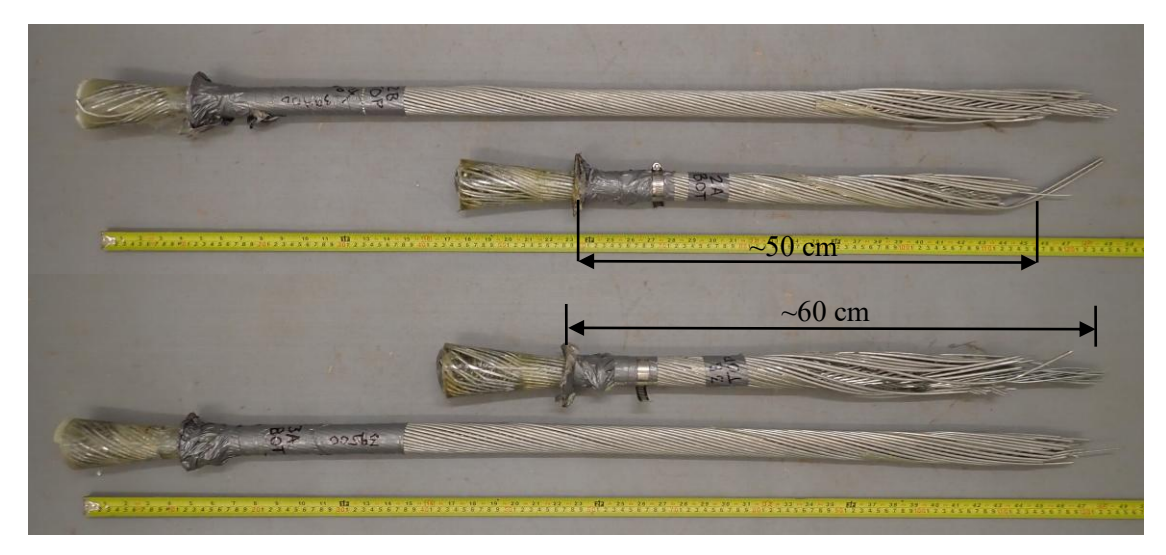


Figure 3-4: Photograph showing the two tensile test samples subsequent to failure. The axial positions of the conductor failures ranged between approximately 50 cm and 60 cm from the beginning of one of the epoxy filled terminations.

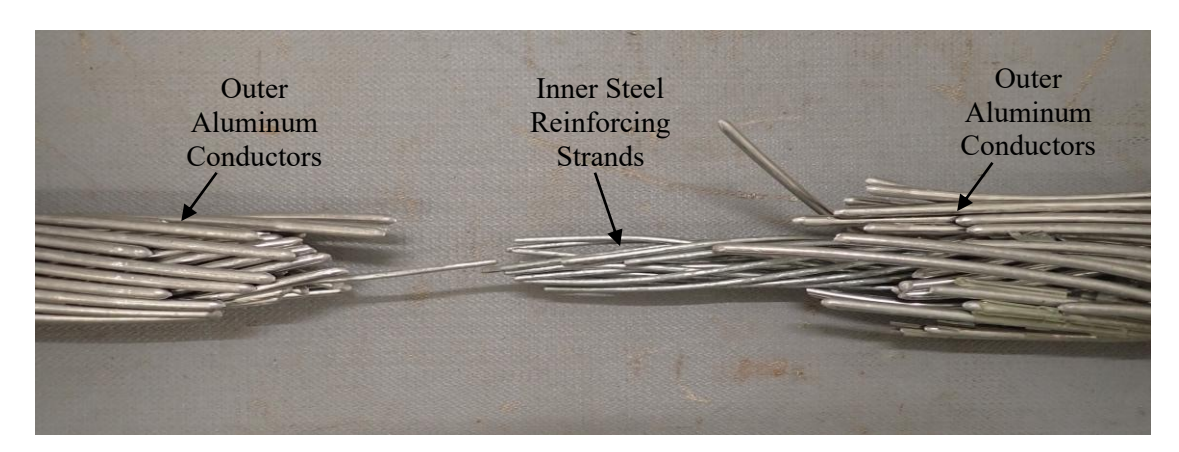


Figure 3-5: Representative example showing the relative positions of the outer aluminum and the inner steel reinforcing wire strand failures subsequent to tension testing.



Figure 3-6: Close-up view of a representative example of the first fracture failure morphology observed for the aluminum strands subsequent to uniaxial tension testing. The first morphology was characterized by a tapered (necked) interval immediately adjacent to the strand fracture surface.



Figure 3-7: Close-up view of a representative example of the second fracture failure morphology observed for the aluminum strands subsequent to uniaxial tension testing. The second morphology was characterized by an oblique fracture plane extending across the diameter of the strand.



Figure 3-8: Close-up view of a representative example of the fracture failure morphology observed for the steel reinforcing core strands subsequent to uniaxial tension testing. The morphology was characterized by a tapered (necked) interval immediately adjacent to the strand fracture surface.



Figure 3-9: Close-up view of a representative example of a partial through wire indication detected in an aluminum strand subsequent to uniaxial tension testing (arrows).

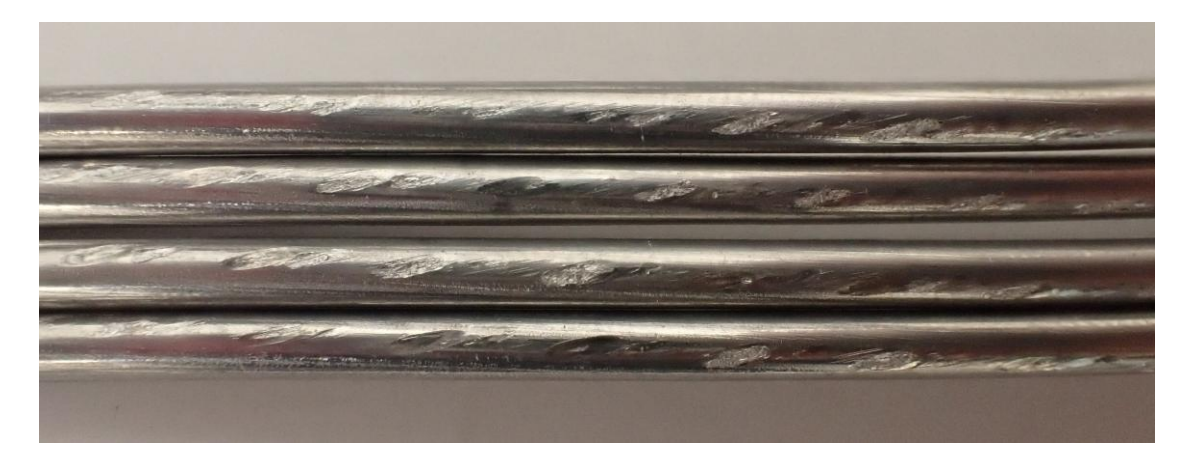


Figure 3-10: Close-up view of a representative example of the strand on strand brinelling (localized deformation) observed on the individual aluminum wire strands subsequent to uniaxial tension testing.

3.2 Dimensional Characterization of Failed Conductor EL-1 Wire Strands

Table 3-1 contains a summary of wire strand diameter results for the 6 layers associated with the failed conductor EL-1 (the detailed measurement results have been provided in Annex B). For Layer 1, Layer 2 and Layer 3 (aluminum conductor strands) the diameters ranged between 3.79 mm to 3.84 mm, 3.79 mm to 3.80 mm and 3.79 mm to 3.80 mm, respectively. For Layer 4, Layer 5 and Layer 6 (zinc coated steel reinforcing strands) the diameters ranged between 2.27 mm to 2.30 mm, 2.27 mm to 2.29 mm and 2.29 mm, respectively. The diameter ranges measured for both the aluminum conductor strands and the zinc coated steel reinforcing strands for conductor EL-1 were generally within reasonable agreement with the specified wire diameter requirements as per ASTM B-232 [4] for a Grackle ACSR 54/19 (size 1192.5 kcmil) conductor .

Figure 3-11 is a sectional SEM backscatter image of a representative example of a zinc coated steel reinforcing strand (additional representative examples are provided in Annex B). The image shows the variation in the thickness of the zinc coating observed around the circumference of the steel reinforcing strand. For the samples evaluated, the thickness ranged between approximately 35.63 µm and 60.70 µm for the strands evaluated. A range of 35.63 µm to 60.70 µm in zinc coating thickness equates to a layer surface density of approximately 312.7 g/m² to 684.2 g/m², respectively. While a variation in the thickness of the zinc coating was observed, it should be noted that a breech through the coating to the steel core was not observed around the circumference (i.e. the cathodic protection provided by the zinc coating remained intact).

Table 3-1: Summary of wire strand diameter results for the 6 layers associated with the failed conductor EL-1. The detailed measurement results have been provided in Annex B.

		Wire Strand Diameter Ranges (mm)						
	Outer	Outer Aluminum Strands Inner Steel Strands						
	Layer 1	Layer 2	Layer 3	Layer 4	Layer 5	Layer 6		
Average	3.81	3.80	3.79	2.28	2.28	2.29		
Maximum	3.84	3.80	3.80	2.30	2.29	2.29		
Minimum	3.79	3.79	3.79	2.27	2.27	2.29		

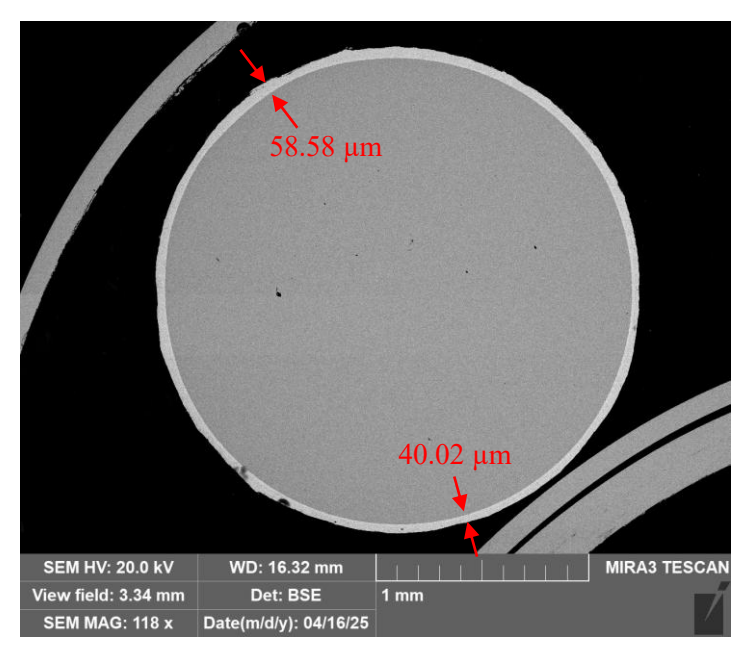


Figure 3-11: SEM backscatter image of a representative example of a zinc coated steel reinforcing strand for the failed conductor EL-1. The image shows the variation in the thickness of the zinc coating observed around the circumference of the steel reinforcing strand.

3.3 Dimensional Characterization of the Tension Test Wire Strands (Subsequent to Testing)

Table 3-2 contains a summary of wire strand diameter ranges for the 6 layers associated with the conductor subjected to a uniaxial tension test of the composite wire assembly. The detailed measurement results have been provided in Annex C. For Layer 1, Layer 2 and Layer 3 (aluminum conductor strands) the diameters ranged between 3.78 mm to 3.81 mm, 3.77 mm to 3.80 mm and 3.79 mm to 3.79 mm, respectively. For Layer 4, Layer 5 and Layer 6 (zinc coated steel reinforcing strands) the diameters ranged between 2.20 mm to 2.26 mm, 2.23 mm to 2.26 mm and 2.23 mm, respectively. The diameter ranges measured for both the aluminum conductor strands and the zinc coated steel reinforcing strands for the conductor were generally within reasonable agreement with the specified wire diameter requirements as per ASTM B-232 [4] for a Grackle ACSR 54/19 (size 1192.5 kcmil) conductor.

Table 3-2: Summary of wire strand diameter ranges for the 6 layers associated with the conductor subjected to a uniaxial tension test. The detailed measurement results have been provided in Annex C.

		Wire Strand Diameter Ranges (mm)						
	Outer	Outer Aluminum Strands Inner Steel Strands						
	Layer 1	Layer 2	Layer 3	Layer 4	Layer 5	Layer 6		
Average	3.80	3.79	3.79	2.24	2.24	2.23		
Maximum	3.81	3.80	3.79	2.26	2.26	2.23		
Minimum	3.78	3.77	3.79	2.20	2.23	2.23		

3.4 Uniaxial Tension Testing of Individual Wire Strands for the Failed Conductor EL-1

Table 3-3 contains a summary of wire strand ultimate uniaxial tension force ranges for the 6 layers associated with the failed conductor EL-1 (the detailed measurement results have been provided in Annex D). For Layer 1, Layer 2 and Layer 3 (aluminum conductor strands) the diameters ranged between 1953 N to 2153 N, 1904 N to 2135 N and 2024 N to 2220 N, respectively. For Layer 4, Layer 5 and Layer 6 (zinc coated steel reinforcing strands) the diameters ranged between 6054 N to 6192 N, 6187 N to 6201 N and 6134 N, respectively. The ultimate tension force ranges measured for the aluminum conductor strands and the zinc coated steel reinforcing strands for the failed EL-1 conductor exceeded the specified wire force requirements for both the aluminum conductor strands (1717 N) and the zinc coated steel reinforcing strands (4952 N) [2].

Table 3-3: Summary of wire strand ultimate force ranges for the 6 layers associated with the failed conductor EL-1. The detailed measurement results have been provided in Annex D.

		Wire Strand Ultimate Tension Force (N)							
	Oute	Outer Aluminum Strands Inner Steel Strands							
	Layer 1 Layer 2 Layer 3 Layer 4 Layer				Layer 5	Layer 6			
Average	2041	2023	2101	6125	6193	6134			
Maximum	2153	2135	2220	6192	6201	6134			
Minimum	1953	1904	2024	6054	6187	6134			

3.5 Uniaxial Tension Testing of Individual Wire Strands Subsequent to the Tension Test of the Composite Conductor Assembly

Table 3-3 contains a summary of wire strand ultimate uniaxial tension force ranges for the 6 layers associated with the intact service exposed conductor (the detailed measurement results have been provided in Annex E). For Layer 1, Layer 2 and Layer 3 (aluminum conductor strands) the force ranged between 1868 N to 2091 N, 1979 N to 2073 N and 1984 N to 2166 N, respectively. For Layer 4, Layer 5 and Layer 6 (zinc coated steel reinforcing strands) the force ranged between 5978 N to 6214 N, 5987 N to 6201 N and 6174N, respectively. The ultimate

tension force ranges measured for the aluminum conductor strands and the zinc coated steel reinforcing strands for the intact service exposed conductor exceeded the minimum specified wire force requirements for both the aluminum conductor strands (1717 N) and the zinc coated steel reinforcing strands (4952 N) [2].

Table 3-4: Summary of wire strand ultimate force ranges for the 6 layers associated with the intact service exposed (used) conductor subsequent to the tension test of the composite wire assembly. The detailed measurement results have been provided in Annex E.

		Wire Strand Ultimate Tension Force (N)						
	Oute	Outer Aluminum Strands Inner Steel Strands						
Layer 1 Layer 2 Layer 3 Layer				Layer 4	Layer 5	Layer 6		
Average	2011	2019	2086	6068	6100	6174		
Maximum	2091	2073	2166	6214	6201	6174		
Minimum	mum 1868 1979 1984 5978 5987 61							

4 METALLURGICAL CHARACTERIZATION OF THE FAILED CONDUCTOR DAMAGE (EL-1)

Samples from several of the outer aluminum wire strands and the steel reinforcing strands, which included the fracture surface associated with the strand failure were removed from conductor EL-1. The samples were prepared for characterization of the topological features associated with the fracture mechanism using scanning electron microscope (SEM) fractographic imaging techniques. Figure 4-1 is a low magnification SEM secondary image of a representative example of the fracture surface associated with the tapered-end geometry observed terminating the failed aluminum wire strands during the preliminary examination of conductor EL-1 (Figure 2-6). The image shows the general cup and cone morphology of the failed end of the wire strand. Figure 4-2 is a high magnification fractographic image within the proximity of the strand centroid showing the topological features associated with the strand fracture mechanism. The image indicates that the strand fracture mechanism was dominated by void coalescence (i.e. ductile fracture) at the site. Figure 4-3 is a low magnification SEM secondary image of a representative example of the fracture surface associated with the oblique geometry observed terminating the failed aluminum wire strands during the preliminary examination of conductor EL-1 (Figure 2-7). Figure 4-4 is a high magnification fractographic image within the proximity of the strand centroid showing the topological features associated with the strand fracture mechanism. Similar to Figure 4-2, the image suggests that the strand fracture mechanism was dominated by void coalescence (i.e. ductile fracture) at the site.

Several samples were also sectioned from the outer aluminum wire strands at locations where evidence of partial through wire indications were observed during the preliminary examination of conductor EL-1 (Figure 2-8). Figure 4-5 is a low magnification SEM backscatter image of a representative example of a partial through wire indication. The image also shows the spacial relationship between the partial through wire indication and the fractured end of the wire strand. Figure 4-6 is a higher magnification SEM backscatter image of the partial through wire indication shown in Figure 4-5. The indication was characterized by a singular propagation morphology which was orientated at an oblique angle with respect to the longitudinal axis of the wire strand.

Several samples were also sectioned from the outer aluminum wire strands at locations where evidence of strand to strand brinelling was observed during the preliminary examination of conductor EL-1 (Figure 2-9). The samples were prepared for metallurgical characterization of the damage using optical microscopy. Figure 4-7 is a sectional view micrograph of a representative example of the strand to strand brinelling observed in conductor EL-1. The image shows the localized severe distortion (plastic deformation) of the external surface material observed on diametrically opposing sides of the wire strand at the site.

Figure 4-8 is a low magnification SEM secondary image of a representative example of the fracture surface associated with the tapered-end geometry observed terminating the failed steel reinforcing strands during the preliminary examination of conductor EL-1 (Figure 2-10). The image shows the general cup and cone morphology of the failed end of the wire strand. Figure 4-9 is a high magnification fractographic image within the proximity of the strand centroid showing the topological features associated with the strand fracture mechanism. The image indicates that the strand fracture mechanism was dominated by void coalescence (i.e. ductile fracture) at the site.

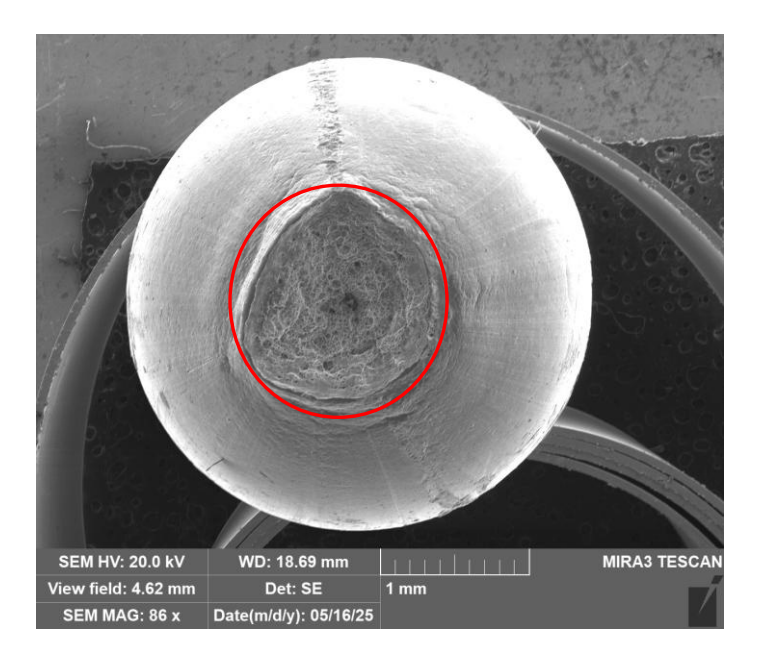


Figure 4-1: Low magnification SEM secondary image of a representative example of the fracture surface (ellipse) associated with the tapered-end (necked) geometry observed terminating the failed aluminum wire strands during the preliminary examination of conductor EL-1 (Figure 2-6). The image shows the general cup and cone morphology of the failed end of the wire strand.

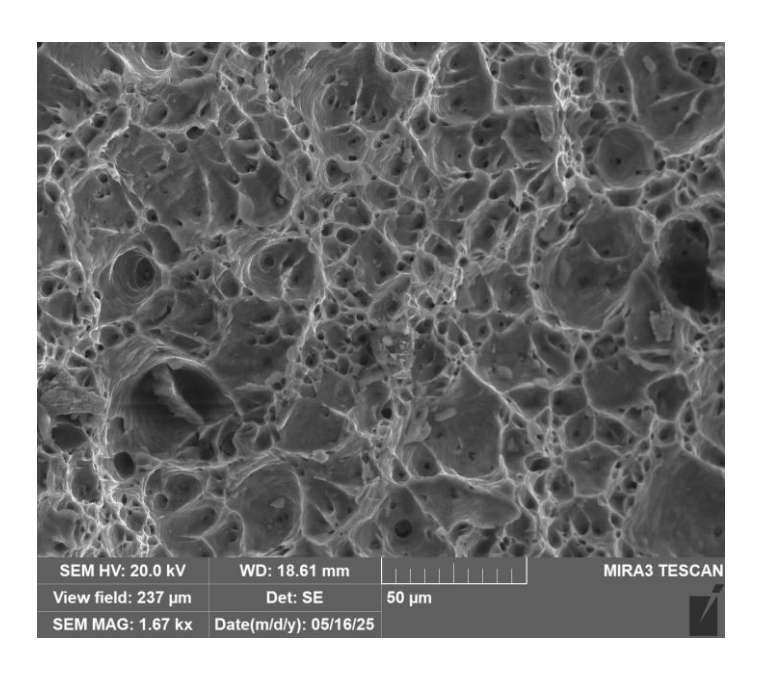


Figure 4-2: High magnification fractographic image within the proximity of the strand centroid shown in Figure 4-1. The image indicates that the strand fracture mechanism was dominated by void coalescence (i.e. ductile fracture) at the site.

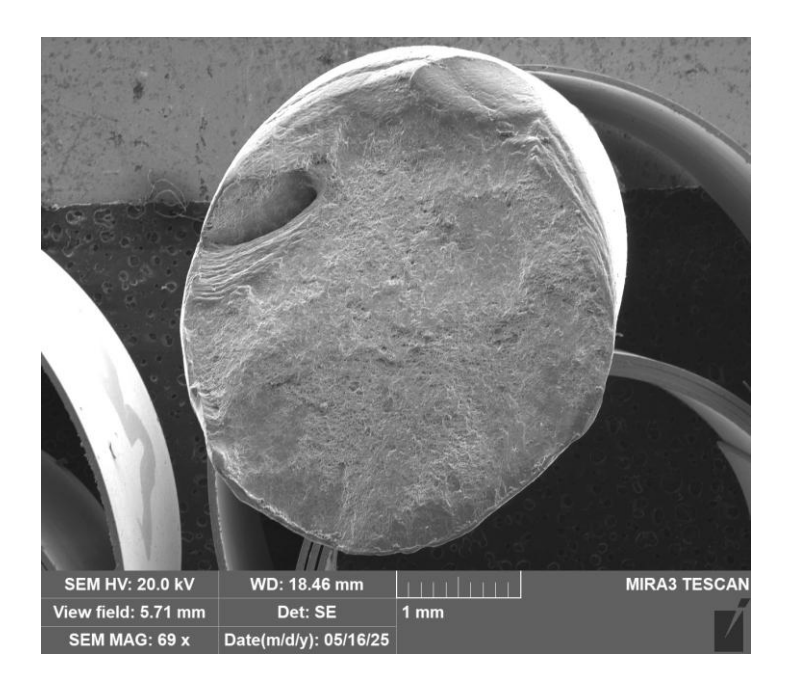


Figure 4-3: Low magnification SEM secondary image of a representative example of the fracture surface associated with the oblique geometry observed terminating the failed aluminum wire strands during the preliminary examination of conductor EL-1 (Figure 2-7).

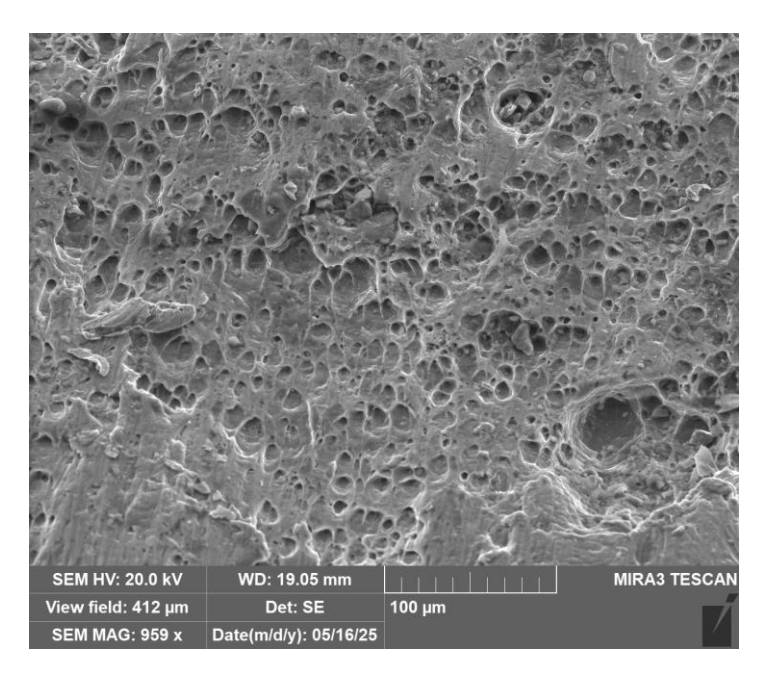


Figure 4-4: High magnification fractographic image within the proximity of the strand centroid shown in Fugure 4-3. The image shows the topological features associated with the strand fracture mechanism. Similar to Figure 4-2, the image suggests that the strand fracture mechanism was dominated by void coalescence (i.e. ductile fracture) at the site.

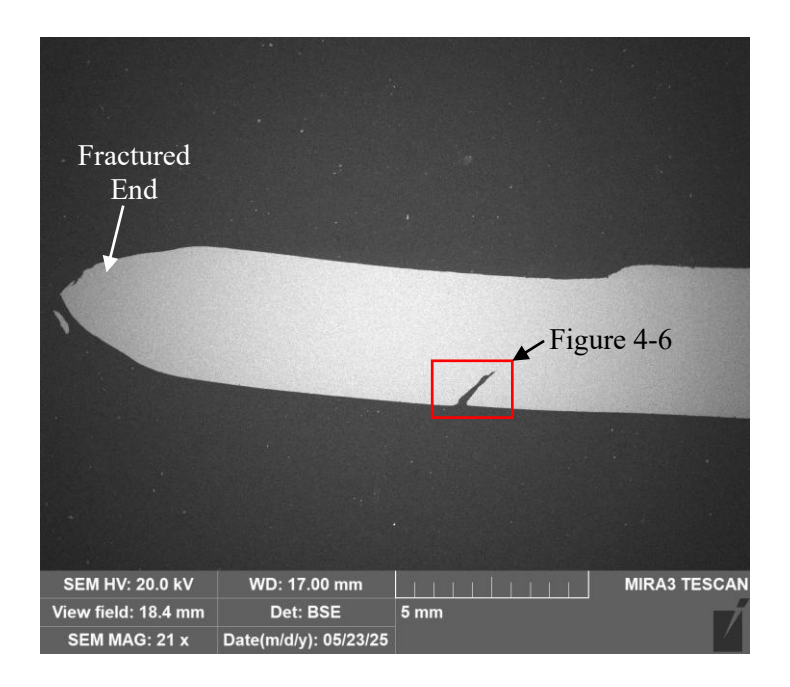


Figure 4-5: Low magnification SEM backscatter image of a representative example of a partial through wire indication (rectangle). The image also shows the spacial relationship between the partial through wire indication and the fractured end of the wire strand.

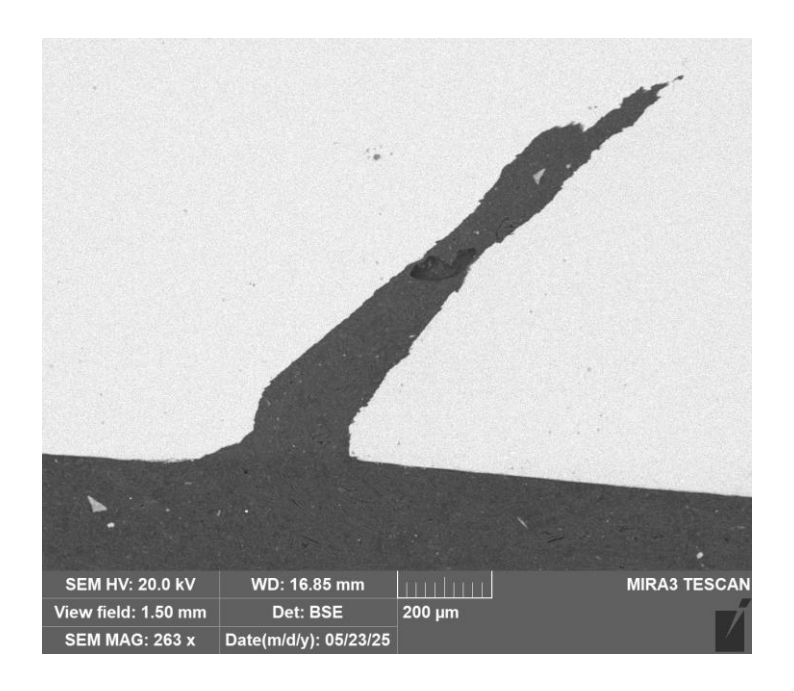


Figure 4-6: Higher magnification SEM backscatter image of the partial through wire indication shown in Figure 4-5. The indication was characterized by a singular propagation morphology which was orientated at an oblique angle with respect to the longitudinal axis of the wire strand.

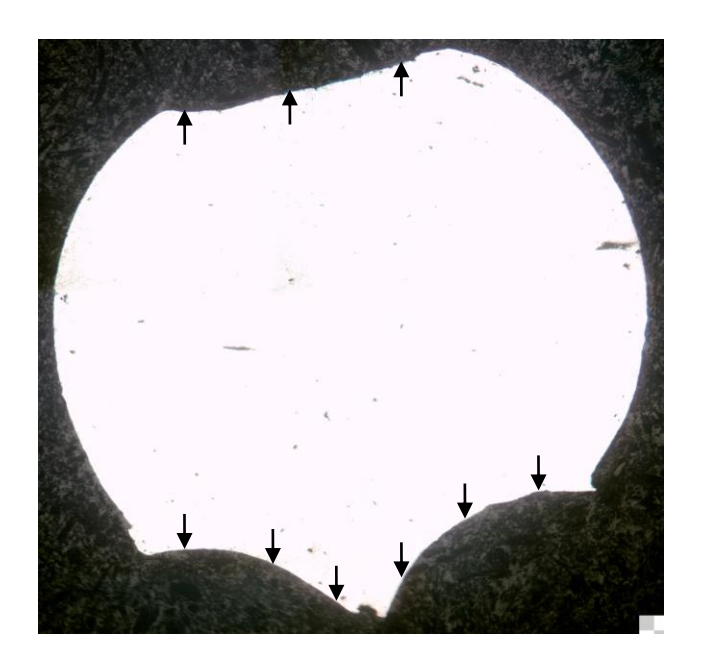


Figure 4-7: Sectional view micrograph of a representative example of the strand to strand brinelling observed in conductor EL-1. The image shows the localized severe distortion (plastic deformation) of the wire material observed at the sites where brinelling was observed on the external surface of the aluminum wire strand (arrows).

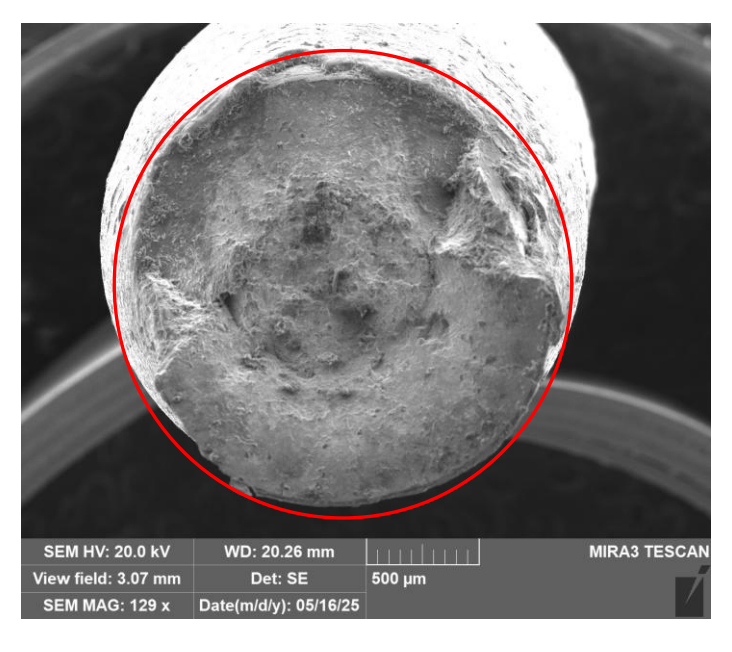


Figure 4-8: Low magnification SEM secondary image of a representative example of the fracture surface (ellipse) associated with the tapered-end (necked) geometry observed terminating the failed steel reinforcing wire strands during the preliminary examination of conductor EL-1 (Figure 2-10). The image shows the general cup and cone morphology of the failed end of the wire strand.

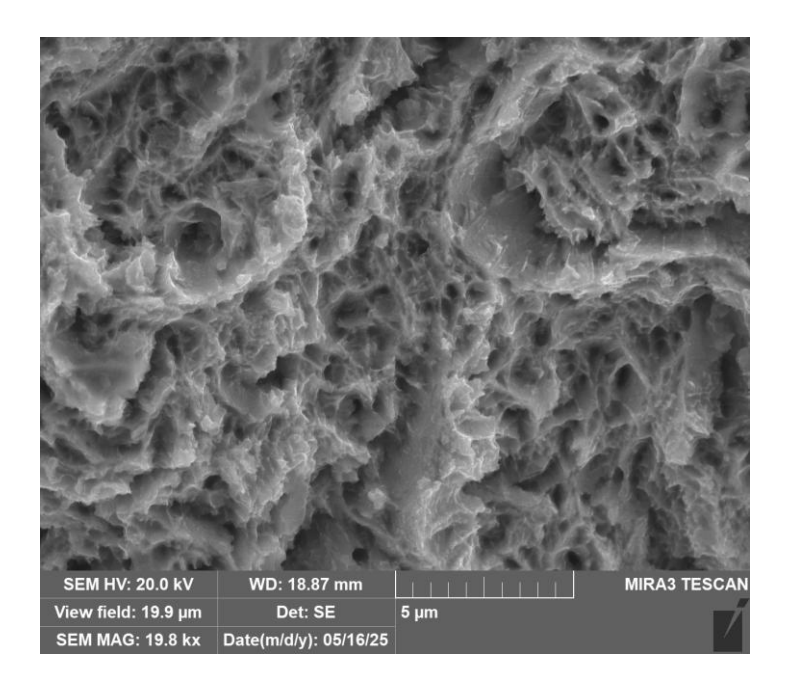


Figure 4-9: High magnification fractographic image within the proximity of the strand centroid shown in Figure 4-8. The image indicates that the strand fracture mechanism was dominated by void coalescence (i.e. ductile fracture) at the site.

5 SUMMARY AND DISCUSSION OF THE PHYSICAL EVIDENCE

5.1 Summary of the Physical Evidence

The following summarizes the physical evidence generated during the investigation for the failed section of conductor EL-1 from suspension Tower #127 and the intact service exposed section of conductor provided for evaluation. The physical evidence includes;

- The field evidence provided by NL Hydro indicated that at Tower #127, the line damage consisted of a complete fracture of conductor EL-1 adjacent to the termination of the insulator wire clamp.
- The fractured ends of the aluminum strands exhibited two general morphologies. The first morphology was characterized by a tapered (necked) interval immediately adjacent to the strand fracture surface. The second morphology was characterized by an oblique fracture plane extending across the diameter of the strand. SEM fractographic analysis indicated that fracture surfaces associated with both morphologies were dominated by void coalescence (i.e. limit load ductile failure).
- Evidence of strand on strand localized brinelling (plastic deformation) and partial through wire indications was observed on the external surfaces of the aluminum strands adjacent to the fractured ends of the wires.
- The fractured ends of the steel strands exhibited a tapered (necked) morphology immediately adjacent to the strand fracture surface. Similar to the aluminum strands, SEM fractographic analysis indicated that fracture surfaces associated with the steel strands were dominated by void coalescence (i.e. limit load ductile failure).
- Measurements of the individual aluminum and steel wire strands for the failed EL-1 conductor indicated that the diameters of the strands remained within reasonable agreement with the specified wire diameter requirements as per ASTM B-232 [4] for a Grackle ACSR 54/19 (size 1192.5 kcmil) conductor.
- Uniaxial tension testing of the individual aluminum and steel wire strands for the failed EL-1 conductor indicated that both the aluminum conductor strands exceeded the minimum specified wire strength requirements for a Grackle ACSR 54/19 (size 1192.5 kcmil) conductor.
- Uniaxial tension testing of duplicate samples from a length of intact service exposed conductor provided by NL Hydro indicated that the ultimate strength of the composite assembly was approximately 6 percent below the specified minimum rated tensile strength for a Grackle ACSR 54/19 (size 1192.5 kcmil) conductor (187 kN).

- Diameter measurements and uniaxial tension testing of the individual strands subsequent to composite conductor assembly tension tests generated similar results to the failed EL-1 conductor.
- Measurements of the zinc coating thicknesses for steel reinforcing strands indicated the surface area density of the coating range was between 312.7 g/m² to 684.2 g/m². It was noted that a breech through the coating to the steel core was not observed around the circumference of the wire strands evaluated (i.e. the cathodic protection provided by the zinc coating remained intact).

5.2 General Discussion

The physical, chemical and metallurgical evidence indicates that the mechanism responsible for the failure of conductor EL-1 at Tower #127 is consistent with ductile limit load fracture of the aluminum and steel reinforcing core wire strands. It was reported that there was significant and unbalanced ice accumulation on the line prior to failure (estimated radial thickness of the ice was in the range between 50 – 75 mm) [1]. The wind velocity was also reported to be between approximately 20 km/h and 35 km/h from a northerly direction (at the closest weather station) on the day of the failure [1]. It has been indicated that for a radial ice accumulation of approximately 25 mm, the design criterion for the maximum wind velocity reduces to 60 km/h [1]. The combination of the ice accumulation and wind velocities reported suggests that the line was operating in excess of the design criteria on the day of the failure. While it has been reported that galloping of the conductors has not been historically observed by NL Hydro in the vicinity of Tower #127 [1], transient forces from galloping cannot be categorically excluded as an additional source of loading on the conductor during the failure event on January 11.

Uniaxial tension testing of duplicate samples from the intact service exposed conductor provided indicated that the ultimate strength of the composite assembly was approximately 6 percent below the specified minimum rated tensile strength for a Grackle ACSR 54/19 (size 1192.5 kcmil) conductor (187 kN). Measurements of the individual aluminum and steel wire strands subsequent to the tension tests indicated that the diameters of the strands remained within reasonable agreement with the specified wire diameter requirements as per ASTM B-232 [4] for a Grackle ACSR 54/19 (size 1192.5 kcmil) conductor. In addition, uniaxial tension testing of the individual aluminum and steel wire strands subsequent to the composite assembly tension tests indicated that both the aluminum conductor strands exceeded the minimum specified wire strength requirements for a Grackle ACSR 54/19 (size 1192.5 kcmil) conductor. Diameter measurements and uniaxial tension testing of the individual strands from the failed EL-1 conductor also generated similar results. The results indicate that both the wire strand dimensional and material strength requirements either met or exceeded the requirements for a Grackle ACSR 54/19 (size 1192.5 kcmil) conductor.

Based on the testing conducted, the chronological order of events associated with the failure of a Grackle ACSR 54/19 conductor is as follows:

a) As monotonic strain is applied to the wire assembly, the applied force increases up to the ultimate breaking strength of the conductor at which point the aluminum strands selectively fracture. At the ultimate breaking strength of the wire assembly, the total

- applied force consists of the sum of the forces sustained by the aluminum strands and the forces sustained by the steel strands.
- b) Immediately subsequent to the selective fracture of the aluminum strands, the remaining applied force exhibited by the assembly consists solely of the elastic response of the steel reinforcing core. Upon the application of additional monotonic strain, the applied force increases up to the ultimate breaking strength of the steel reinforcing core resulting in the fracture failure of the steel strands.

One possible explanation for the lower than specified composite conductor assembly ultimate strength observed is a lower than normal force partitioning ratio between the sum of the steel core strand forces to the sum of the aluminum conductor strand forces for a given unit of conductor strain. There are several scenarios which may account for an abnormal force partitioning ratio, all of which would require significantly more sophisticated testing than that conducted during the current investigation.

While a decrease in the ultimate breaking strength of the conductor assembly may have contributed to the failure of the EL-1 conductor, both the current failure on January 11, 2025 and a previous failure investigated by Wayland Engineering [5], which occurred on March 30, 2024, have been primarily attributed to the combination of accumulated ice and wind conditions which exceeded the design criteria for the conductor. Thus, it is recommended that NL Hydro consider exploring either mechanical and/or thermal methods which effectively reduce ice accumulation on the transmission lines when atmospheric conditions are conducive to ice build-up.

6 CONCLUSIONS AND RECOMMENDATIONS

The conclusions and recommendations inferred by the investigation for the failed section of conductor EL-1 from suspension Tower #127 include:

- The physical, chemical and metallurgical evidence indicates that the mechanism responsible for the failure of conductor EL-1 at Tower #127 is consistent with ductile limit load fracture (i.e. overload) of the aluminum and steel reinforcing core wire strands.
- Uniaxial tension testing of duplicate samples from a length of intact service exposed conductor provided by NL Hydro indicated that the ultimate strength of the composite assembly was approximately 6 percent below the specified minimum rated tensile strength for a Grackle ACSR 54/19 (size 1192.5 kcmil) conductor.
- Diameter measurements and uniaxial tension testing of the individual strands from the failed EL-1 conductor and the intact service exposed conductor indicated that both the wire strand dimensional and material strength requirements either met or exceeded the requirements for a Grackle ACSR 54/19 (size 1192.5 kcmil) conductor.
- While the decrease in the ultimate breaking strength of the conductor assembly observed may have contributed to the failure of the EL-1 conductor, both the current failure on January 11, 2025 and a previous failure investigated by Wayland Engineering, which occurred on March 30, 2024, have been primarily attributed to the combination of accumulated ice and wind conditions which exceeded the design criteria for the conductor.
- It is recommended that NL Hydro consider exploring either mechanical and/or thermal methods which effectively reduce ice accumulation on the transmission lines when atmospheric conditions are conducive to ice build-up.

References

- [1] Various E-mails provided by M. Veitch, Newfoundland and Labrador Hydro, May, 2025.
- [2] Various E-mails provided by M. Veitch, Newfoundland and Labrador Hydro, June-September, 2024.
- [3] ASTM A931, "Standard Test Method for Tension Testing of Wire Ropes and Strand", ASTM International
- [4] ASTM B232, "Standard Specification for Concentric-Lay-Stranded Aluminum Conductors, Coated Steel Reinforced (ACSR)", ASTM International.
- [5] Wayland Engineering Report No. J2413A, "NL Hydro Transmission Line Failure (Conductor EL-1 and EL-2 at Suspension Tower 1225)", October 2024.

Annex A Data Sheet for the ACSR Grackle (Zinc Coated) Conductor

Table A-1 is the manufacturer's data sheet summary for the ACSR Grackle conductor with a zinc coated steel reinforcing core.

Table A-1: Manufacturer's data sheet for the ACSR Grackle conductor (zinc coated steel reinforcing core).





Annex B Dimensional Characterization of the Failed Section of ACSR Grackle (Zinc Coated) Conductor EL-1

Table B-1 summarizes the outer aluminum conductor and inner steel reinforcing wire strand diameter measurements for the failed section of conductor EL-1. Figure B-1 shows representative examples of the thickness of the zinc coating present on the steel reinforcing wire strands.

Table B-1: Summary of the outer aluminum conductor and inner steel reinforcing wire strand diameter measurements for the failed section of conductor EL-1.

XX/*	Wire Strand Diameter (mm)							
Wire	Outer	Aluminum S	Strands	Inn	er Steel Stra	ınds		
Strand No.	Layer 1	Layer 2	Layer 3	Layer 4	Layer 5	Layer 6		
1	3.82	3.79	3.79	2.29	2.29	2.29		
2	3.82	3.79	3.79	2.28	2.29			
3	3.84	3.80	3.79	2.27	2.28			
4	3.82	3.80	3.79	2.27	2.28			
5	3.84	3.79	3.79	2.29	2.27			
6	3.81	3.80	3.79	2.29	2.28			
7	3.80	3.79	3.80	2.27				
8	3.82	3.80	3.79	2.30				
9	3.81	3.79	3.80	2.28				
10	3.81	3.80	3.80	2.28				
11	3.81	3.80	3.80	2.28				
12	3.79	3.79	3.80	2.29				
13	3.81	3.80						
14	3.80	3.80						
15	3.81	3.79						
16	3.80	3.80						
17	3.80	3.80						
18	3.79	3.80						
19	3.81							
20	3.80							
21	3.80							
22	3.82							
23	3.81							
24	3.80							
Average	3.81	3.80	3.79	2.28	2.28	2.29		
Maximum	3.84	3.80	3.80	2.30	2.29	2.29		
Minimum	3.79	3.79	3.79	2.27	2.27	2.29		

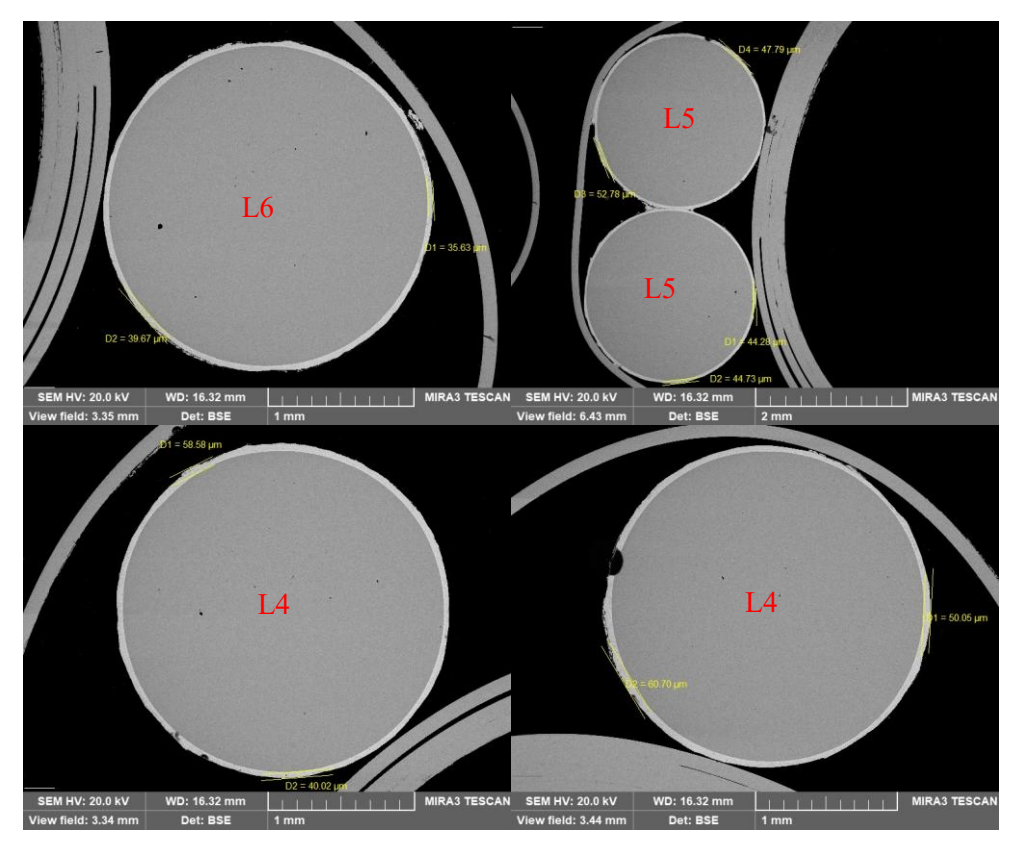


Figure B-1: SEM backscatter image of representative examples of the zinc coated steel reinforcing strands for failed conductor EL-1. The image shows the variation in the thickness of the zinc coating observed around the circumference of the steel reinforcing strands.

Annex C Dimensional Characterization of the Intact Service Exposed Section of ACSR Grackle (Zinc Coated) Conductor Provided for Uniaxial Tension Testing

Table C-1 summarizes the outer aluminum conductor and inner steel reinforcing wire strand diameter measurements for the used intact conductor provided for uniaxial tension testing.

Table C-1: Summary of the outer aluminum conductor and inner steel reinforcing wire strand diameter measurements for the used intact service exposed conductor provided for uniaxial tension testing.

XX.7*	Wire Strand Diameter (mm)								
Wire	Outer	Aluminum S	Strands	Inner Steel Strands					
Strand No.	Layer 1	Layer 2	Layer 3	Layer 4	Layer 5	Layer 6			
1	3.79	3.79	3.79	2.23	2.26	2.23			
2	3.79	3.79	3.79	2.26	2.23				
3	3.81	3.79	3.79	2.26	2.23				
4	3.81	3.79	3.79	2.26	2.23				
5	3.79	3.79	3.79	2.25	2.23				
6	3.79	3.79	3.79	2.23	2.23				
7	3.81	3.79	3.79	2.2					
8	3.79	3.8	3.79	2.23					
9	3.81	3.77	3.79	2.24					
10	3.79	3.77	3.79	2.24					
11	3.81	3.8	3.79	2.26					
12	3.79	3.77	3.79	2.26					
13	3.81	3.79							
14	3.81	3.79							
15	3.79	3.79							
16	3.81	3.79							
17	3.79	3.8							
18	3.78	3.8							
19	3.79								
20	3.79								
21	3.79								
22	3.78								
23	3.78								
24	3.79								
Average	3.80	3.79	3.79	2.24	2.24	2.23			
Maximum	3.81	3.80	3.79	2.26	2.26	2.23			
Minimum	3.78	3.77	3.79	2.20	2.23	2.23			

Annex D Uniaxial Tension Test Results of Individual Wire Strands for the Failed Conductor EL-1

Table D-1 summarizes the ultimate uniaxial tension force results for select individual outer aluminum conductor and inner steel reinforcing wire strands for the failed conductor EL-1.

Table D-1: Summary of the ultimate uniaxial tension force results for select individual outer aluminum conductor and inner steel reinforcing wire strands for the failed conductor EL-1.

Wire Strand No.	Wire Strand Ultimate Tension Force (N)												
	(ands		Inner Steel Strands									
	Layer 1		Layer 2		Layer 3		Layer 4		Layer 5		Layer 6		
1	2028	C	2077	C/S	2028	C/S			6192	С	6134	С	
2	2082	C							6201	С			
3	1993	C	1993	C	2117	C/S	6054	С					
4							6192	С					
5	1957	C	2099	C	2171	C/S	6156	С	6187	С			
6							6147	С					
7	2046	C/S	1904	C	2220	C/S							
8							6143	С					
9			1948	C/S	2024	С							
10							6058	С					
11	2113	C	2082	C/S									
12					2046	С							
13			2002	C									
14													
15	2024	C	1966	C									
16													
17			2135	C									
18	2019	C											
19													
20	2086	C											
21													
22	2153	C/S								·			
23	2033	C/S											
24	1953	C											
Average	2041		2023		2101		6125		6193		6134		
Maximum	2153		2135		2220		6192		6201		6134		
Minimum	1953		1904		2024		6054		6187		6134		

C indicates a tapered end failure morphology (i.e. cup and cone), whereas S indicates an oblique failure morphology (i.e. shear failure).

Annex E Uniaxial Tension Testing of Individual Wire Strands Subsequent to the Tension Test of the Composite Conductor Assembly

Table E-1 summarizes the ultimate uniaxial tension force results for select individual outer aluminum conductor and inner steel reinforcing wire strands for the used intact conductor provided for uniaxial tension testing.

Table E-1: Summary of the ultimate uniaxial tension force results for select individual outer aluminum conductor and inner steel reinforcing wire strands for the used intact service exposed conductor provided for uniaxial tension testing.

Wire Strand No.	Wire Strand Ultimate Tension Force (N)												
	(ands		Inner Steel Strands									
	Layer 1		Layer 2		Layer 3		Layer 4		Layer 5		Layer 6		
1			2019	С					5987	С	6174	С	
2							5987	С					
3	1997	С					6080	С	6201	С			
4	1944	С	2073	C/S	2051	С							
5					2086	C/S			6112	С			
6	1868	С			2099	C/S							
7					2166	C/S							
8			2006	S									
9	1979	С					6214	С					
10			2059	С			6080	С					
11			1979	S	2131	C/S	5978	С					
12	2055	С	1979	С	1984	C/S	6067	С					
13													
14	2019	С	2006	С									
15	2086	С											
16			1997	С									
17													
18	2006	С	2055	C/S									
19	2091	С											
20													
21													
22	2028	С											
23	2064	С											
24	1993	С											
Average	2011		2019		2086		6068		6100		6174		
Maximum	2091		2073		2166		6214		6201		6174		
Minimum	1868		1979		1984		5978		5987		6174		

C indicates a tapered end failure morphology (i.e. cup and cone), whereas S indicates an oblique failure morphology (i.e. shear failure).